



5-2007

Experimental Investigation of Reinforced Concrete Beams with Lapped Reinforcement

Mary Elizabeth Griffey
University of Tennessee, Knoxville

Recommended Citation

Griffey, Mary Elizabeth, "Experimental Investigation of Reinforced Concrete Beams with Lapped Reinforcement. " Master's Thesis, University of Tennessee, 2007.
https://trace.tennessee.edu/utk_gradthes/4435

This Thesis is brought to you for free and open access by the Graduate School at Trace: Tennessee Research and Creative Exchange. It has been accepted for inclusion in Masters Theses by an authorized administrator of Trace: Tennessee Research and Creative Exchange. For more information, please contact trace@utk.edu.

To the Graduate Council:

I am submitting herewith a thesis written by Mary Elizabeth Griffey entitled "Experimental Investigation of Reinforced Concrete Beams with Lapped Reinforcement." I have examined the final electronic copy of this thesis for form and content and recommend that it be accepted in partial fulfillment of the requirements for the degree of Master of Science, with a major in Civil Engineering.

John Ma, Major Professor

We have read this thesis and recommend its acceptance:

Edwin G. Burdette, Richard Bennett

Accepted for the Council:

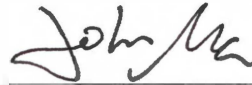
Dixie L. Thompson

Vice Provost and Dean of the Graduate School

(Original signatures are on file with official student records.)

To the Graduate Council:

I am submitting herewith a thesis written by Mary Elizabeth Griffey entitled "Experimental Investigation of Reinforced Concrete Beams with Lapped Reinforcement". I have examined the final paper copy of this thesis for form and content and recommend that it be accepted in partial fulfillment of the requirements for the degree of Master of Science, with a major in Civil Engineering.

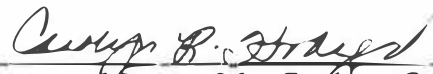


John Ma, Major Professor

We have read this thesis
and recommend its acceptance:



Accepted for the Council:



Vice Provost and Dean of the Graduate School

Thesis
2007
.G75

**Experimental Investigation of Reinforced Concrete Beams with
Lapped Reinforcement**

**A Thesis
Presented for the
Master of Science
Degree
The University of Tennessee, Knoxville**

**Mary Elizabeth Griffey
May 2007**

Acknowledgements

I wish to thank Dr. John Ma's support and guidance in introducing me to the research process and technical writing. I would also like to acknowledge all of Dr. Ma's research team, especially Lungui Li and Austin Batemen, for their work and contribution to the research project discussed in this thesis. Specifically Austin Bateman helped design and test the first two specimens. Lungui Li assisted the testing of the other six specimens. I would also like to acknowledge Ken Thomas, the electric and instrument shop supervisor, and Larry Roberts, the department's design technician, with their assistance with the testing setups. Ross Prestressed Concrete, Inc. donated the concrete materials and helped with the casting of the specimens. Headed Reinforcement Corporation donated the headed bar reinforcement, and Oklahoma Steel and Wire Co., Inc. provided the welded wire reinforcement (WWR). The research work reported here is part of the NCHRP 12-69 project "Design and Construction Guidelines for Long-span Decked Precast, Prestressed Concrete Girder Bridges", sponsored by the National Research Council of the National Academy of Sciences through the National Cooperative Highway Research Program. I would also like to thank Dr. Edwin G. Burdette and Dr. Richard Bennett for serving on my committee.

ABSTRACT

One of the great contributions made by President Dwight D. Eisenhower was his influence in the implementation of the National Interstate and Defense Highways Act of 1956. The National Highway System serves an important role in American citizen's ground transportation. Now more than a half of a century in age, there is a high priority to repair existing infrastructure as well as the need for expansion. Repair and expansion must be achieved efficiently by reducing construction time and improving the capacity and durability of the structure. Precast, prestressed decked bulb tees (DBTs) serve as an excellent solution to ensure quality from an on-site precast concrete fabricator and also to reduce construction time. This thesis focuses on the research involved in the interface connections of these DBTs. Eight specimens of reinforced concrete with two connection details at the center span of the beam were tested, and the results serve as a conservative estimate to the behavior of the jointed interface. Two different prospective joint designs were tested in this project. One type was a headed bar reinforcement which was tested in various spacing and lap lengths. The second type of joint was welded wire reinforcement with varying wire spacing. In order to accelerate bridge construction, it is desirable to narrow the width of the jointed zone. However, the width has to be wide enough to accommodate non-contact lapped reinforcement as well as to develop strength in the joint. According to the moment versus steel stress comparison from the strain gauge results, the 6 inch lap length specimens with headed bars behaved as a continuous reinforced specimen. Moment curvature suggests that the 6 inch lap length provides the design moment capacity and ductility. With the same 6 inch lap length, it was found that the specimen with 4 inch spacing of reinforcement provided 1.5 times the moment capacity of the 6 inch spacing of reinforcement without significantly compromising ductility.

Table of Contents

CHAPTER 1 Introduction.....	1
Highway Infrastructure Repair	1
Project Scope	1
Applications of Headed Bar Reinforcement	3
CHAPTER 2 Development Length of Reinforcement in Tension	4
Bond Stress	4
ACI Code for Straight Bars in Tension.....	5
ACI Code for Hooked Bars in Tension.....	6
Texas Research on Headed Bars.....	7
CHAPTER 3 Experimental Program	13
Description of the Test Specimens	13
Strain Gauge Installation.....	15
Testing Setup	18
Moment Capacity.....	19
Strain Gauge Data.....	19
Moment-Curvature.....	46
CHAPTER 4 Discussion of Results.....	51
Moment Capacity.....	51
Strain Comparisons.....	51
Moment-Curvature Discussion	60
Failure Types	61
CHAPTER 5 Conclusions and Recommended Future Research.....	62
List of References	64
Vita.....	67

LIST OF TABLES

Table 2-1: Comparison of Required Development Length..... 12
Table 3-1: Beam Specimen Design..... 13
Table 3-2: Concrete Cylinder Strength..... 15
Table 3-3: Moment Capacity and Curvature of Specimens..... 19

LIST OF FIGURES

Figure 1-1: Model Specimen in Relation to the Long Span Deck and DBT System	2
Figure 1-2: Model Specimen with Headed Bar Reinforcement.....	2
Figure 2-1: Steel, Concrete, and Bond Stress in a Cracked Beam (MacGregor 2005).....	4
Figure 2-2: Anchorage and Lap Splice Lengths (Thompson, 2006).	7
Figure 2-3: C_1 and C_2 for the Specimens with 6" and 4" Spacing	9
Figure 3-1: Control, Headed Bar, and WWR sample layouts.....	14
Figure 3-2: Strain Gauge Installation and Specimen Fabrication.....	16
Figure 3-3: Testing Setup.....	18
Figure 3-4: Plan View of Rebar location and Detail A of the Control, Specimen C1.....	20
Figure 3-5: Moment vs. Strain Curves (Specimen C1).....	21
Figure 3-6: Plan View of Rebar location and Detail A of Specimen H-6-6.....	22
Figure 3-7: Moment vs. Strain Curves (Specimen H-6-6).....	23
Figure 3-7. Continued.	24
Figure 3-8: Plan View of Rebar location and Detail A of Specimen H-2.5-6.....	25
Figure 3-9: Moment vs. Strain Curves (Specimen H-2.5-6).....	26
Figure 3-10: Plan View of Rebar location and Detail A of Specimen H-6-4.....	28
Figure 3-11: Moment vs. Strain Curves (Specimen H-6-4).....	29
Figure 3-12: Plan View of Rebar location and Detail A of Specimen H-2.5-4.....	32
Figure 3-13: Moment vs. Strain Curves (Specimen H-2.5-4).....	33
Figure 3-14: Plan View of Rebar location and Detail A of Specimen H-4-6.....	36
Figure 3-15: Moment vs. Strain Curves (Specimen H-4-6).....	37
Figure 3-16: Plan View of Rebar location and Detail A of Specimen W-4-4.....	39
Figure 3-17: Moment vs. Strain Curves (Specimen W-4-4).....	40
Figure 3-18: Plan View of Rebar Location and Detail A of Specimen W-4-6.....	43
Figure 3-19: Moment vs. Strain Diagrams (Specimen W-4-6).....	44
Figure 3-20: Moment vs. Curvature Diagrams for Headed Bar Specimens	47
Figure 3-21: Moment vs. Curvature Diagrams for 4 in. Spacing	48
Figure 3-22: Moment vs. Curvature Diagrams for 6 in. Spacing and $f'_c=10,000$ psi.....	49
Figure 3-23: Moment vs. Curvature Diagrams for 6 in. Spacing and $f'_c=8,300$ psi.....	49
Figure 3-24: Moment vs. Curvature Diagrams for WWR Specimens.....	50
Figure 4-1: Cross Section Before Cracking and Stress Distribution	52
Figure 4-2: Cross Section After Cracking and Stress Distribution.....	53
Figure 4-3: Moment versus Steel Stress Comparison for Specimen H-6-6.....	55
Figure 4-4: Moment versus Steel Stress Comparison for Right Side of Specimen H-6-4.....	56
Figure 4-5: Moment versus Steel Stress Comparison for Left Side of Specimen H-6-4.....	57
Figure 4-6: Moment versus Steel Stress Comparison for Specimen H-2.5-4.....	58
Figure 4-7: Moment versus Steel Stress Comparison for Specimen H-2.5-6.....	58
Figure 4-8: Moment versus Steel Stress Comparison for Specimen H-4-6.....	59
Figure 4-9: Failure Types.....	61

CHAPTER 1 Introduction

Highway Infrastructure Repair

For the first 50 years of the life of the interstate system, the Federal Highway Administration's main priority was construction expansion and development across the country. These highways now require significant repair to the roads and bridges that have been in use for a half century. The focus now turns to efficient highway construction which consists of quality work and rapid construction. The headed bar reinforcement can assist in improving the quality of product by reducing the required jointed interface and improving the moment capacity and strength of the girders. For this reason, researchers have an interest in the behavior of headed reinforcement at the jointed interface. The findings discussed in this thesis are involved with a portion of the research effort from NCHRP project 12-69, Design and Construction Guidelines for Long-span Decked Precast, Prestressed Concrete Girder Bridges.

Project Scope

The National Cooperative Highway Research Program project 12-69 objective is to investigate and improve the performance and construction time for long-span decked precast, prestressed concrete girder bridges. These girders can be constructed at a precast concrete plant and shipped to the construction site. The girders will then be erected and connected through special design. The research done on the jointed interface and behavior of headed bar reinforcement connections will aid in the project's objective of improving the structural integrity and reducing the construction time (NCHRP, 2005). In order to investigate the behavior of headed bar and WWR connections, eight specimens were designed and tested. Figure 1-1 shows a typical decked bulb tee and bridge deck, and the dashed jointed interface is the interest in this thesis. The shaded beam shows the specimens fabricated to conservatively model the actual behavior of the prestressed concrete girders. Figure 1-2 shows a sample beam with the headed bar reinforcement and a lapped connection interface at the center span of the beam. The model specimens were

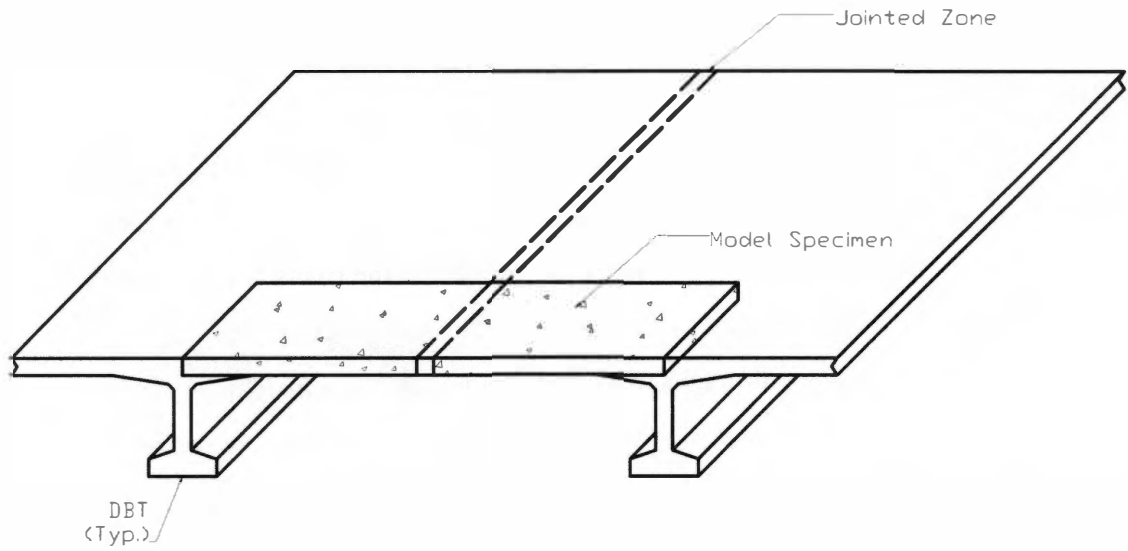


Figure 1-1: Model Specimen in Relation to the Long Span Deck and DBT System

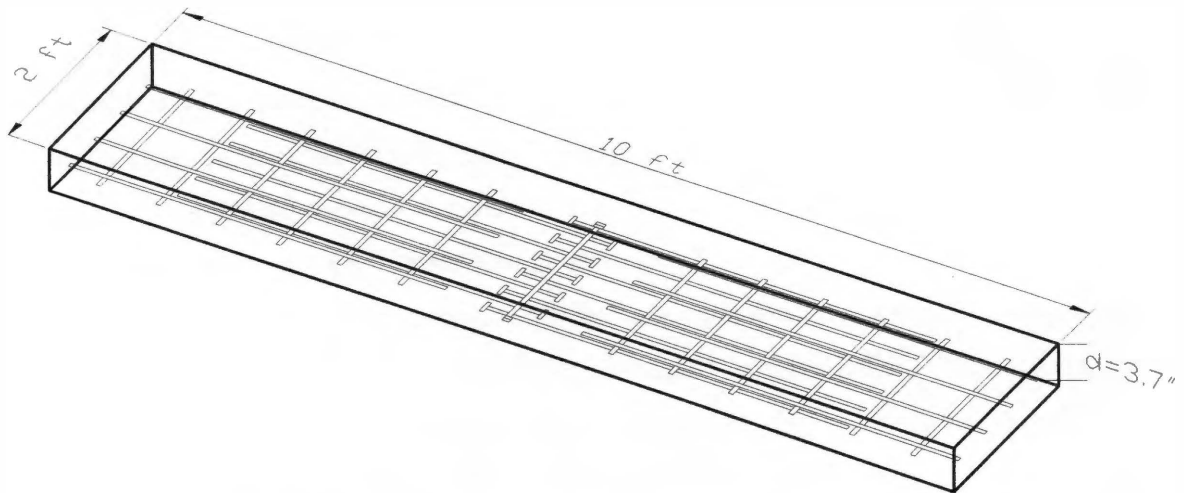


Figure 1-2: Model Specimen with Headed Bar Reinforcement

fabricated to test the reinforcement connections at the center of the span. To isolate the reinforcement layout at the connection as the testing variable, the beams were cast monolithically with concrete. Typically, the joint zone would be connected after the casting of the flanges of the girders with a high strength grout. The specimens did not have the grouted joint zone, and the testing focused on the non contact lapped reinforcement connections at the center span of the beam. Five of the specimens were constructed with three different lap lengths and two different spacings. Another specimen served as a control specimen with continuous straight bars running through the connection. The last two of the eight specimens consisted of welded wire reinforcement at different spacing. Through the analysis of strain gauge data, moment curvature, and moment capacity, a better understanding of the performance of headed bar reinforcement and welded wire reinforcement connections can be achieved.

Applications of Headed Bar Reinforcement

Headed bar reinforcement provides two improvements in reinforced concrete when designing a connection. One improvement would be that the headed bars provide a shorter required development length than that of a straight bar. This reduces the jointed interface width required and resolves any issues pertaining to having enough development length within the dimensions of the structure. Hooked bars are another type of reinforcement used to reduce the required development length, but the large diameter hook can make a connection much more congested. The reduced overcrowding of reinforcement serves as the second improvement provided by headed reinforcement (Thompson, 2003).

While headed bar reinforcement currently has no design code provisions, this type of reinforcement could become popular in many concrete structures such as girders in bridges. The purpose of this thesis is to determine the required joint interface width between non contact headed bar lap length through strain gauge and moment curvature analysis of the eight specimens. The test results will be compared with previous research on headed reinforcement in the joint interface.

CHAPTER 2 Development Length of Reinforcement in Tension

Bond Stress

In order for reinforcement to provide the tensile capacity and concrete to provide the compressive capacity of a beam, the two materials must act as a composite material to transfer forces within the specimen. This action describes bonding. If bond stress does not develop, then the reinforcement will pull out of the concrete causing the steel tensile capacity to go to zero and fail. The bond stress will vary along the length of the beam due to cracks in the concrete. When concrete cracks, bond stress cannot form between the reinforcement and concrete. Figure 2-1 describes the stresses within a cracked beam that is simply supported with two point loads creating a constant moment region between the loads. The steel stress at the cracks is equal to the moment at the crack divided by the internal lever arm and the area of steel. The concrete stress goes to zero at the cracks and

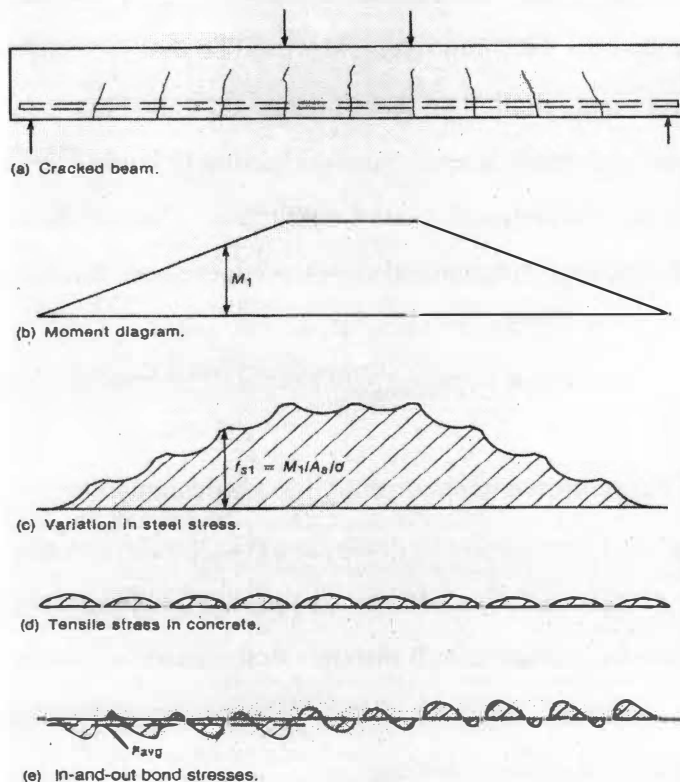


Figure 2-1: Steel, Concrete, and Bond Stress in a Cracked Beam (MacGregor 2005).

increases to the center distance between to cracks. The average bond stress within the constant moment region is equal to zero because the shear is zero. The in and out bond stresses transfer stress into the reinforcement and back out again (MacGregor 2005).

ACI Code for Straight Bars in Tension

The American Concrete Institute International, ACI, develops the standards and code for concrete design. Chapter 12 of the ACI 318-05 code (ACI 2005) discusses the development and splices of reinforcement. Development length is the term used to describe the adequate length in which a reinforcement bar can be developed to its full yield capacity. This length is the distance required for a bar to develop its stress from zero to yield stress. For a straight bar, the required development length, according to the code for a specimen with clear spacing of bars not less than twice the bar diameter and clear cover not less than one bar diameter, which is the case for all specimens tested in this project, is illustrated in the Equation 2-1.

$$L_d = \frac{f_y \Psi_t \Psi_e \lambda}{25 \sqrt{f'_c}} d_b \quad (\text{Eq. 2-1}) \quad (\text{Straight Bar ACI Code})$$

- f_y is the specified yield strength of the reinforcement which will be approximated as 60 ksi.
- Ψ_t is a bar location factor. For situations where there is more than 12 inches of concrete cast below the developed bar, Ψ_t is 1.3. For other cases Ψ_t is 1.0. For this project, the concrete cast below the headed bars is less than 12 inches, and the bar location factor is 1.0. Note that $\Psi_t \Psi_e$ must be less than 1.7. $\Psi_t \Psi_e$ is 1.2.
- Ψ_e is an epoxy coating factor. For epoxy coated bars with cover less than three times the bar diameter or clear spacing less than six times the bar diameter, Ψ_e is equal to 1.5. For all other cases with epoxy coated reinforcement, Ψ_e is equal to 1.2. For uncoated reinforcement Ψ_e is 1.0. For this project, Ψ_e is 1.2.
- λ is a lightweight concrete factor, and λ is 1.0 for normal weight concrete which was the type of concrete used for this project.

- d_b for the headed bars was 5/8 inches, and the concrete strength of the beam varied between specimens and is approximated as 8,500 psi.

$$L_d = \frac{60,000 \text{ psi} * 1.0 * 1.2 * 1.0}{25\sqrt{8,500 \text{ psi}}} * 5/8 \text{ in.} = 19.52 \text{ in. (Straight Bar ACI Code)}$$

Once the development length is determined, Article 12.14 discusses the required conditions to have non contact splices. The code requires that the lap splices shall not be used for No. 11 bars or larger, and the minimum spacing for non-contact splices in flexure must be smaller than one-fifth the required lap splice length or 6 inches. Both of these requirements are satisfied with all headed bar specimens in this research. Article 12.15 covers the splices of deformed bars in tension. The minimum length for a tension lap splice is divided between Class A and Class B splice and shall not be permitted to be less than 12 inches. For the specimens, 100% of the steel area is spliced within the required lap length which puts the splices in Class B. For Class B splices, the minimum lap length is 1.3 times the development length and not less than 12 inches.

$$\text{Required Lap Length} = 1.3(L_d) \text{ (Eq. 2-2)}$$

$$\text{Required Lap Length} = 1.3 * 19.52 \text{ in.} = 25.4 \text{ in. (Straight Bar ACI code)}$$

ACI Code for Hooked Bars in Tension

Article 12.5 of the ACI code also specifies the required development length for hooked anchors. The code does not identify the development length for headed bars, but it can be inferred that the headed bars will improve the bond development and decrease the required development length. The required lap length for headed bars can more closely be estimated through the equation for development length for hooked bars. The equation to calculate this length is shown in Equation 2-3. The length shall not be less than 8 times the bar diameter or 6 inches. For the specimens tested, the bar diameters are 5/8 in. which makes the required development length for hooks to be at least 6 inches.

$$l_{dh} = \frac{0.02\psi_e \lambda f_y}{\sqrt{f'_c}} d_b \text{ (Eq. 2-3) (Hooked Bar ACI Code)}$$

$$l_{dh} = \frac{0.02 * 1.2 * 1.0 * 60,000 \text{ psi}}{\sqrt{8,500 \text{ psi}}} * 5/8 \text{ in.} = 9.76 \text{ in.}$$

The hooked development length is then multiplied by a factor from ACI 12.5.3 to account for the confinement by stirrups. Confinement will reduce the possibility of early hook failure by concrete splitting. The multiplier depends upon the cover, hook type, bar size, and stirrup presence. For a 180° or 90° hook type with a No. 11 bar and smaller reinforcement, no stirrups, and less than a 2.5 in. side cover, the multiplier is 0.7. This multiplier's conditions are similar to the conditions of the 6 in. spaced headed bar specimen. Therefore, the modified hooked development length will equal 6.8 in.

$$l_{dh} = 9.76in.*0.7 = 6.8in.$$

Texas Research on Headed Bars

The University of Texas at Austin (UTA) performed research of the anchorage behavior of headed reinforcement sponsored by the Texas Department of Transportation (Thompson, 2006). The project investigated the development length and proposed a design method for the required development of headed bars to be included in the American Concrete Institute code. The design method included two length variables for determining the overlap length shown in Figure 2-2. The anchorage length is the measurement from the point of maximum bar stress to the bearing face of the head. The lap splice length is then determined from an appropriate strut-and-tie model and the known anchorage length. For the applications in this thesis, the lap splice length was determined by the recommended 55° struts from the UTA research (Thompson, 2006).

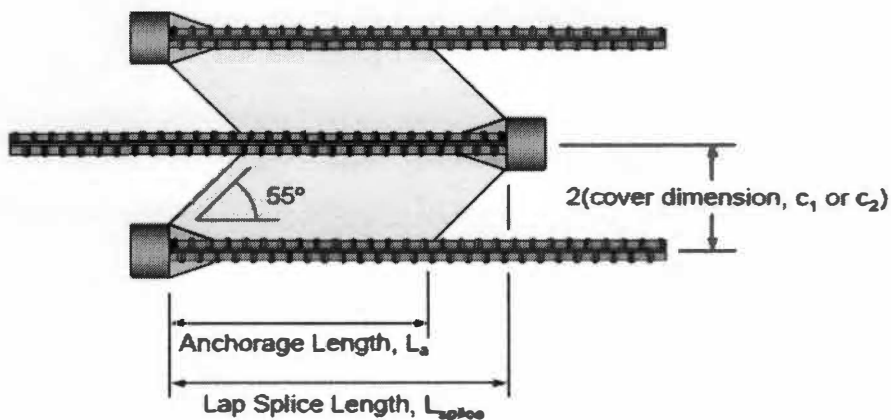


Figure 2-2: Anchorage and Lap Splice Lengths (Thompson, 2006).

An estimate of the required lap length for headed bar specimens using the design provisions written from the UTA research is also included as a comparison to the results found in this project. The proposed design additions for required lap length of headed bar reinforcement is discussed in the “Anchorage Behavior of Headed Reinforcement” report (Thompson, 2003) and is included as follows:

12.6.2 Test results showing the adequacy of mechanical devices *other than headed bars* shall be presented to the building official. *Headed bars are permitted provided they conform to the provisions of 12.6.3 through 12.6.4.*

12.6.3 Development of reinforcement shall be permitted to consist of a combination of mechanical anchorage plus *bond along the anchorage length* of reinforcement between the point of maximum bar stress and the mechanical anchorage. *The stress provided by bearing of a head ($f_{s,head}$) shall conform to 12.6.3.1 and the stress provided by bond ($f_{s,bond}$) shall conform to the provisions of 12.6.3.2. The total bar stress for headed reinforcement shall be the sum of $f_{s,head} + f_{s,bond}$.*

12.6.3.1 The bar stress provided by bearing of the head, $f_{s,head}$, shall be computed by

$$f_{s,head} = 1.4 * \sqrt{\frac{A_{nh}}{A_b}} * \left(\frac{c_1}{d_b}\right) * \psi * f'_c$$

$$\psi = 0.6 + 0.4 * \left(\frac{c_2}{c_1}\right) \leq 2.0$$

- A_{nh} is the net bearing area of the head (neglecting the bar area), in². For the headed bar specimens, the diameter of the head was 2 inches, and the diameter of the bar was 5/8 inch. The A_{nh} was 2.835 in².

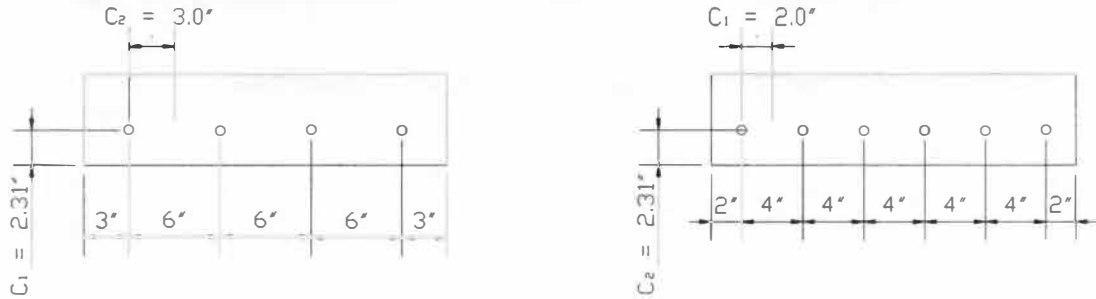


Figure 2-3: C_1 and C_2 for the Specimens with 6" and 4" Spacing

- C_1 is the minimum of half the center-to-center bar spacing or the least overall cover dimension measured to the center of the bar, in. As shown in Figure 2-3, C_1 is 2.31 inches for the 6 inch spacing, and C_1 is 2.0 inches for the 4 inch spacing of headed bars.
- C_2 is the dimension orthogonal to C_1 in. If C_1 is determined by half the center-to-center bar spacing, C_2 is the lesser of the cover in the orthogonal direction measure to center-to-center bar spacing orthogonal to C_1 . (C_2 must always be greater than or equal to C_1 .) From Figure 2-3, C_2 is 3.0 inches for the 6 inch spacing of reinforcement, and C_2 is 2.31 inches for the 4 inch spacing.
- A_b is the cross-sectional area of the bar. For this project, a #5 bar was used with A_b equal to 0.31 in².
- d_b is the diameter of the bar. For this project, d_b is equal to 5/8 inch.
- f'_c is the concrete compressive strength. An average compressive strength of all specimens will be taken as approximately 8,500 psi.
- Ψ is the radial disturbance factor.

For the 6 in. spacing, $\Psi = 0.6 + 0.4*(3.0in./2.31in.) = 1.12$

For the 4 in. spacing, $\Psi = 0.6 + 0.4*(2.32in./2.0in.) = 1.06$

A minimum anchorage length of $6d_b$ is required for the above equation to be valid.

12.6.3.2 The bar stress provided by bond, $f_{s,bond}$, shall be computed by

$$f_{s,bond} = \chi * f_y * \left(\frac{L_a}{L_d} \right)$$

- ***L_a is the bonded anchorage length as determined by the provision of 12.6.3, in.*** This will be the variable of interest which will be calculated.
- ***L_d is the development length of a non-headed bar of the same diameter as determined from the provisions of 12.2, in.*** L_d was determined under the section “ACI Code for Straight Bars in Tension” and was equal to 19.52 inches.
- ***χ is the reduction factor for head size which must be greater than 0.3.*** A more exact expression was determined in the “Behavior and Capacity of Headed Reinforcement”, (Thompson 2006), which is expressed below. For this project, χ is equal to 0.3.

$$\chi = 1 - 0.7 \left(\frac{A_{nh} / A_b}{5} \right) \geq 0.3$$

$$\chi = 1 - 0.7 \left(\frac{2.835 \text{in}^2 / 0.31 \text{in}^2}{5} \right) = -0.28 \quad \text{Therefore, } \chi = 0.3$$

The anchorage length, L_a , shall be measured from the point of maximum bar stress to the bearing face of the head. An anchorage length of at least $6d_b$ must be provided. Appropriate strut-and-tie models shall be used to determine the critical section at which the maximum bar stress occurs.

12.6.4 Any connection between the head and bar shall be permitted provided the full bar stress expected from the head can be developed at the connection without the slip of the reinforcement relative to the head. Furthermore, the head shall be sufficiently

rigid to provide optimal bearing across the entire head area. Test results demonstrating the adequacy of the head-bar connection shall be provided to the appropriate building official. (The requirements of this provision should be addressed by ASTM. At the time when a suitable provision exists, the language of this text can be adjusted to reference ASTM specifications.)

Equation 2-4 expresses the required anchorage length, L_a , in terms of required bond stress. This expression was used to determine the projected anchorage length and lap splice length under the conditions of the specimens in the test.

$$\text{If } f_{s, \text{bond}} = f_y - f_{s, \text{head}} \geq 0, \quad L_a = \left(\frac{f_{s, \text{bond}} * L_d}{\chi * f_y} \right) \quad (\text{a})$$

$$\text{If } f_{s, \text{bond}} = f_y - f_{s, \text{head}} \leq 0, \quad L_a = 6 * d_b \quad (\text{b}) \quad (\text{Eq. 2-4})$$

4 in. Spacing:
$$\psi = 0.6 + 0.4 * \left(\frac{2.31 \text{in.}}{2 \text{in.}} \right) = 1.06$$

$$f_{s, \text{head}} = 1.4 * \sqrt{\frac{2.835 \text{in}^2}{0.31 \text{in}^2}} * \left(\frac{2 \text{in.}}{5/8 \text{in.}} \right) * 1.06 * 8,500 \text{psi} = 122.1 \text{ksi}$$

$$f_y - f_{s, \text{head}} \leq 0 \quad \text{Therefore, } L_a = 6 * d_b = 6 * (5/8 \text{in.}) = 3.75 \text{in.}$$

$$L_{\text{splice}} = (3.75 \text{in.}) + [4 \text{in.} - (5/8) \text{in.} - 0.688 \text{in.}] / \tan(55^\circ) = 5.63 \text{in.}$$

6 in. Spacing:
$$\psi = 0.6 + 0.4 * \left(\frac{3 \text{in.}}{2.31 \text{in.}} \right) = 1.12$$

$$f_{s, \text{head}} = 1.4 * \sqrt{\frac{2.835 \text{in}^2}{0.31 \text{in}^2}} * \left(\frac{2.31 \text{in.}}{5/8 \text{in.}} \right) * 1.12 * 8,500 \text{psi} = 149 \text{ksi}$$

$$f_y - f_{s, \text{head}} \leq 0 \quad \text{Therefore, } L_a = 6 * d_b = 6 * (5/8 \text{in.}) = 3.75 \text{in.}$$

$$L_{\text{splice}} = (3.75 \text{in.}) + [6 \text{in.} - (5/8) \text{in.} - 0.688 \text{in.}] / \tan(55^\circ) = 7.03 \text{in.}$$

The headed bar lap length calculations considers the same bar size, concrete strength, and spacing of the previous development length calculations. For the 4 in. spacing and 6 in. spacing, the anchorage length results from the minimum development length of $6d_b$. Note that the calculations for the lap splice length assumes recommended strut line angle of 55° from the end of the anchorage length.

Table 2-1 summarizes the required development lengths and lap lengths for the three methods discussed in this chapter. The ACI code for a straight bar will require the largest required lap length, because it does not consider the contribution of the head to the increased development of bond stress. The proposed method by University of Texas at Austin produced varying required lap lengths depending on the spacing of the reinforcement specimen.

Table 2-1: Comparison of Required Development Length

Method	Required Development Length	Minimum Required Development Length	Required Lap Splice Length
ACI (Straight Bar)	19.5 in.	12 in.	25.4 in.
ACI (Hooked Bar)	6.8 in.	6 in.	N/A
Proposed Method by University of Texas at Austin (4" Spacing)	3.75 in. (Required Anchorage Length)	3.75 in.	5.63 in.
Proposed Method by University of Texas at Austin (6" Spacing)	3.75 in. (Required Anchorage Length)	3.75 in.	7.03 in.

CHAPTER 3 Experimental Program

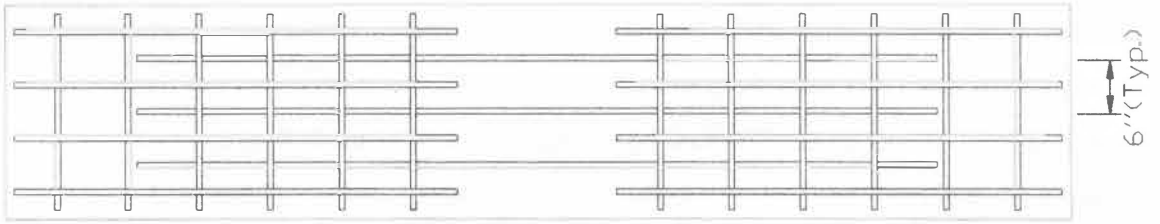
Description of the Test Specimens

Table 3-1 describes the specifications of the reinforcement for each of the eight beam specimens designed for testing in this project. Each beam was two feet wide, ten feet long, and six inches deep. The first beam was a control beam with a layer of continuous rebar across the joint interface. The following five beams were reinforced with Grade 60 #5 headed bars provided by the Headed Reinforcement Corporation (www.hrc-usa.com) with a standard 2 in. diameter friction welded head. The headed bars meet ASTM A 970 (ASTM 2007). Two beams were reinforced in the joint interface with welded wire reinforcement (WWR) which was Grade 60 Epoxy Coated Welded Wire Reinforcement with a “D31” size provided by Oklahoma Steel and Wire Co., Inc. (www.oklahomasteel.com).

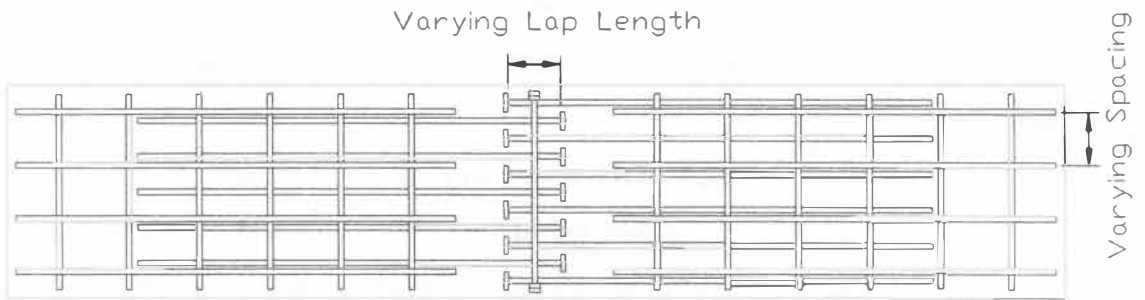
Figure 3-1 shows the plan view of the beams fabricated and tested in this research. The beam in Figure 3-1 (a) is the Control Specimen which had #5 continuous bars spaced 6 in. apart. Figure 3-1 (b) shows a sample of the headed bar reinforced connections. Five specimens had this reinforcement connection with vary lap lengths and spacing discussed in Table 3-1. Figure 3-1 (c) is the WWR beam with a 4 in. lap length connection at the center span. Two specimens had this reinforcement connection with a 4 in. lap length and either a 4 in. or 6 in. spacing.

Table 3-1: Beam Specimen Design

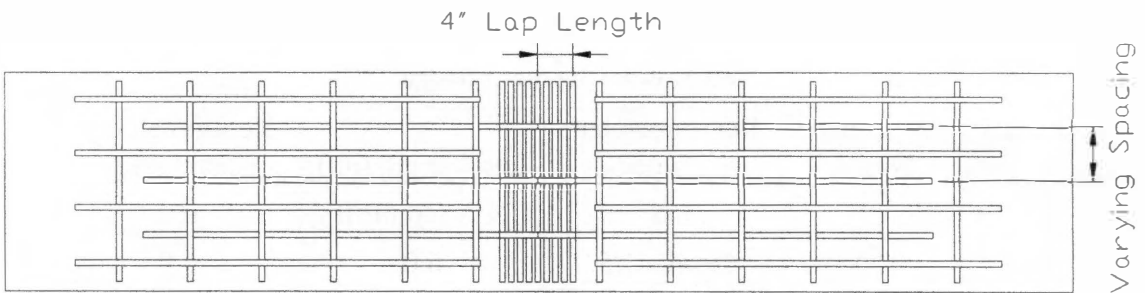
Specimen #	Specimen Name	Reinforcement Type	Lap Length (in.)	Reinforcement Spacing (in.)
1	C1	#5	N/A (control)	6.0
2	H-6-6	Headed #5	6.0	6.0
3	H-2.5-6	Headed #5	2.5	6.0
4	H-6-4	Headed #5	6.0	4.0
5	H-2.5-4	Headed #5	2.5	4.0
6	H-4-6	Headed #5	4.0	6.0
7	W-4-6	WWR D31	4.0	6.0
8	W-4-4	WWR D31	4.0	4.0



(a) Control Specimen



(b) Typical Headed Bar Specimen



(c) Typical WWR Specimen

Figure 3-1: Control, Headed Bar, and WWR sample layouts.

Table 3-2: Concrete Cylinder Strength

Specimen Name	Date of Concrete Casting	Date of Specimen Testing	Age (days)	Concrete Strength at Testing (psi)
C1	7/12/2006	7/20/2006	8	10,542*
H-6-6	7/12/2006	7/25/2006	13	10,542*
H-2.5-6	9/13/2006	10/06/2006	23	8,230
H-6-4	9/13/2006	10/16/2006	33	8,860
H-2.5-4	9/13/2006	11/08/2006	56	8,950
H-4-6	11/01/2006	11/25/2006	24	8,480
W-4-6	11/01/2006	11/17/2006	16	7,750
W-4-4	11/01/2006	12/01/2006	30	8,352

* Based on testing results on 7/21/2006

The concrete mix design used to cast all eight of the beam specimens was provided from Ross Prestressed, Inc., who has provided service to the Tennessee Department of Transportation. Table 3-2 describes the date of testing, the concrete cylinder strength, and the age of the cylinders. The concrete strength will have an effect on the performance of the beam, and it must be considered when evaluating each of the connection designs. The design compressive strength of the concrete mix was 7000 psi at 28 days.

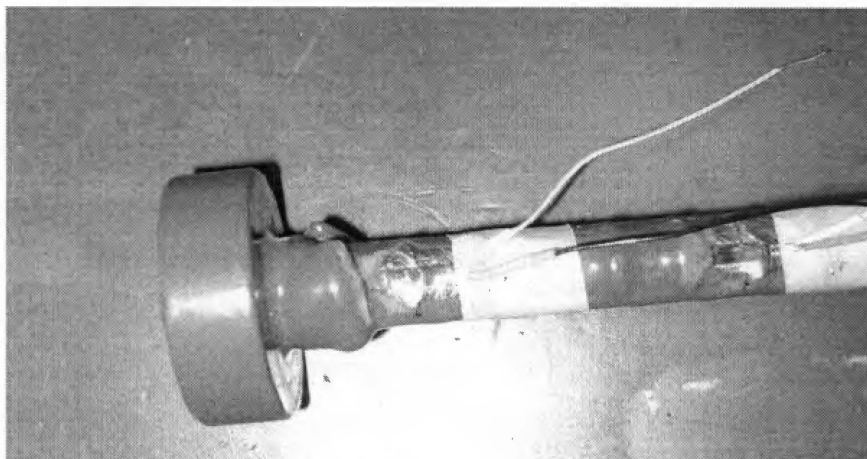
Strain Gauge Installation

The strain gauges from Vishay Micro Measurement (www.vishay.com) were used. The general purpose strain gauges recommended for this project had resistances of 120 ohm and 350 ohm, and they varied in length of either 0.125 or 0.25 inches. The reason for varying resistances and length for the gauges was due to availability.

In order to ensure the quality of the data produced by the strain gauges, the following steps were followed. The first step was to prepare the rebar for installation by grinding a smooth surface which removed the epoxy coating and ridges at the desired location of a gauge with a handheld grinding wheel. All reinforcement was epoxy coated. The second step was solvent degreasing with Isopropyl Alcohol which removes any debris, oils, greases, organic contaminants, and soluble chemical residues. The third

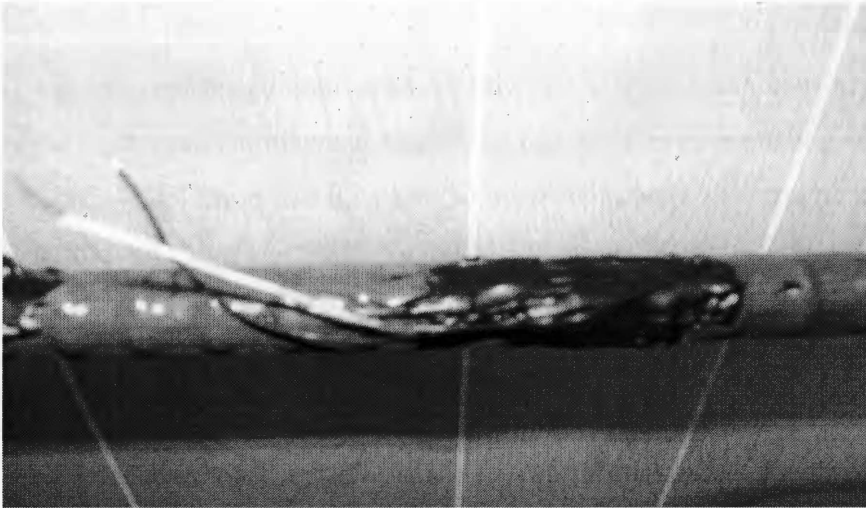
step was surface abrading which was done initially with 220 grit sand paper and followed with a finer 320 grit sand paper and a conditioning solution. The fourth step was to draw lines to accurately locate the position of the strain gauge and orient the strain gauge parallel to the rebar. The fifth step was to apply a conditioner solvent on the site and then wipe clean. The sixth step was to apply the neutralizer solution on the area in order to reach a preferred alkalinity of 7.0 to 7.5 pH. The final step was to attach the strain gauges with an M-Bond AE-10 adhesive. The adhesive and solutions were provided by Vishay Micro Measurements.

Once the strain gauges were installed on the reinforcement, the lead wires on the gauges were soldered to wires that will hook up to the data acquisition system. After the soldering was finished, shrink wrap is installed over the new soldered connection for protection. Following the soldering, the gauge and soldered connection was coated with M-Coat J-1 Kit to prevent water damage once the specimens are cast in concrete. The curing of the M-Coat J-1 requires a 24 hour period. Figure 3-2 (a) shows a strain gauge attached and soldered to the headed bar with the heat wrap over the soldered wires, and Figure 3-2 (b) shows a strain gauge that is coated and ready to be set in the form. Figure 3-2 (c) shows the tying of the reinforcement with the gauges attached, and Figure 3-2 (d) shows the pouring of the concrete in the specimen forms.



(a) Soldered Strain Gauge

Figure 3-2: Strain Gauge Installation and Specimen Fabrication.



(b) Strain Gauge Coated in M-Bond



(c) Tied Rebar in Form for the Control Specimen



(d) Concrete Pour

Figure 3-2. Continued.

Testing Setup

All eight specimens were tested with the same loading set-up. The specimens were 10 feet long and 6 inches deep, and the beams were simply supported with supports spanning 8 feet apart. The specimens were loaded with two point loads spaced 40 inches apart. Figure 3-3 shows the set up for the beam specimen testing. The jointed interface for all specimens was located in the center of the span between the two point loads, and the jointed interface will experience the maximum moment of the beam. The maximum moment remains constant within the two point loads. The constant moment between the point loads can be calculated by multiplying the applied load, P , times the distance between one support and the point load. This distance between the support and point load was 28 inches which is shown in Figure 3-3. This moment at the jointed interface will be plotted versus the strain gauge readings discussed later in the thesis. The extension and compression reading shown at the top and bottom of the specimen was used to calculate the curvature of the beam at a given moment. The moment versus curvature graphs are also plotted in the testing results.

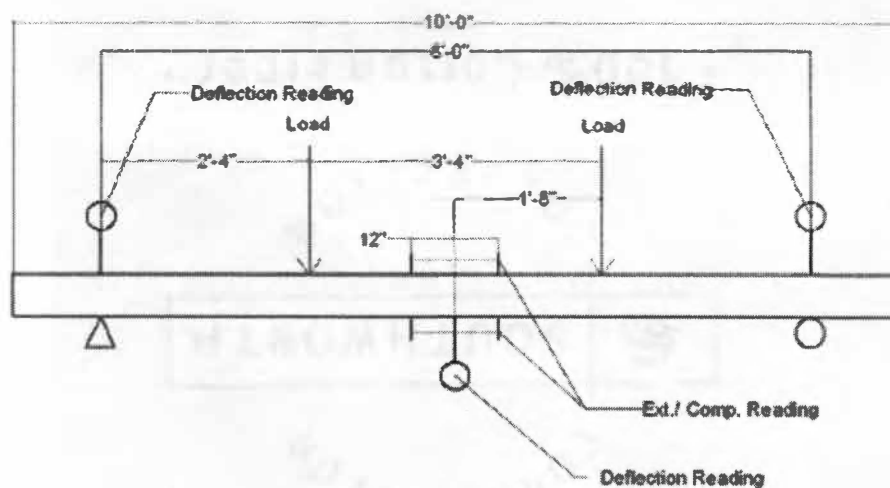


Figure 3-3: Testing Setup.

Moment Capacity

The moment capacity, failure mode, strain behavior, and moment curvature are all key elements to be considered in the performance of each specimen. Table 3-3 compiles the maximum moment and maximum curvature of each specimen. The curvature was calculated from the extension and compression readings. The curvature is an important factor. A beam with a high moment capacity and a low curvature will be undesirable in the industry because the failure will be brittle and quick. Three of the specimens failed prematurely, and the maximum curvature could not be reported.

Strain Gauge Data

The first step of the analysis of the strain gauge data was to plot the data in moment versus strain diagrams. A figure with the plan view of the reinforcement spacing and lap length and a detail view of the strain gage locations are included before each specimen's moment versus strain plot. The detail figures include the notation for each strain gauge and the distance of the center of the strain gauge to the centerline of the beam's span. Each moment versus strain plot includes a line representing maximum moment experienced and the yield strain of the 60 ksi strength reinforcement. Figure 3-4 through Figure 3-19 show the schematic layout of each specimen and their strain gauges followed by the plots of the moment versus strain behavior.

Table 3-3: Moment Capacity and Curvature of Specimens

Specimens	Moment Capacity M_n (ft-kips)	Maximum Curvature rad/(10 ⁶ in.)	
		Corresponding to M_n	Maximum
C1	25.19	10,827	12,930
H-6-6	25.83	7,657	9,490
H-2.5-6	17.4	2,180	3,715
H-6-4	39.4	6,320	8,850
H-2.5-4	35.82	3,407	Failed Suddenly
H-4-6	19.8	3,540	No Data Collected
W-4-4	4.74	711	Failed Suddenly
W-4-6	3.68	1,967	Failed Suddenly

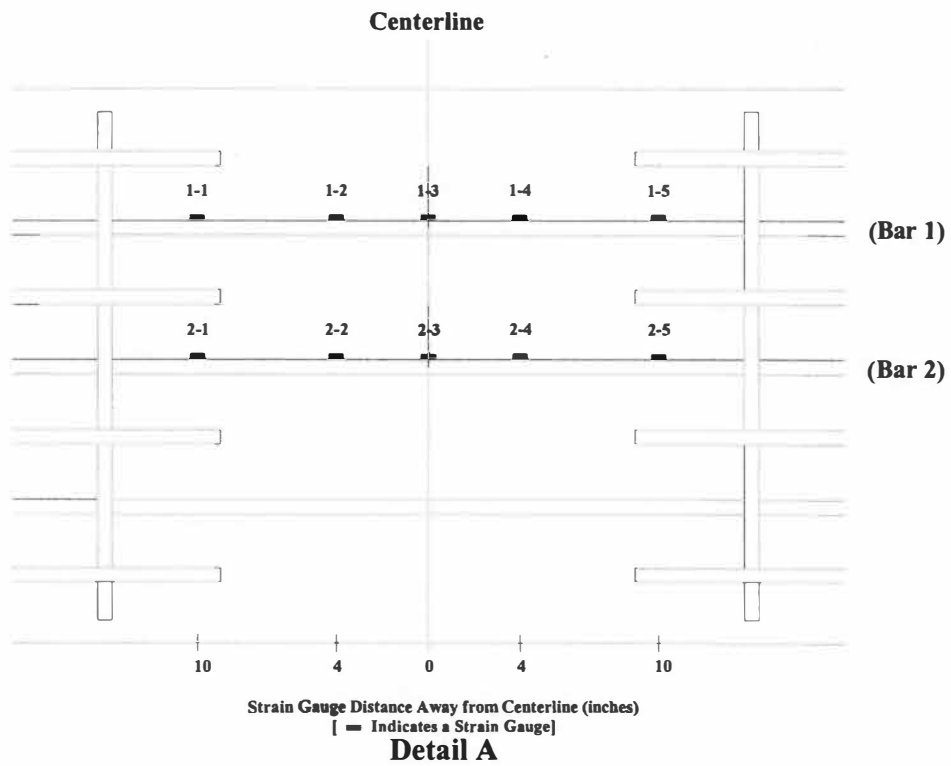
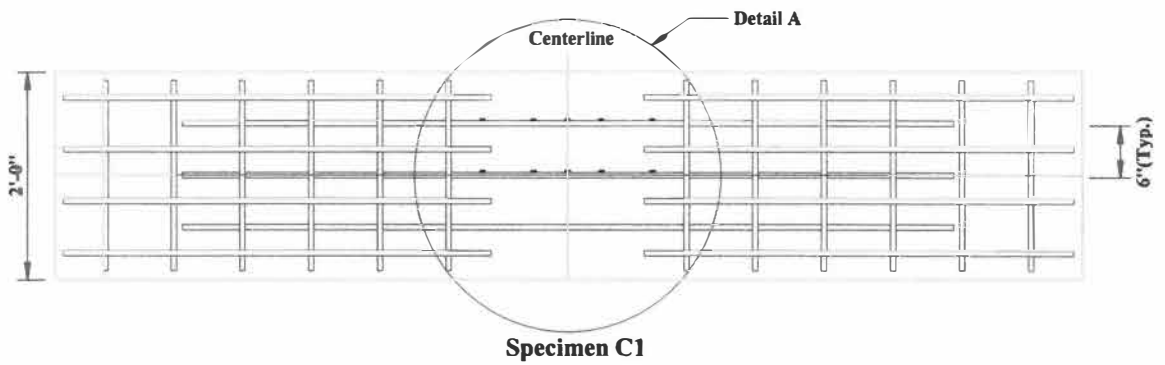
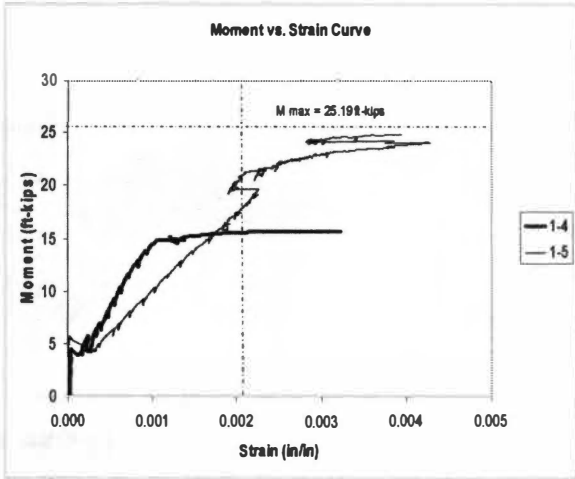
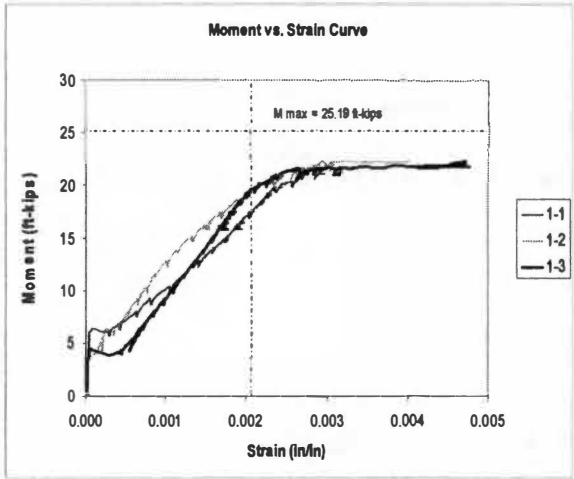
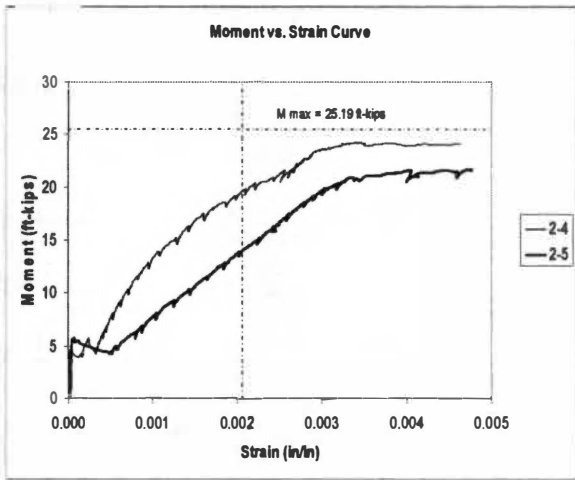
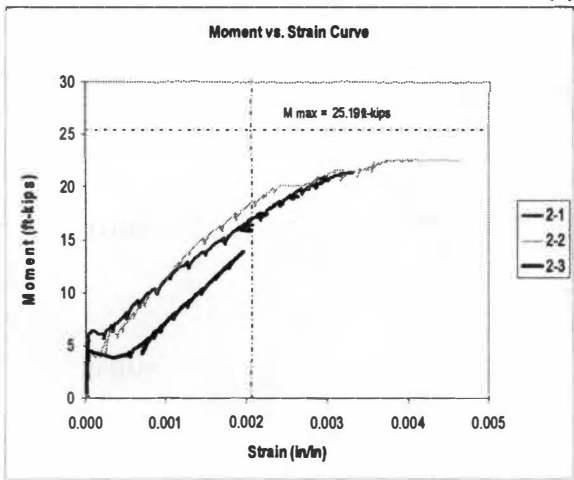


Figure 3-4: Plan View of Rebar location and Detail A of the Control, Specimen C1.



(a) Bar 1



(b) Bar 2

Figure 3-5: Moment vs. Strain Curves (Specimen C1).

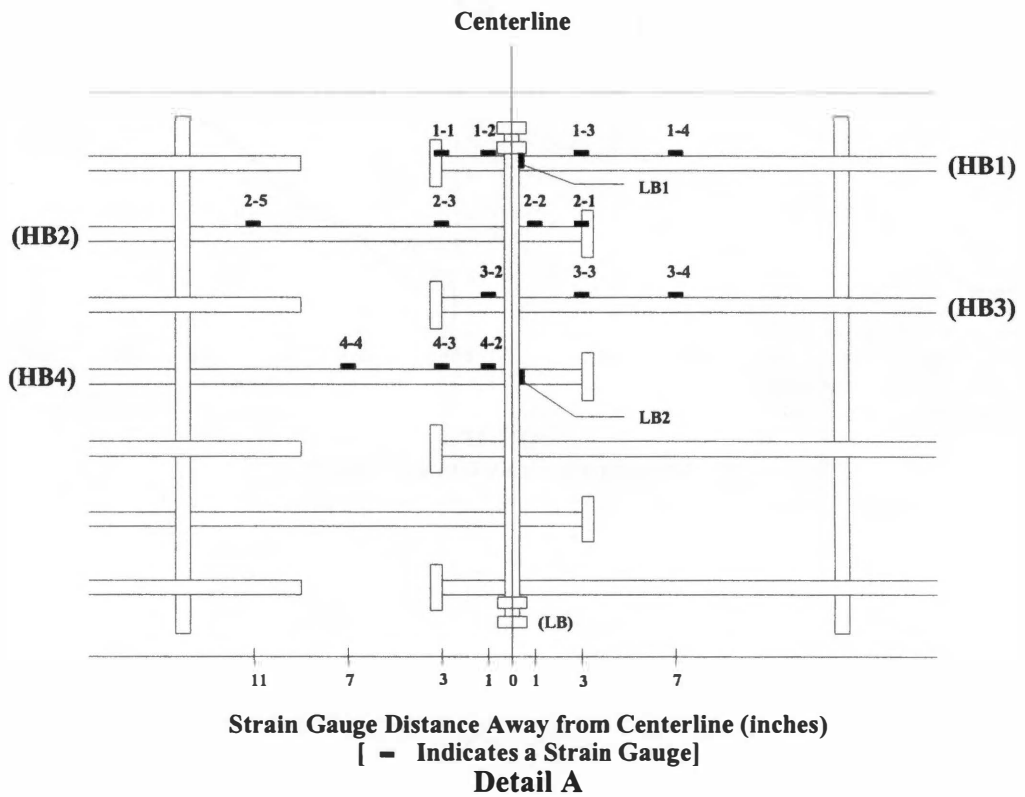
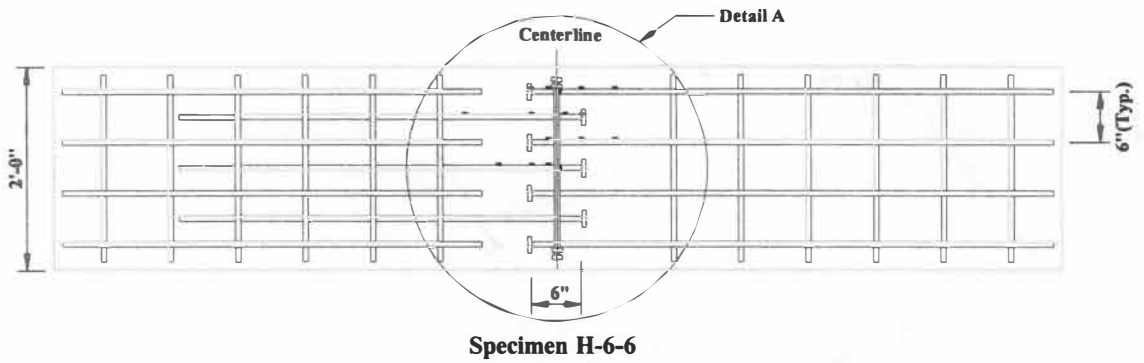
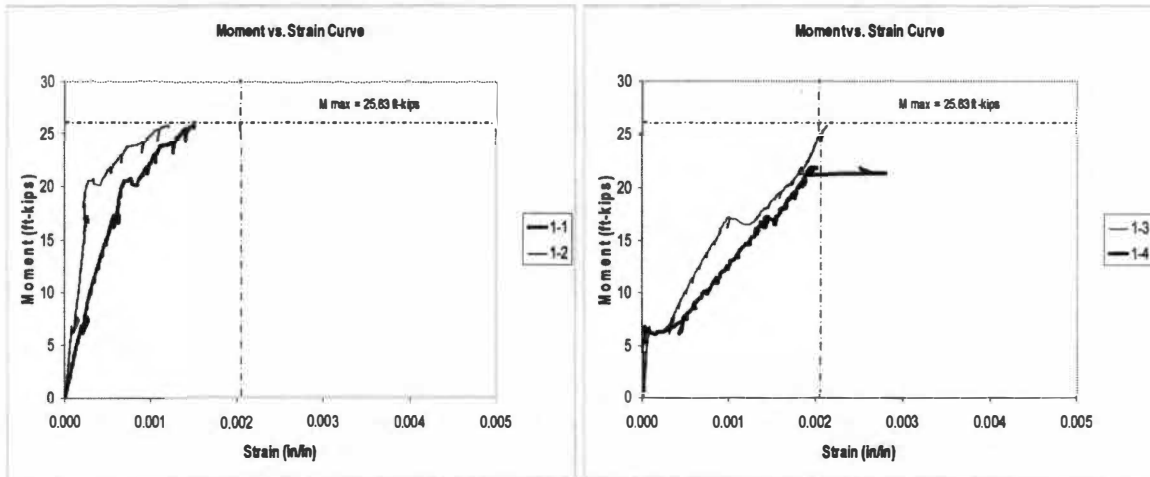
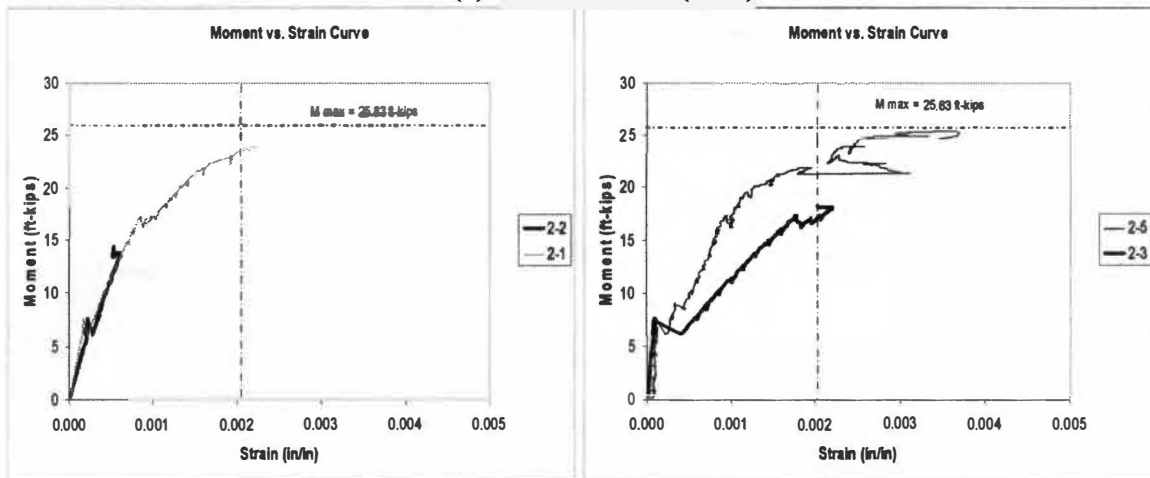


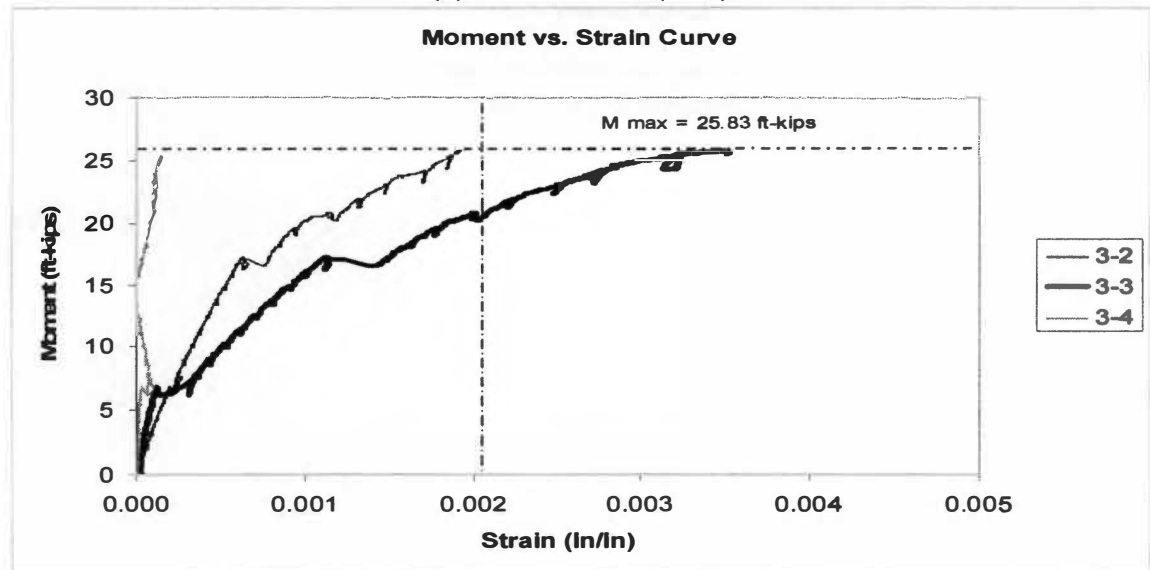
Figure 3-6: Plan View of Rebar location and Detail A of Specimen H-6-6.



(a) Headed Bar 1 (HB1)

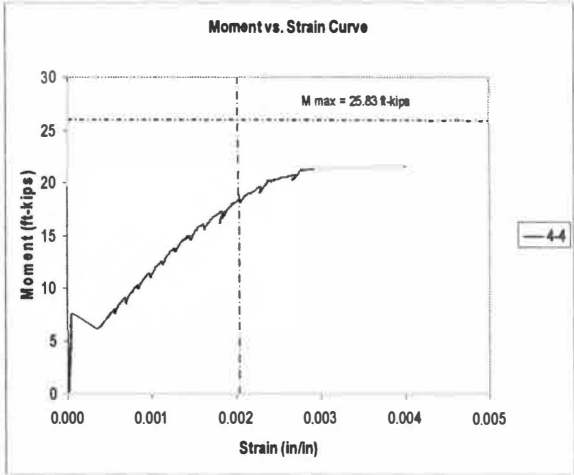
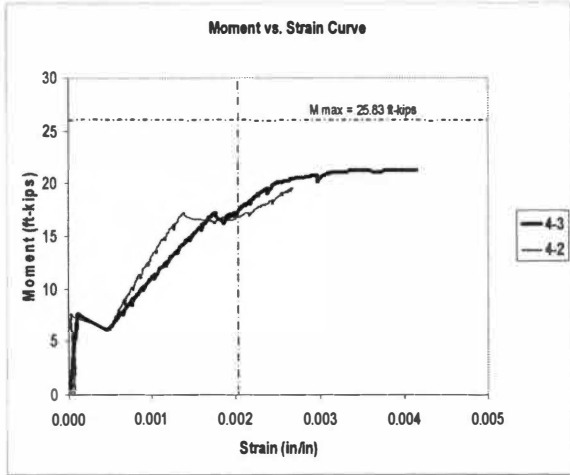


(b) Headed Bar 2 (HB2)

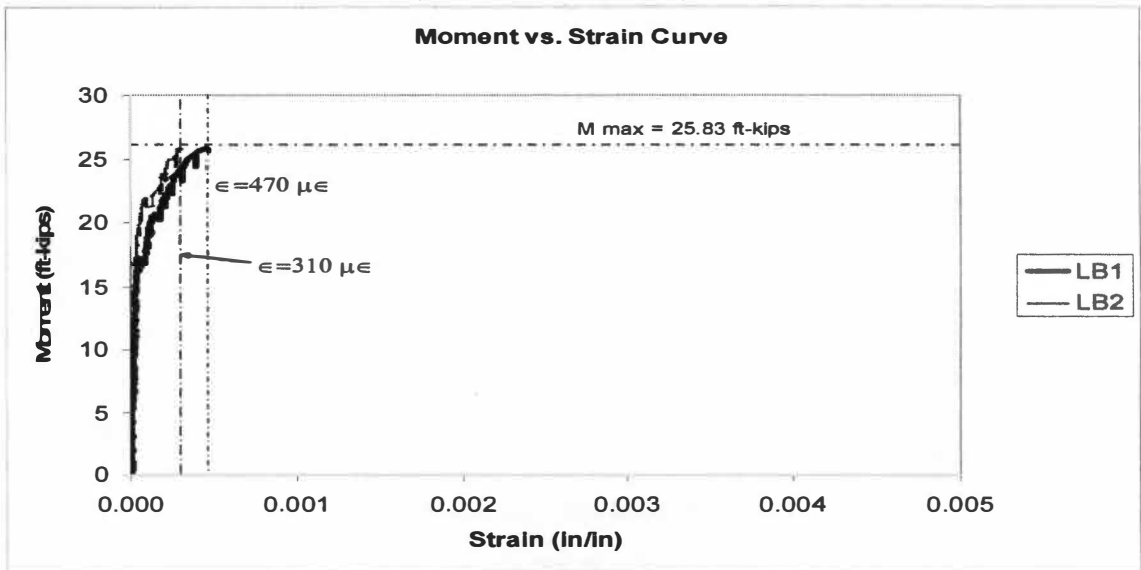


(b) Headed Bar 3 (HB3)

Figure 3-7: Moment vs. Strain Curves (Specimen H-6-6).



(d) Headed Bar 4 (HB4)



(e) Longitudinal Bar (LB)
Figure 3-7. Continued.

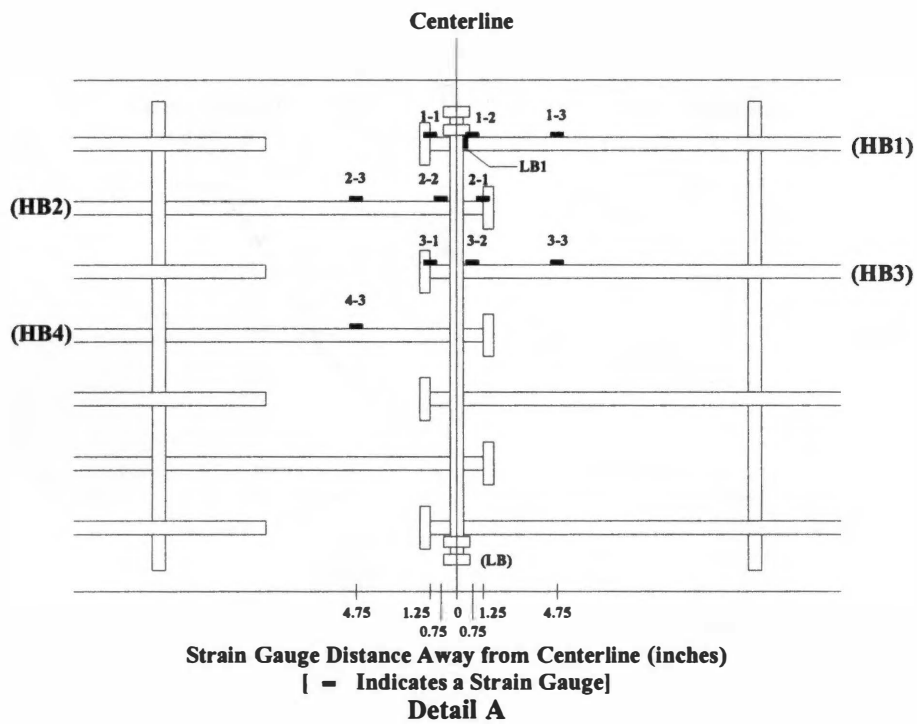
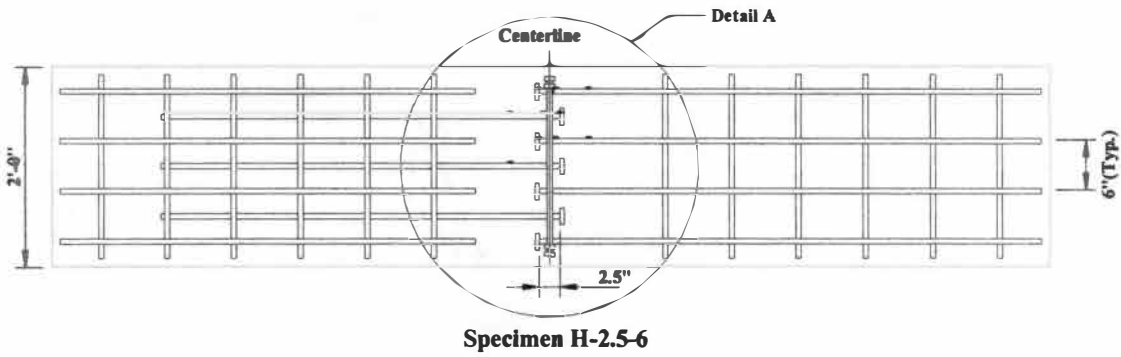
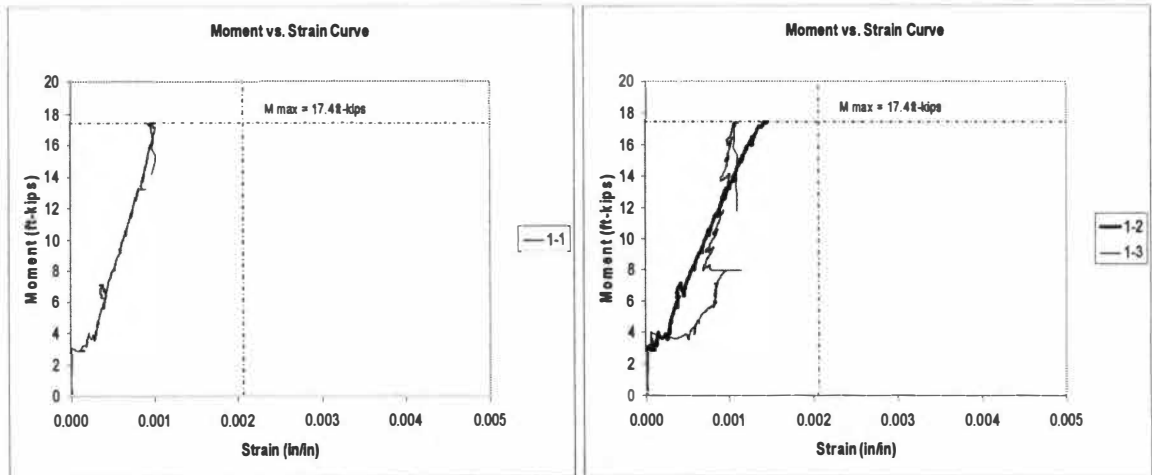
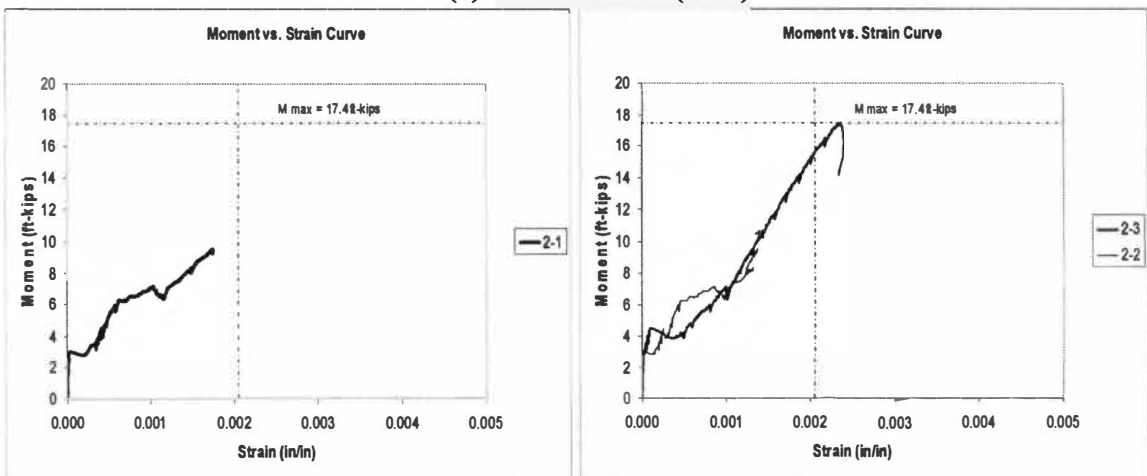


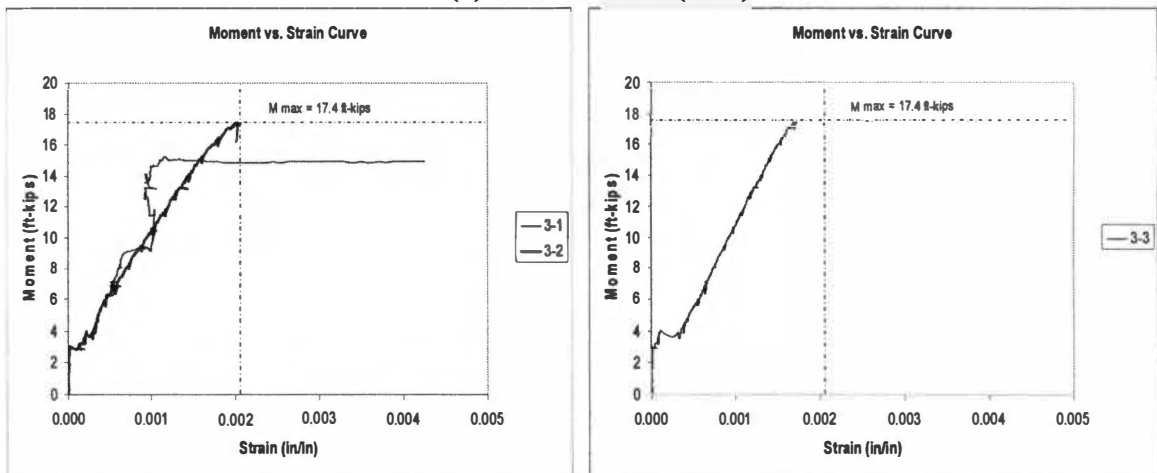
Figure 3-8: Plan View of Rebar location and Detail A of Specimen H-2.5-6.



(a) Headed Bar 1 (HB1)

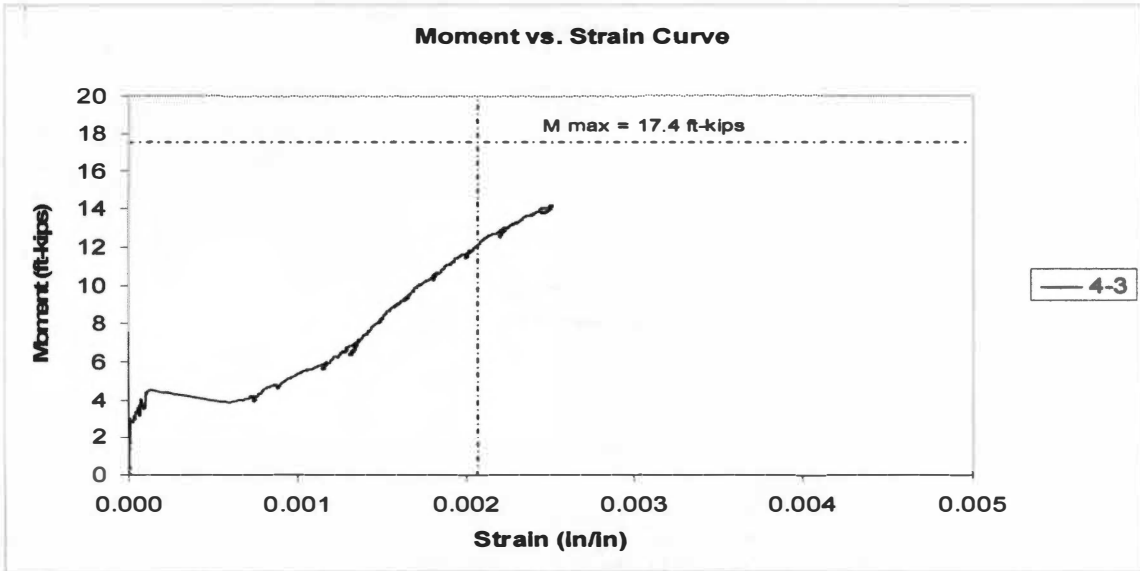


(b) Headed Bar 2 (HB2)

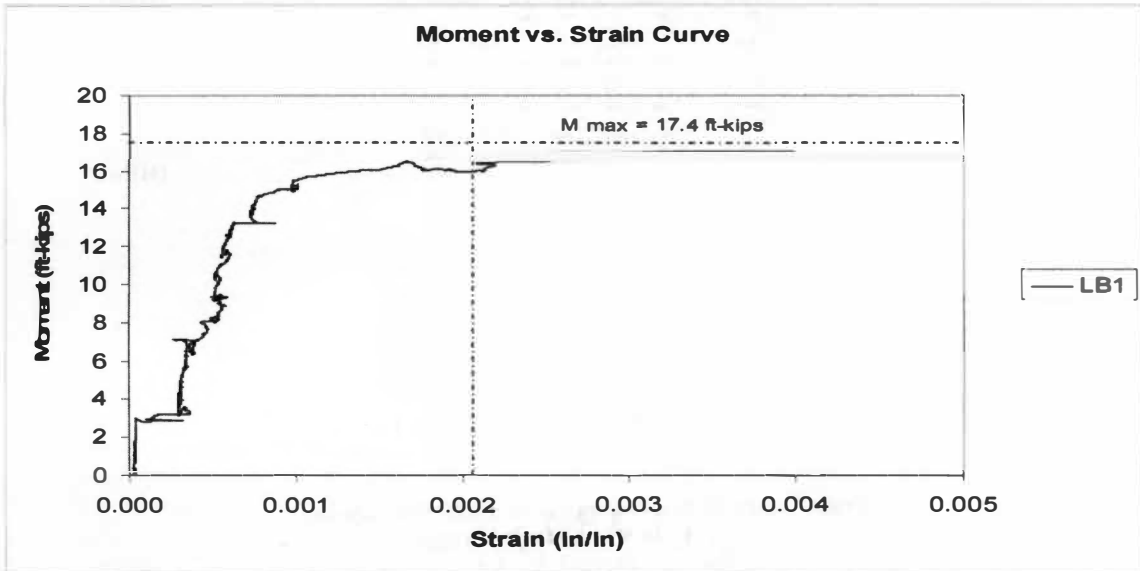


(c) Headed Bar 3 (HB3)

Figure 3-9: Moment vs. Strain Curves (Specimen H-2.5-6).



(d) Headed Bar 4 (HB4)



(e) Longitudinal Bar (LB)

Figure 3-9. Continued.

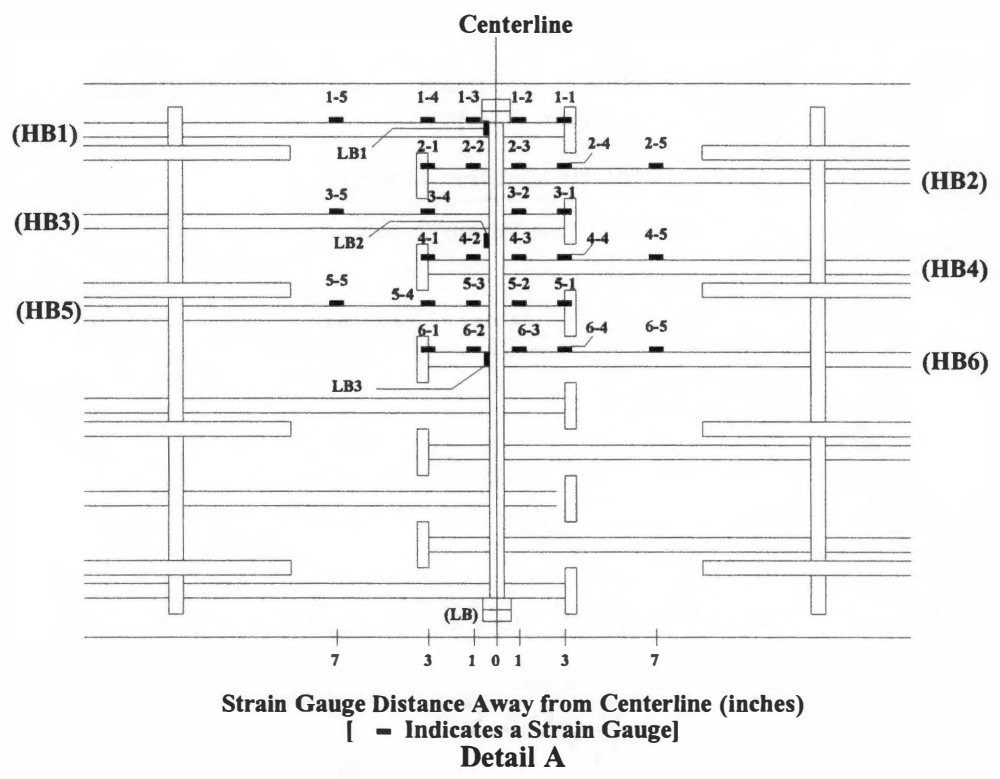
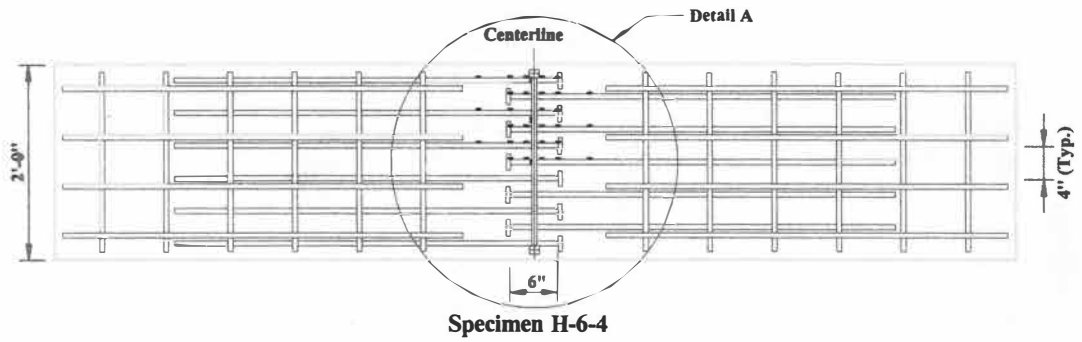
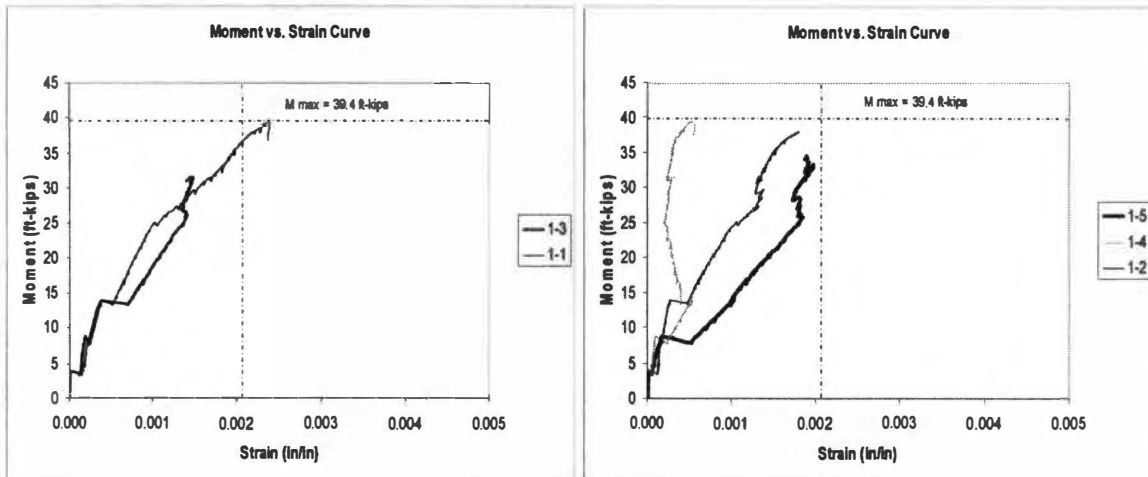
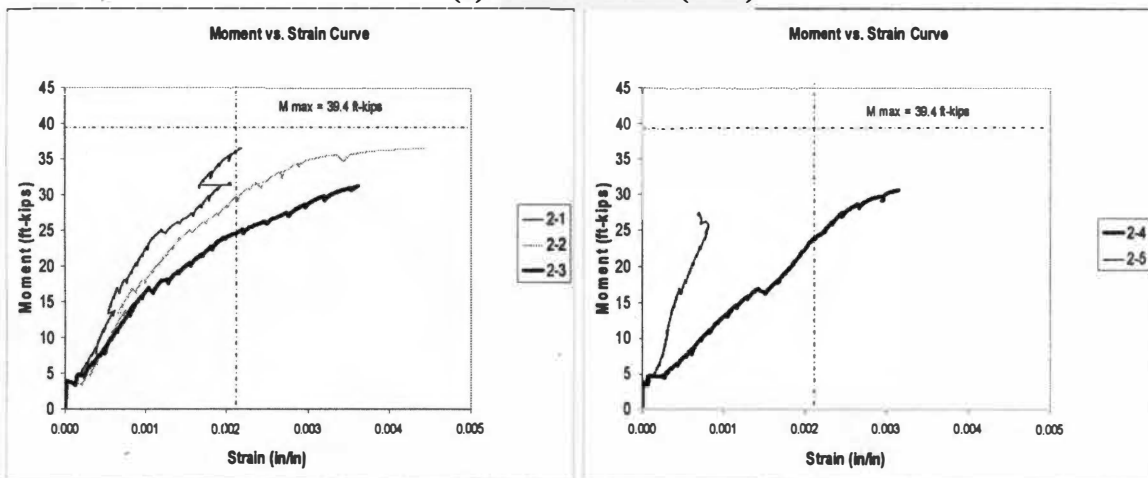


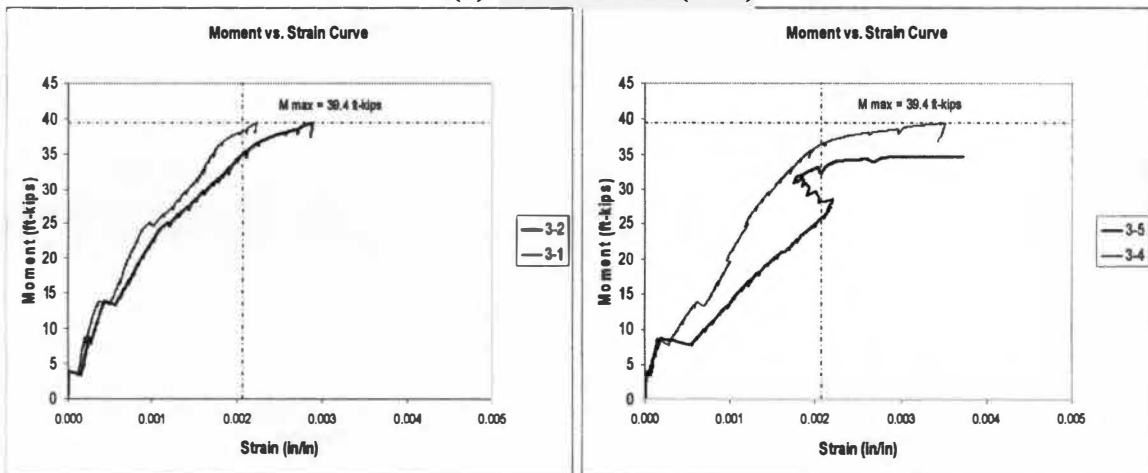
Figure 3-10: Plan View of Rebar location and Detail A of Specimen H-6-4.



(a) Headed Bar 1 (HB1)

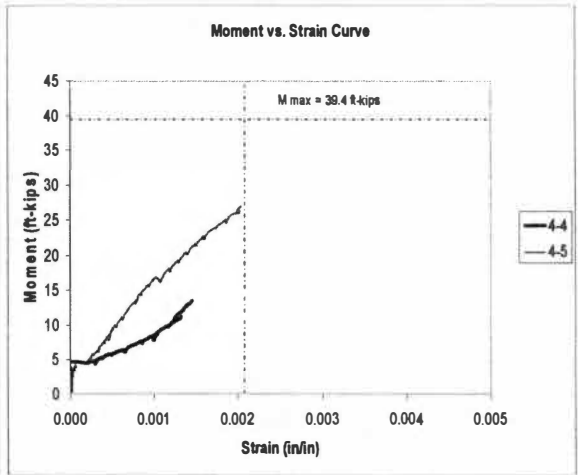
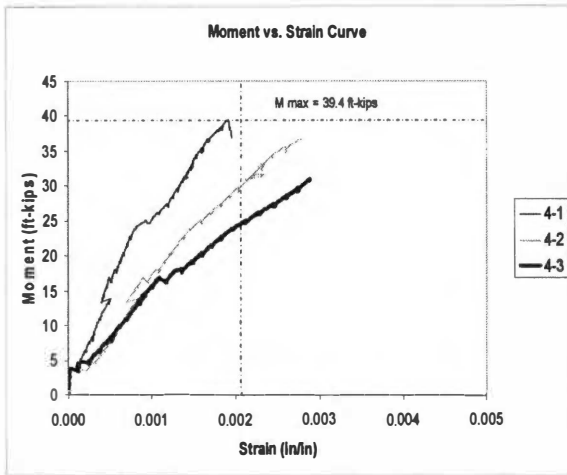


(b) Headed Bar 2 (HB2)

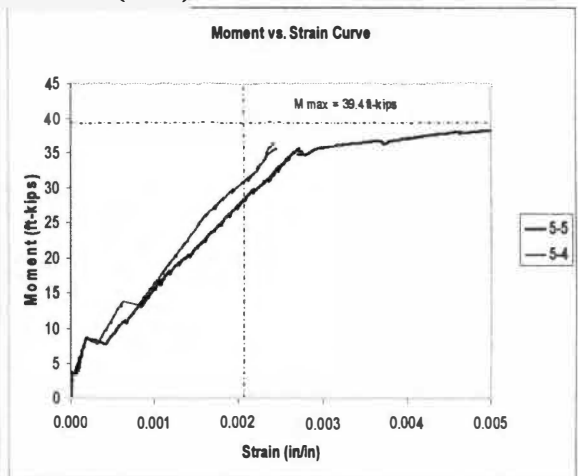
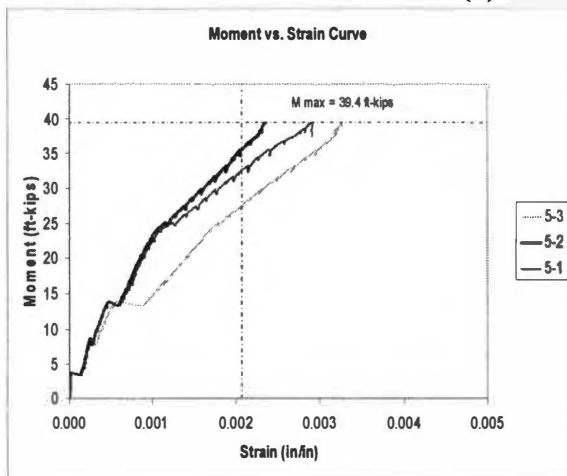


(c) Headed Bar 3 (HB3)

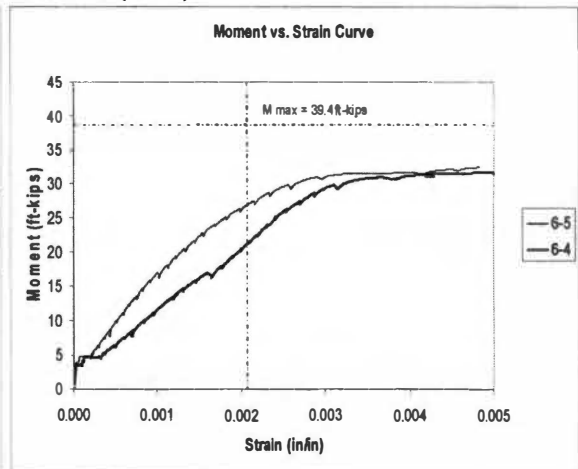
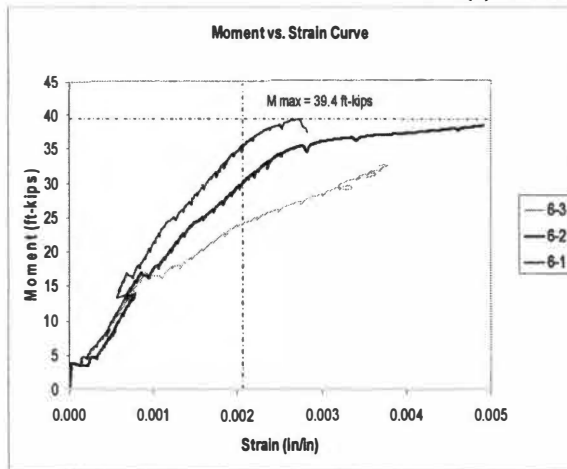
Figure 3-11: Moment vs. Strain Curves (Specimen H-6-4).



(d) Headed Bar 4 (HB4)

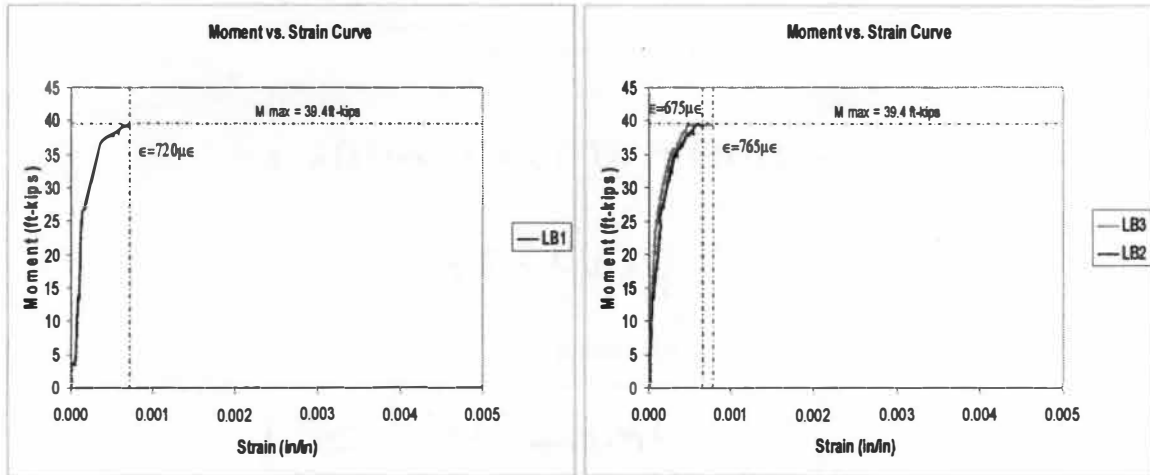


(e) Headed Bar 5 (HB5)



(f) Headed Bar 6 (HB6)

Figure 3-11. Continued.



(g) Longitudinal Bar (LB)
Figure 3-11. Continued.

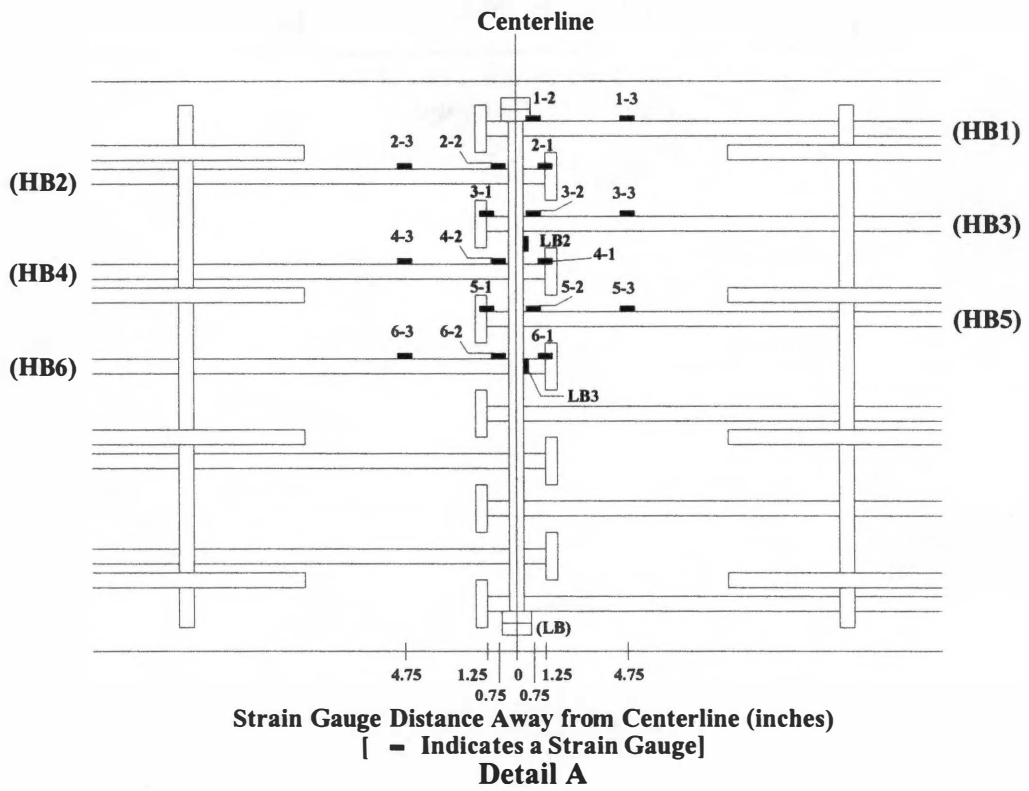
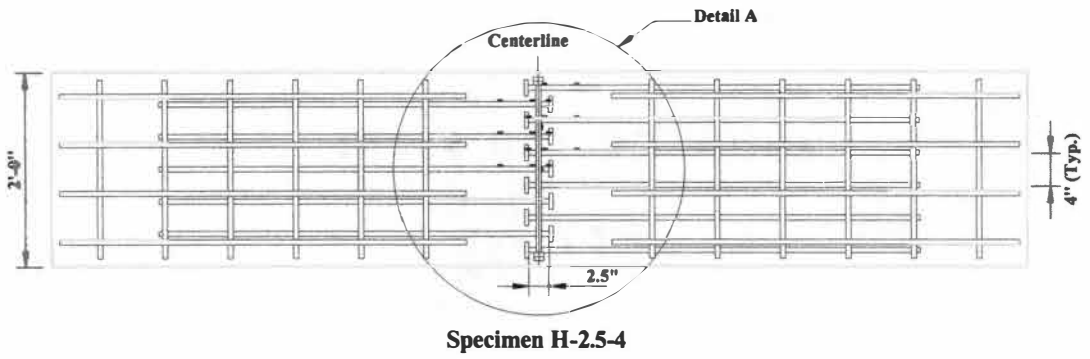
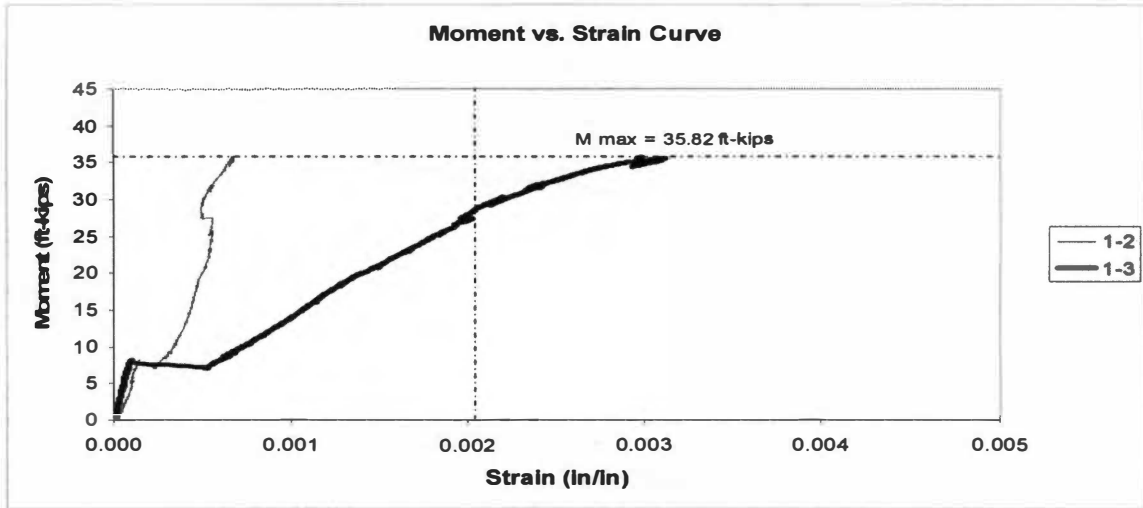
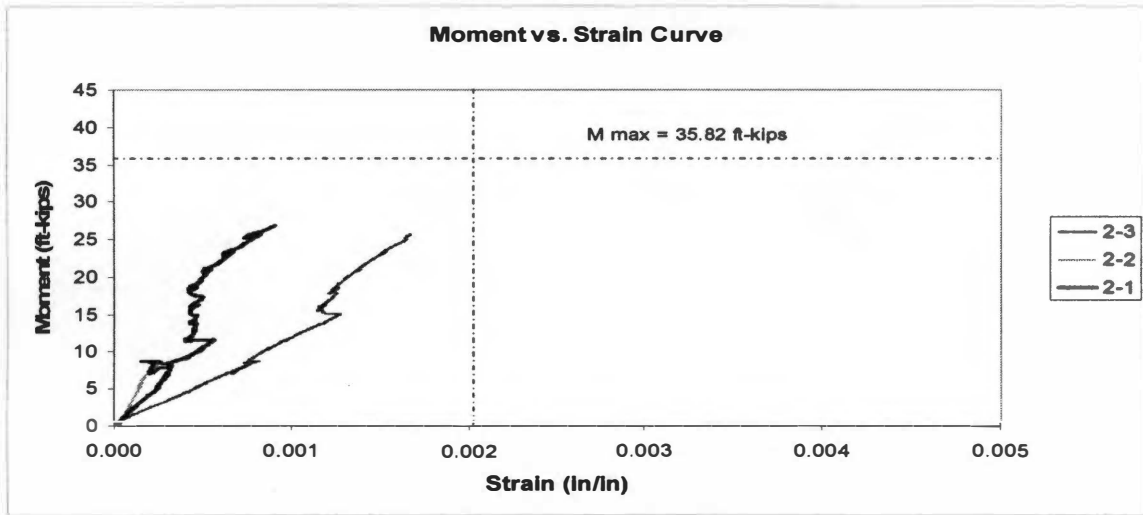


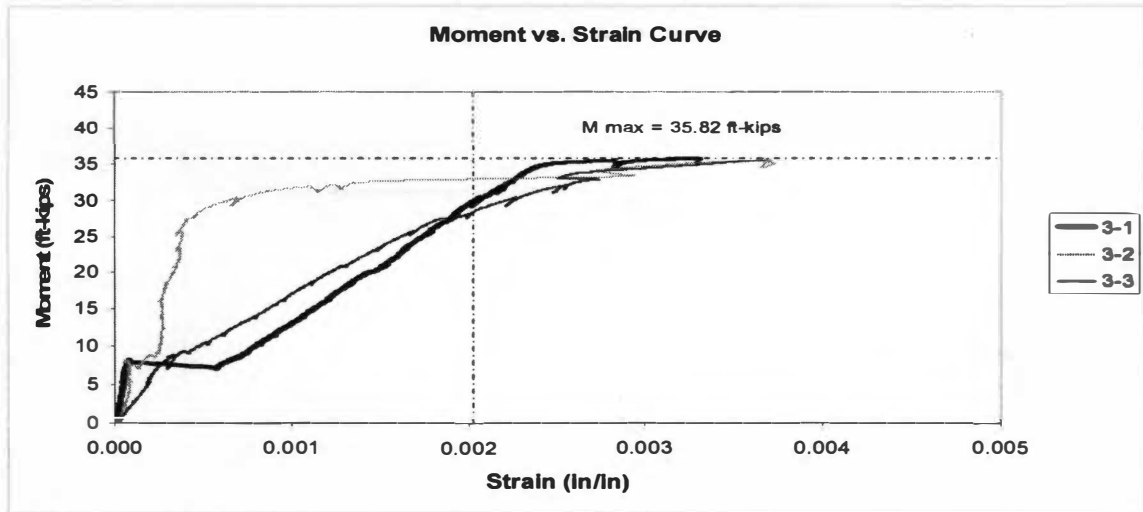
Figure 3-12: Plan View of Rebar location and Detail A of Specimen H-2.5-4.



(a) Headed Bar 1 (HB1)



(b) Headed Bar 2 (HB2)



(c) Headed Bar 3 (HB3)

Figure 3-13: Moment vs. Strain Curves (Specimen H-2.5-4).

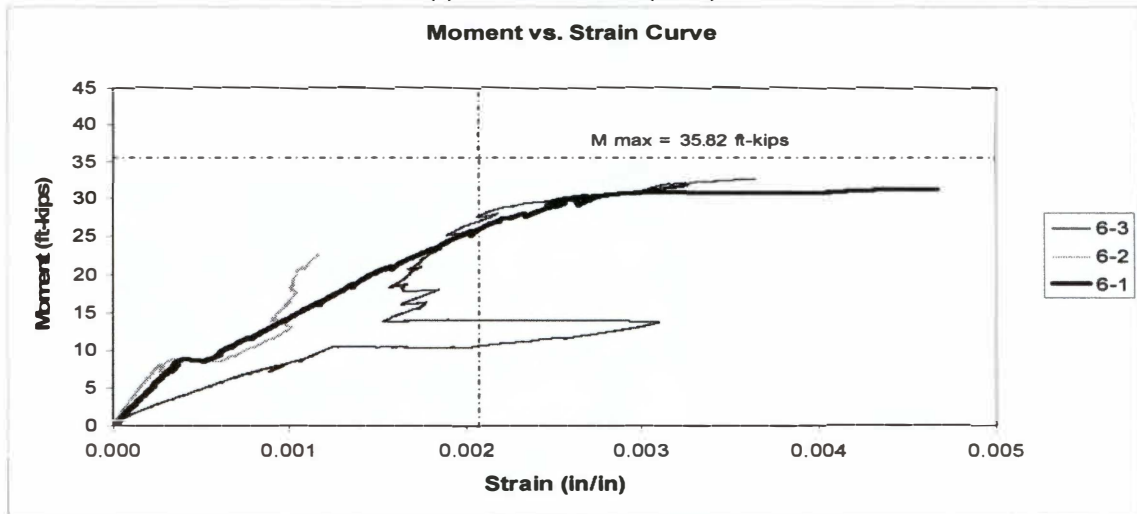
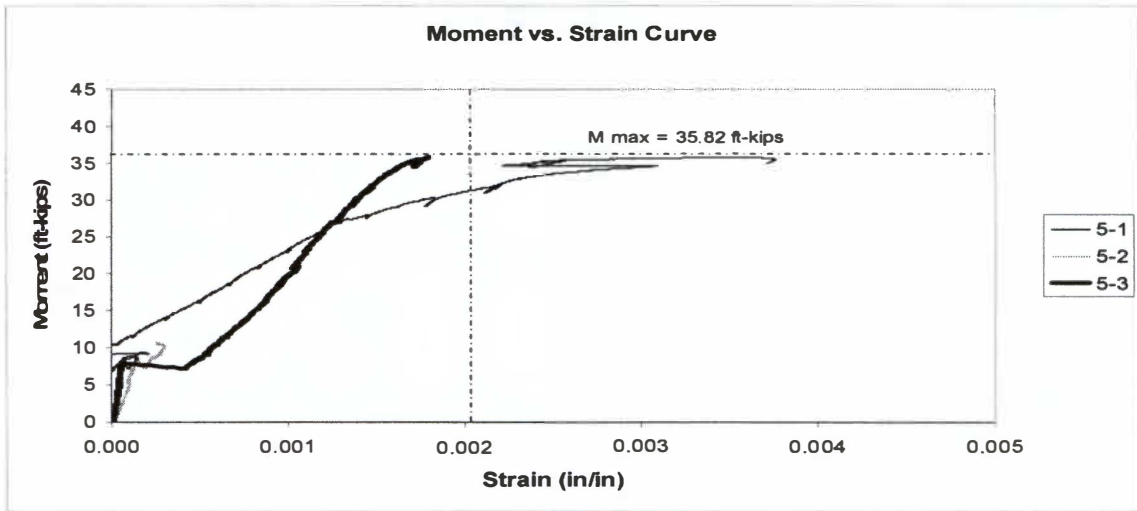
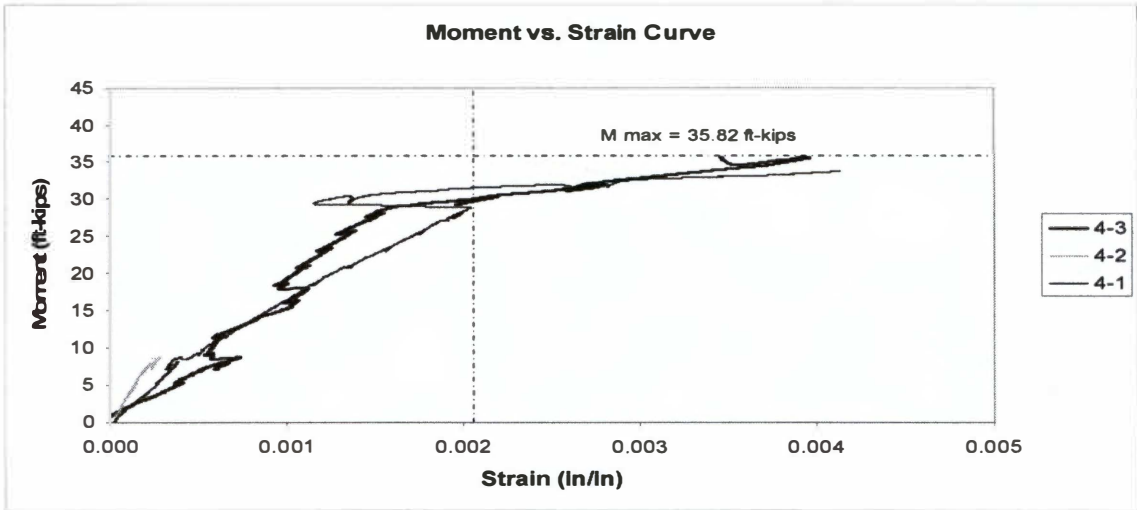
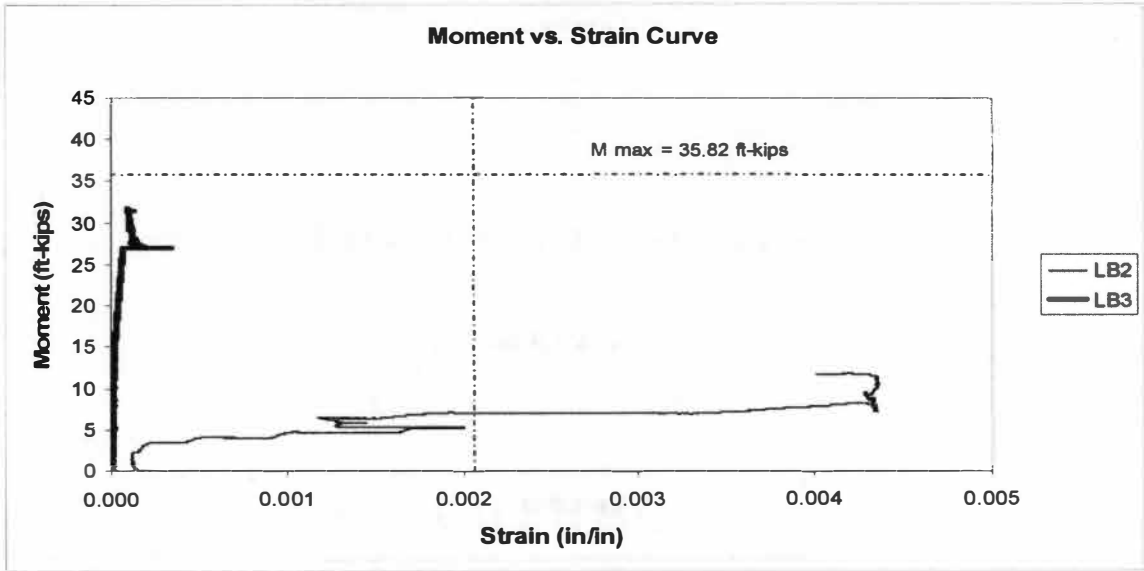


Figure 3-13. Continued.



(g) Longitudinal Bar 1 (LB1)
Figure 3-13. Continued.

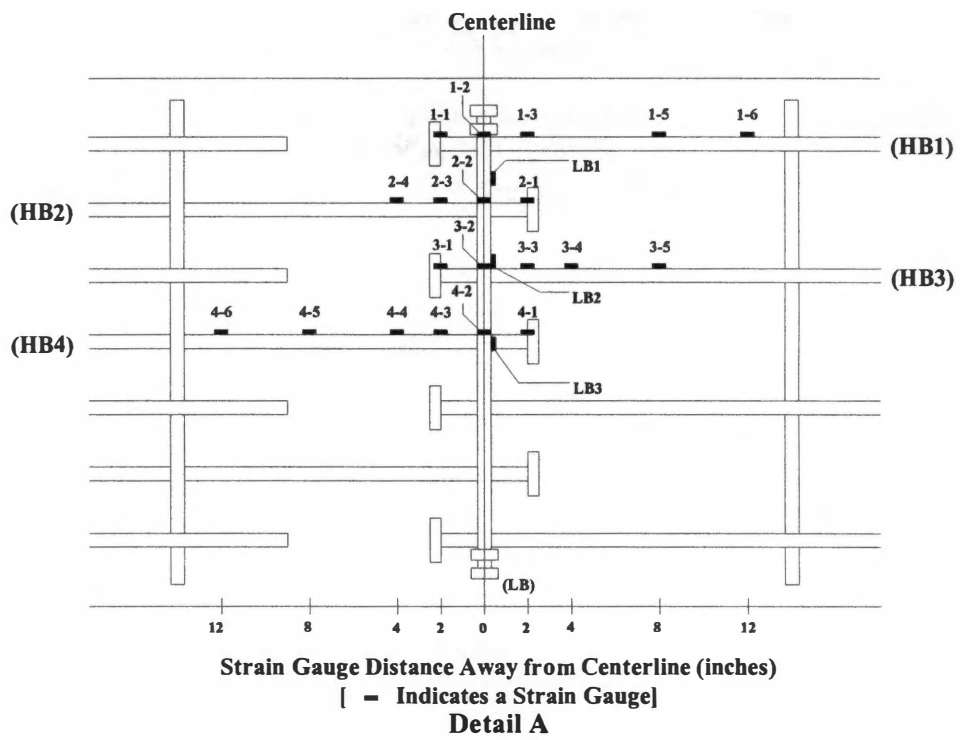
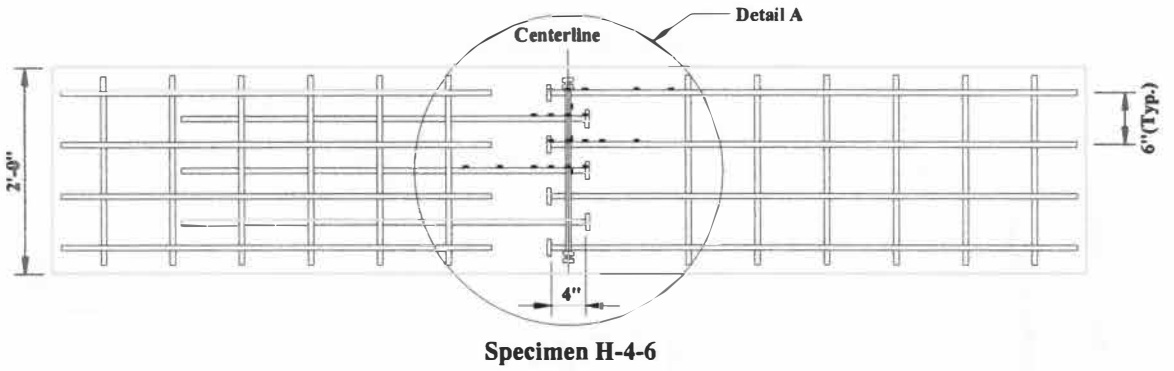
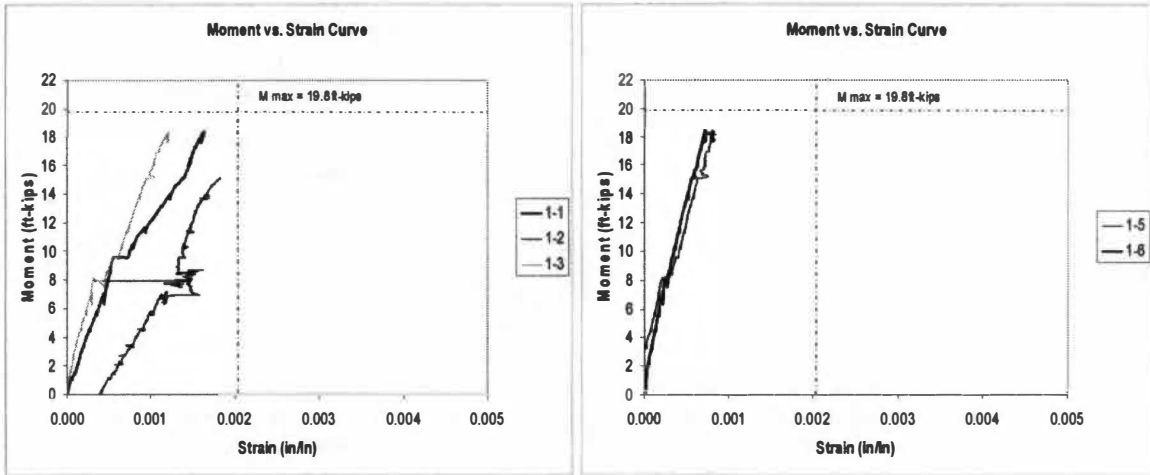
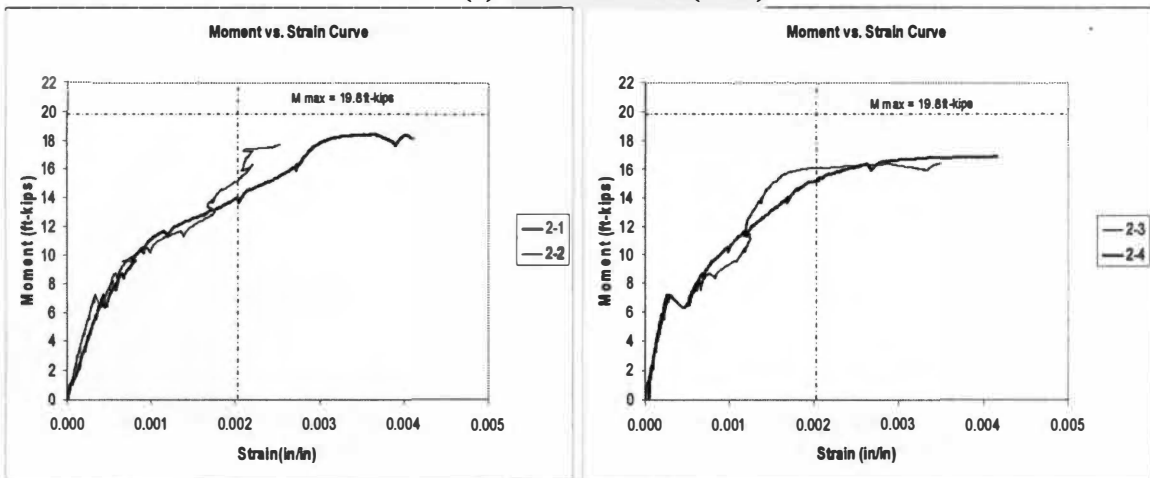


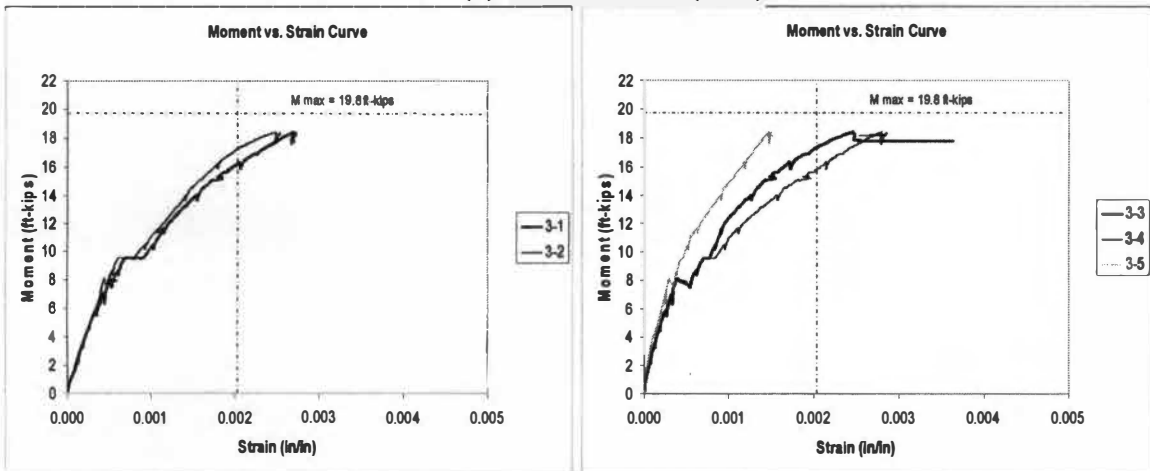
Figure 3-14: Plan View of Rebar location and Detail A of Specimen H-4-6



(a) Headed Bar 1 (HB1)

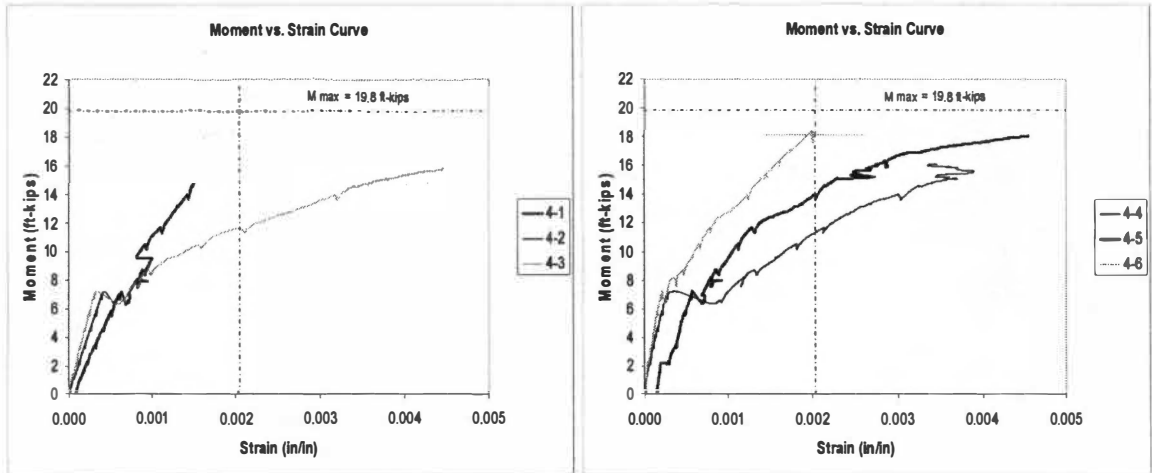


(b) Headed Bar 2 (HB2)

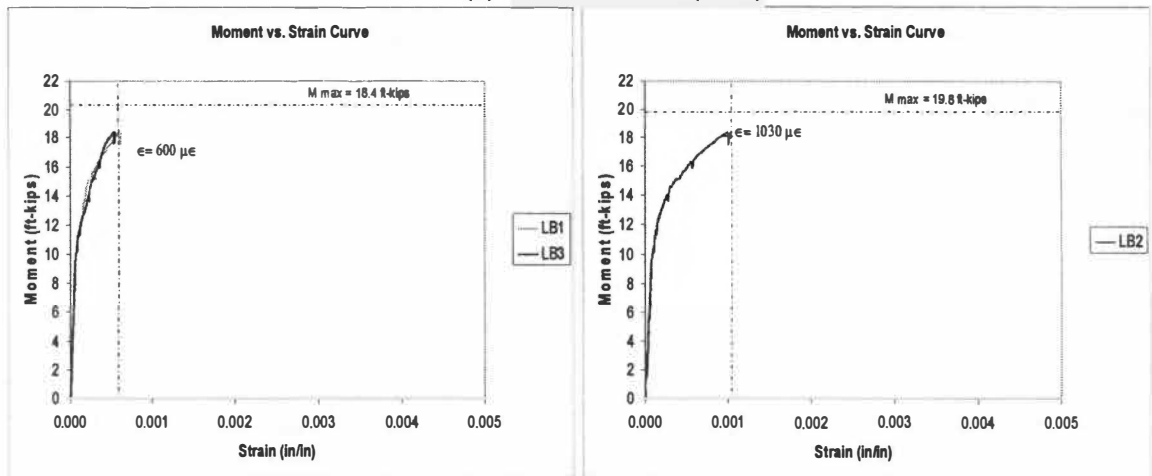


(c) Headed Bar 3 (HB3)

Figure 3-15: Moment vs. Strain Curves (Specimen H-4-6).

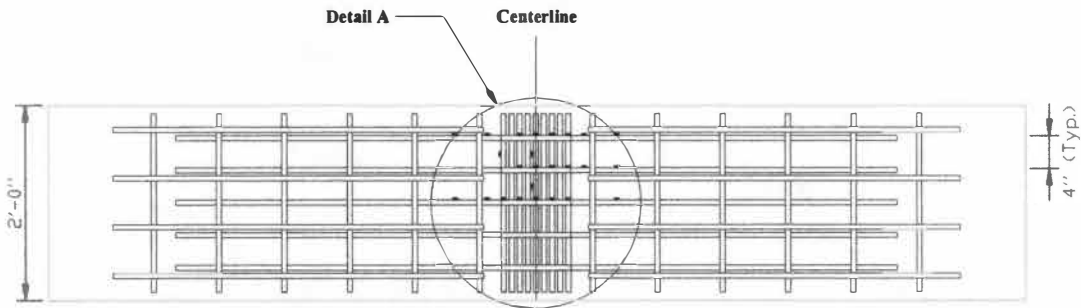


(d) Headed Bar 4 (HB4)

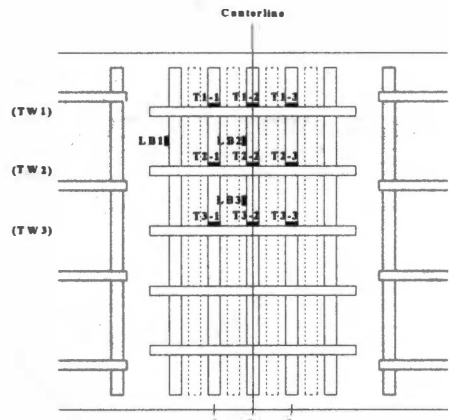


(e) Longitudinal Bar (LB)

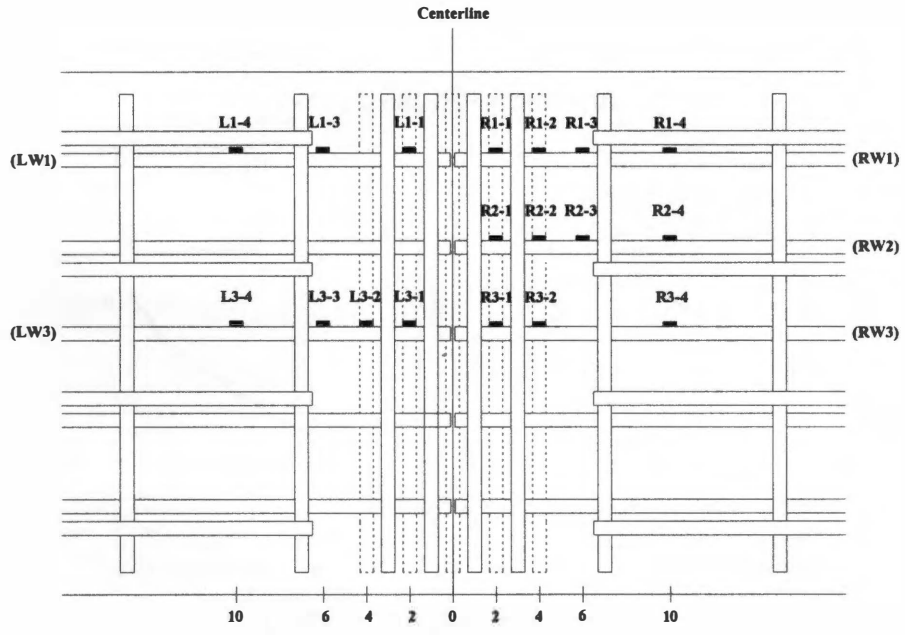
Figure 3-15. Continued.



Specimen W-4-4



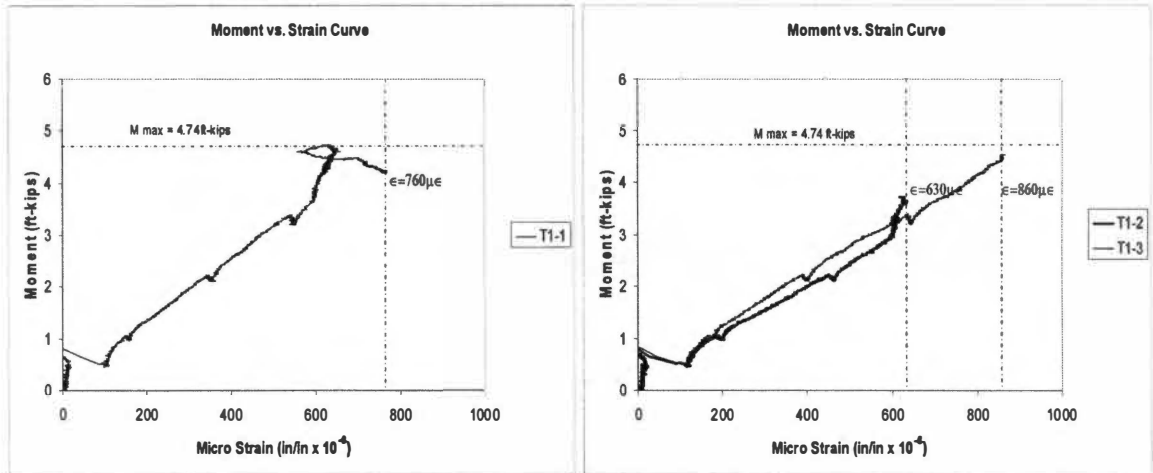
Strain Gauge Distance Away from Centerline (Inches)
 [= Indicates a Strain Gauge]
Detail A: Top WWR (TW)



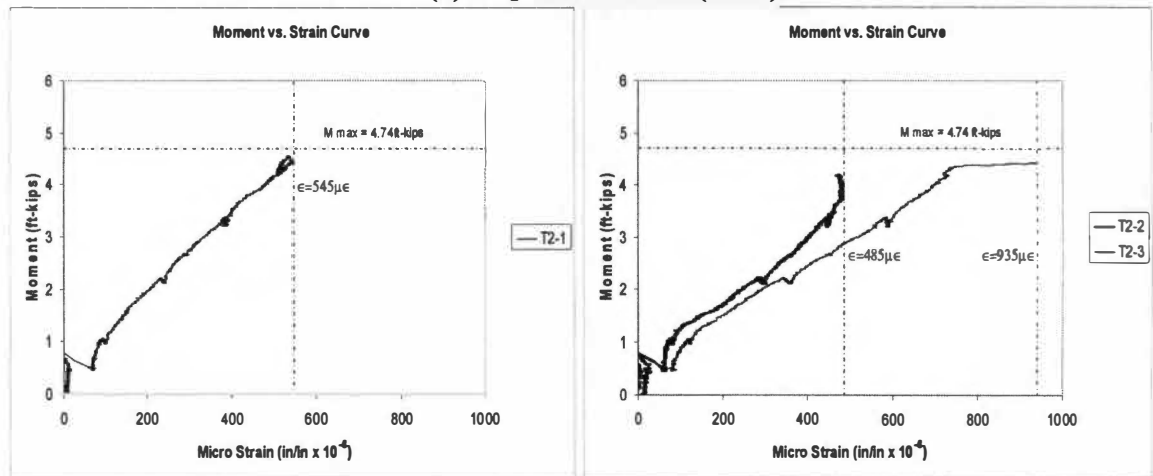
Strain Gauge Distance Away from Centerline (Inches)
 [= Indicates a Strain Gauge]

Detail A: Left WWR (LW) and Right WWR (RW)

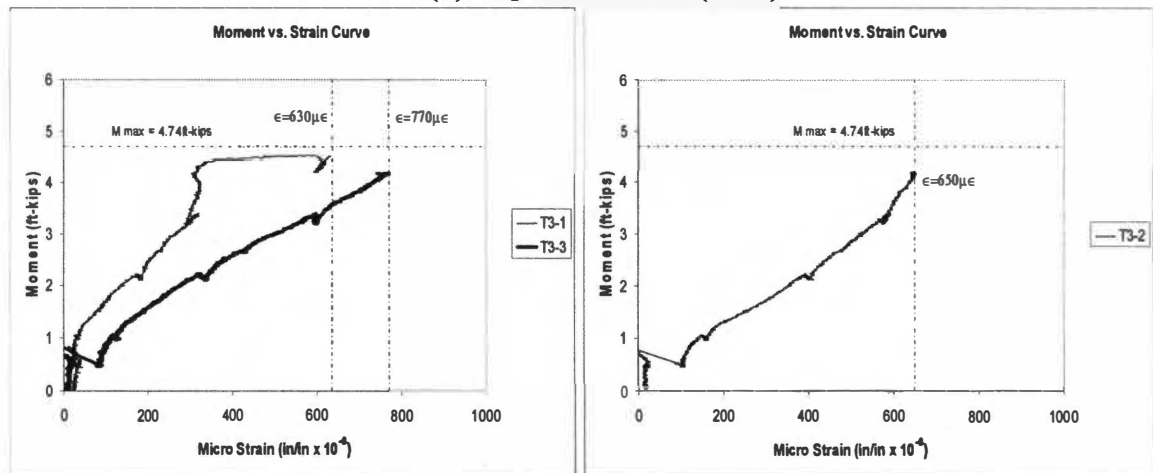
Figure 3-16: Plan View of Rebar location and Detail A of Specimen W-4-4.



(a) Top WWR Bar 1 (TW1)

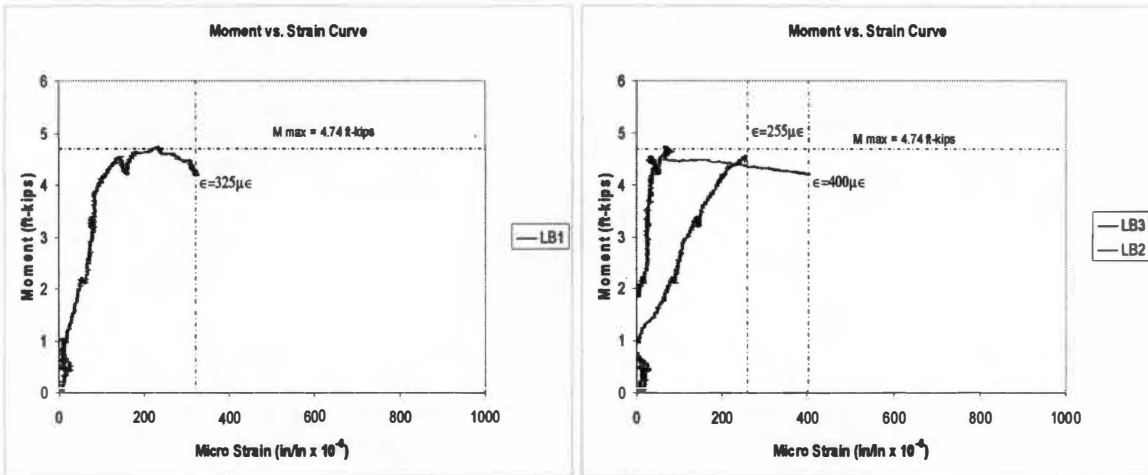


(b) Top WWR Bar 2 (TW2)

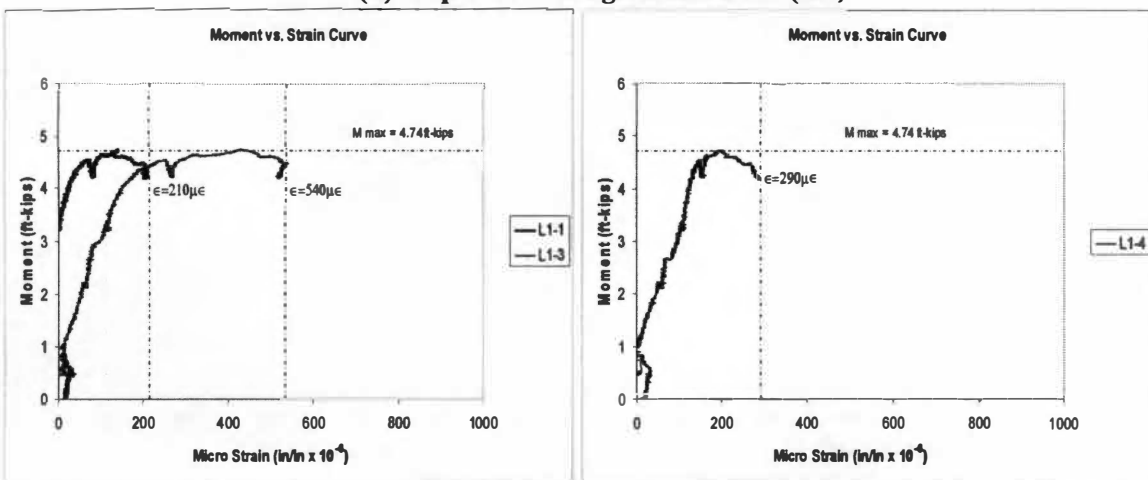


(c) Top WWR Bar 3 (TW3)

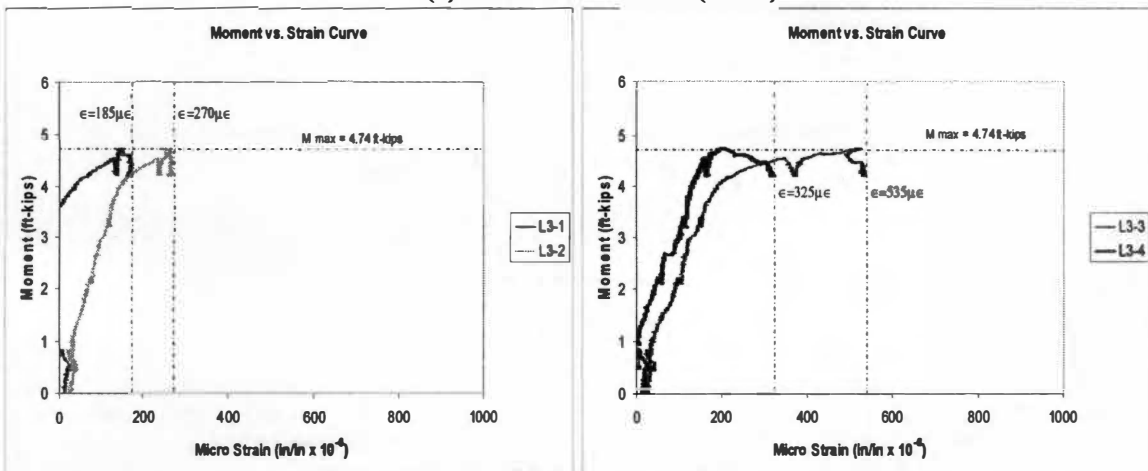
Figure 3-17: Moment vs. Strain Curves (Specimen W-4-4).



(d) Top WWR Longitudinal Bars (LB)

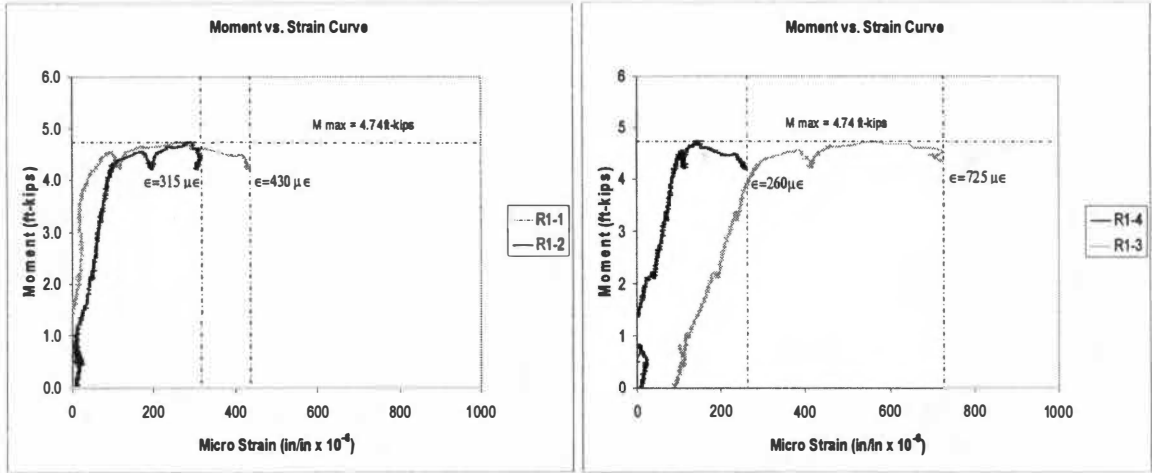


(e) Left WWR Bar 1 (LW1)

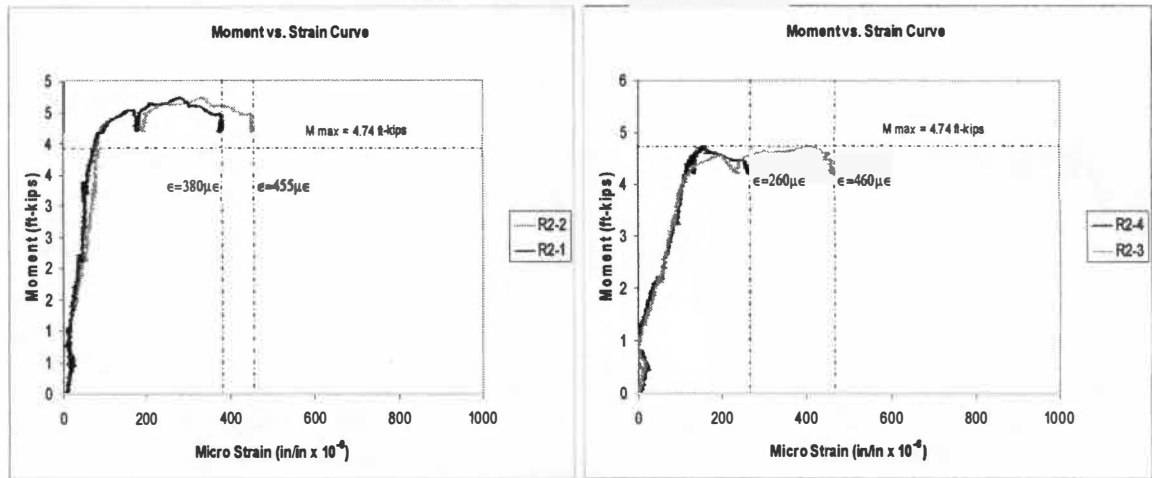


(f) Left WWR Bar 3 (LW3)

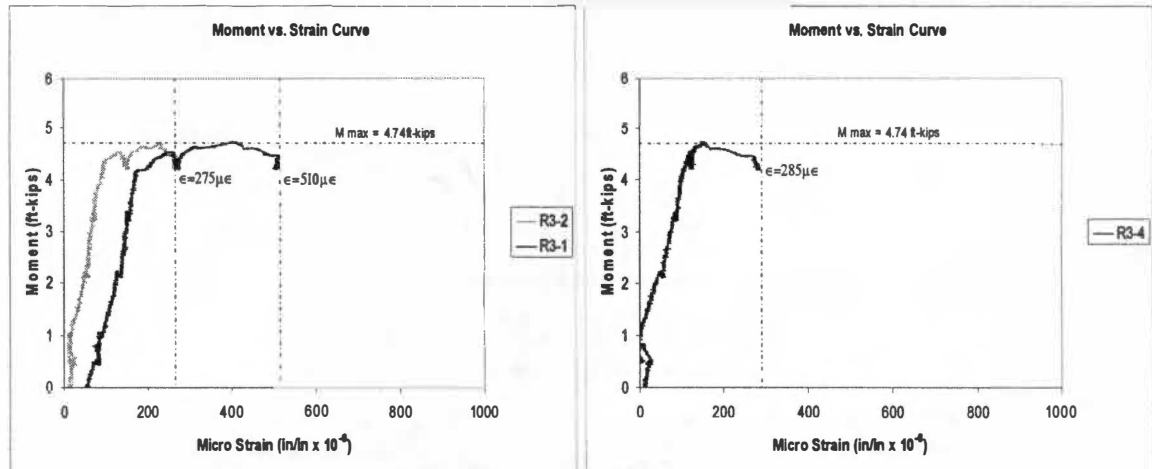
Figure 3-17. Continued.



(g) Right WWR Bar 1 (RW1)

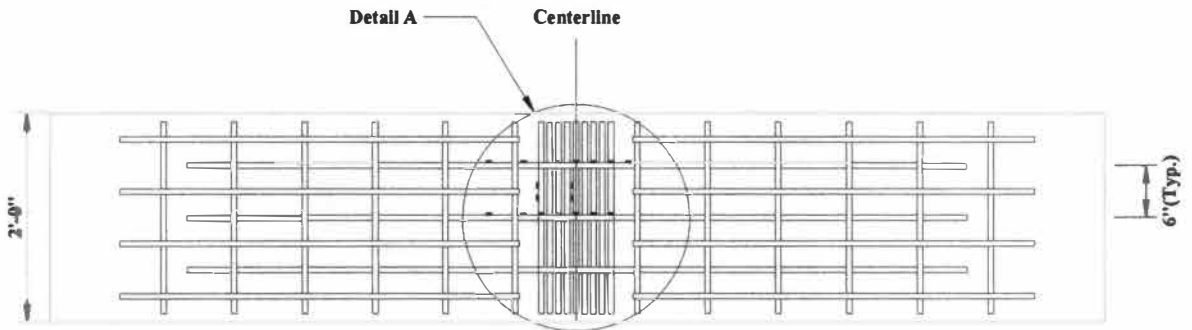


(h) Right WWR Bar 2 (RW2)

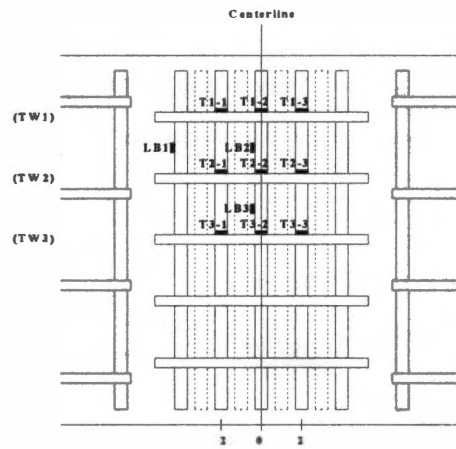


(i) Right WWR Bar 3 (RW3)

Figure 3-17. Continued.



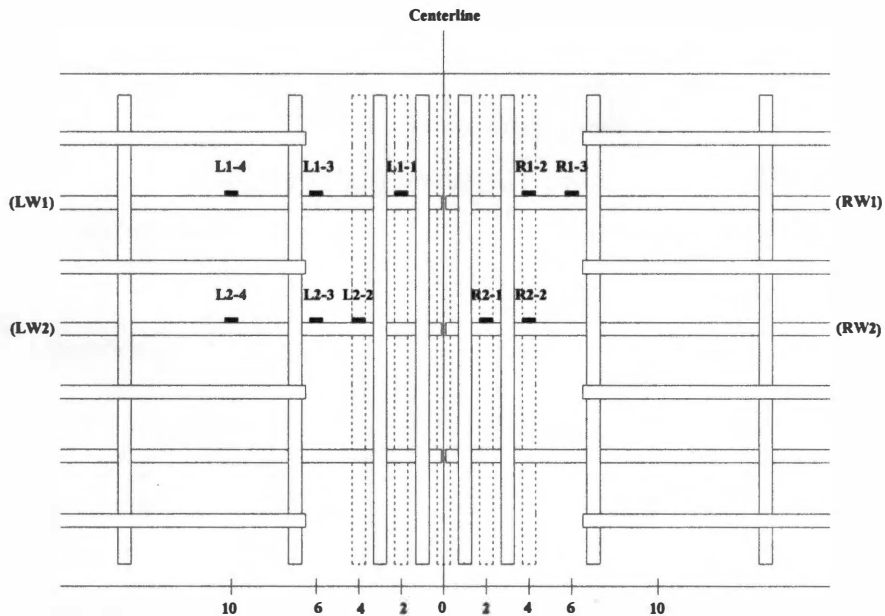
Specimen W-4-6



Strain Gauge Distance Away from Centerline (Inches)

— Indicates a Strain Gauge

Detail A: Top WWR (TW)

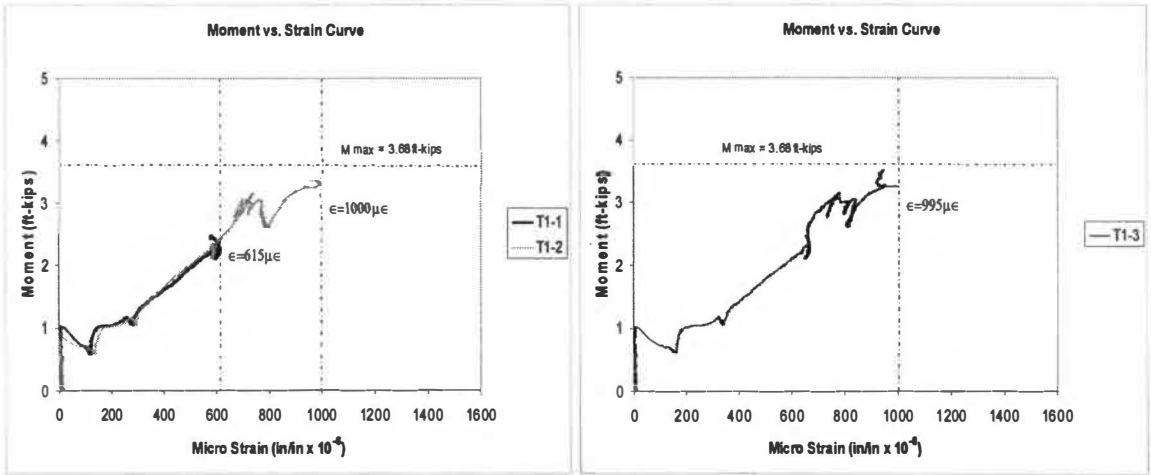


Strain Gauge Distance Away from Centerline (Inches)

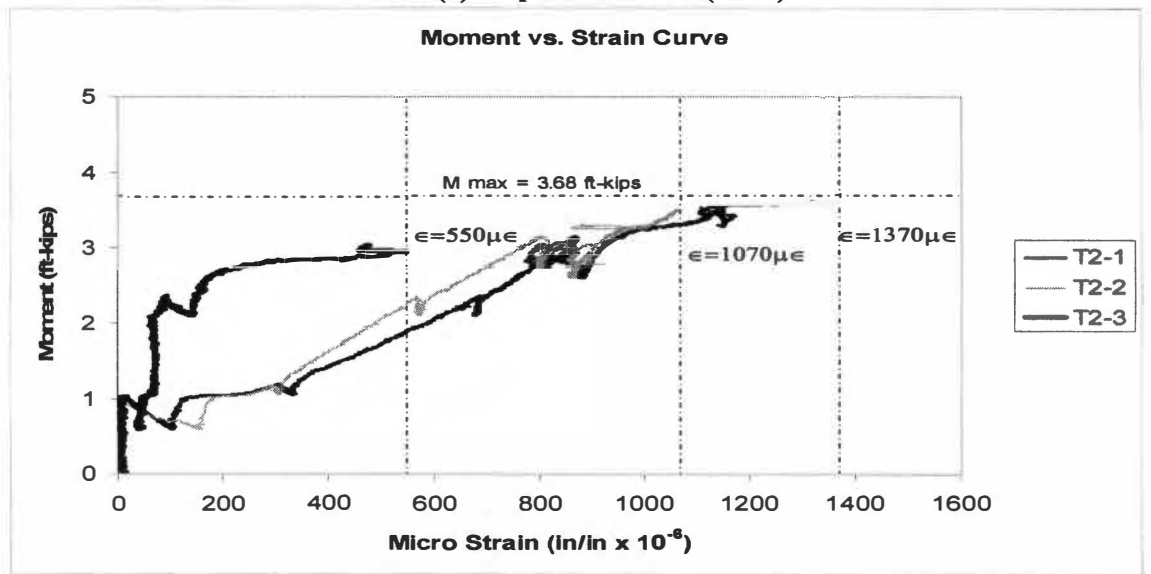
— Indicates a Strain Gauge

Detail A: Left WWR (LW) and Right WWR (RW)

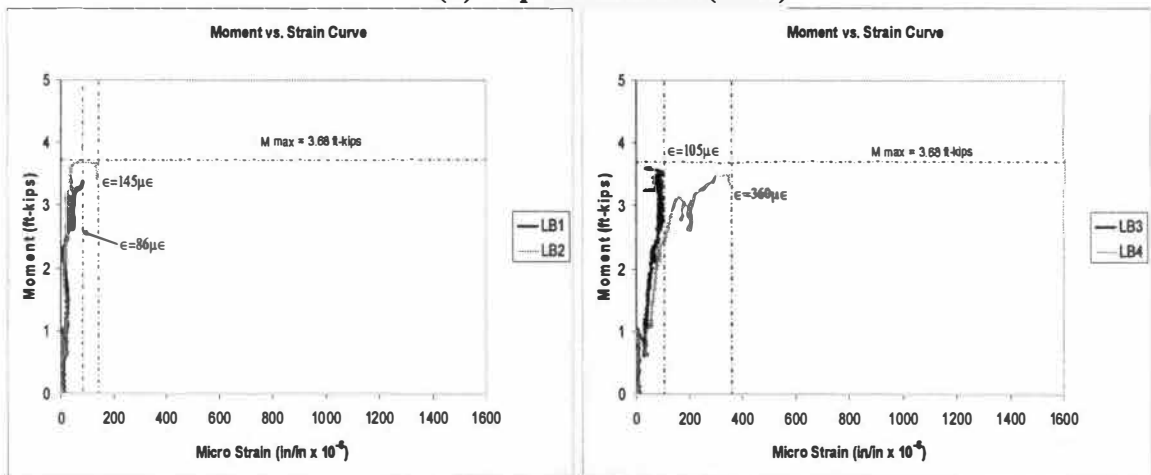
Figure 3-18: Plan View of Rebar Location and Detail A of Specimen W-4-6.



(a) Top WWR Bar 1 (TW1)

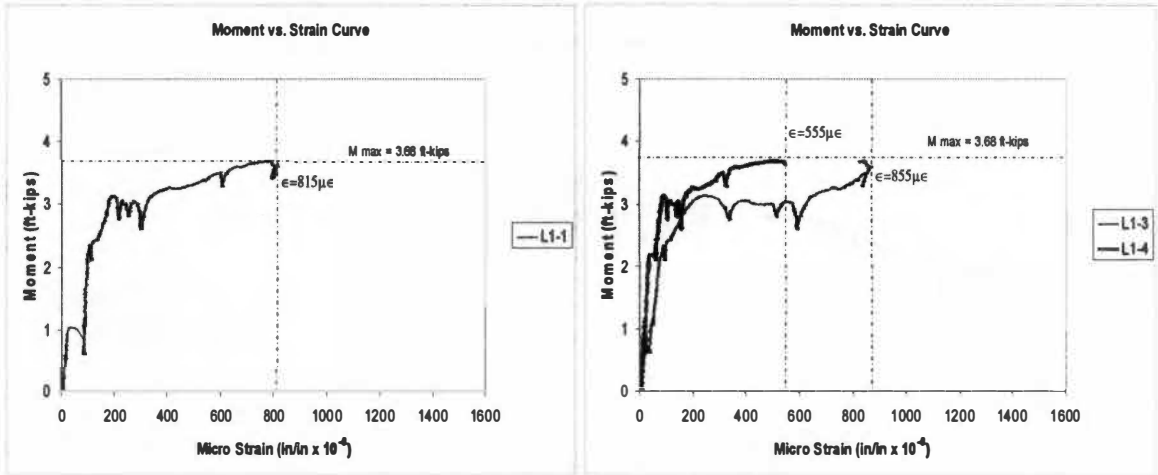


(b) Top WWR Bar 2 (TW2)

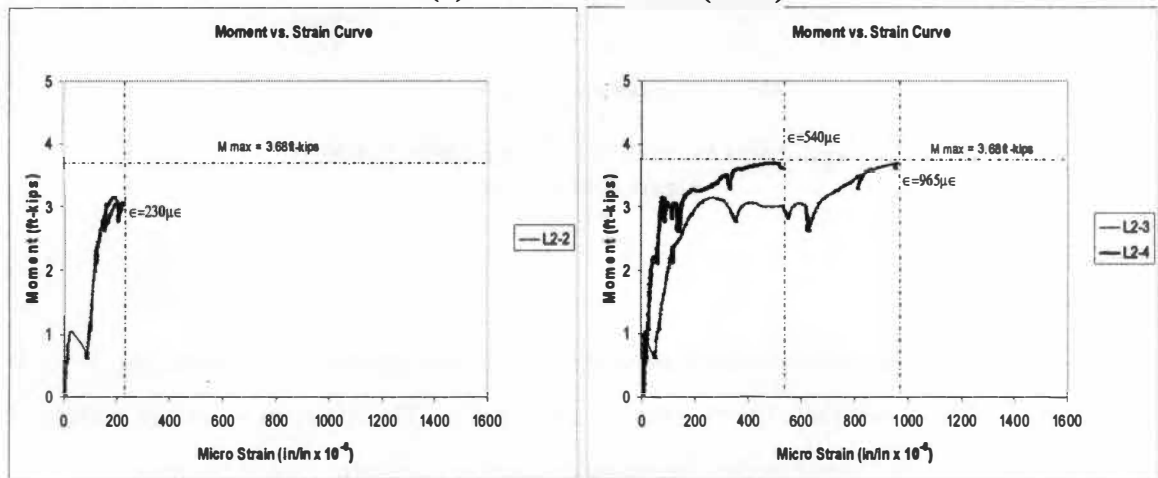


(c) Top WWR Longitudinal Bars (LB)

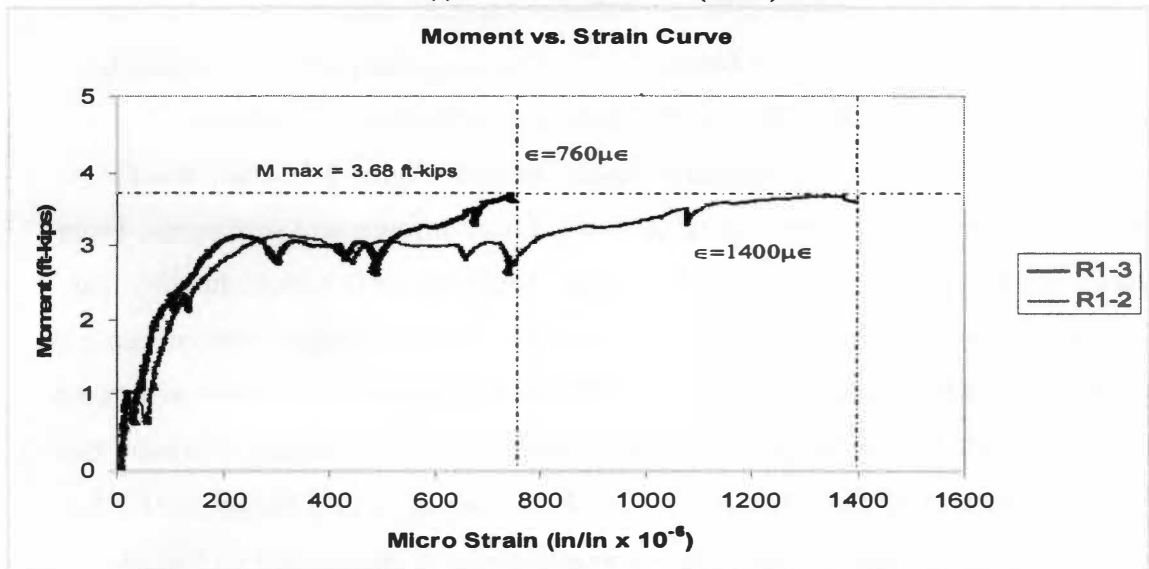
Figure 3-19: Moment vs. Strain Diagrams (Specimen W-4-6).



(d) Left WWR Bar 1 (LW1)

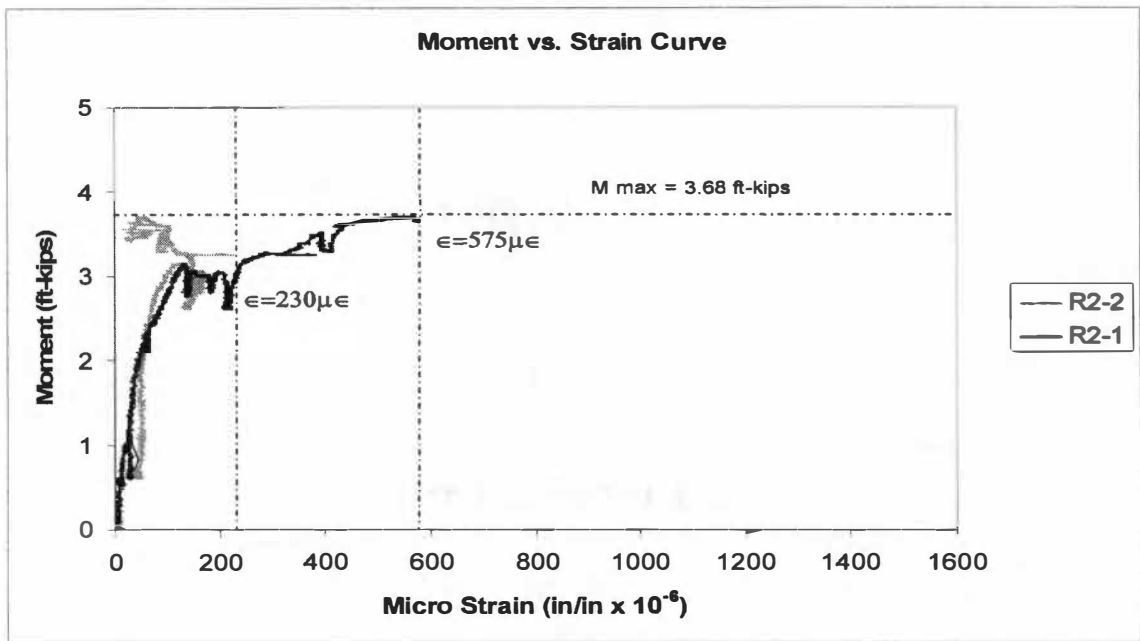


(e) Left WWR Bar 2 (LW2)



(f) Right WWR Bar 1 (RW1)

Figure 3-19. Continued.



(g) Right Welded Wire Fabric Bar 2 (RW2)
Figure 3-19. Continued.

Moment-Curvature

The extension and compression readings, shown in Figure 3-2, recorded the length change used to calculate the curvature of the beam. The moment versus curvature was then plotted for each specimen. The notation used to describe each specimen is defined in Table 3-1. Response 2000 is a software program used to predict the behavior of reinforced concrete structures (Bentz, 2000). This computer program was used to predict the moment curvature behavior of specimens with either 4 in. or 6 in. reinforcement spacing and a particular concrete strength. Figure 3-20 compares the moment curvature response for each of the headed bar reinforcement specimens. From Figure 3-20, it can be concluded that the 6 in. lap length provides a more ductility than the 2.5 in. or 4 in. lap length. Also, the 4 in. spacing provides a higher moment capacity than the 6 in. reinforcement because the smaller spacing provides more steel in the cross section. For example, Specimen H-6-4 had a moment capacity that was 50% more than the moment capacity of Specimen H-6-6. For the 2.5 in. lap length, Specimen H-2.5-4 had a maximum moment 2.25 times the moment capacity of Specimen H-2.5-6. A

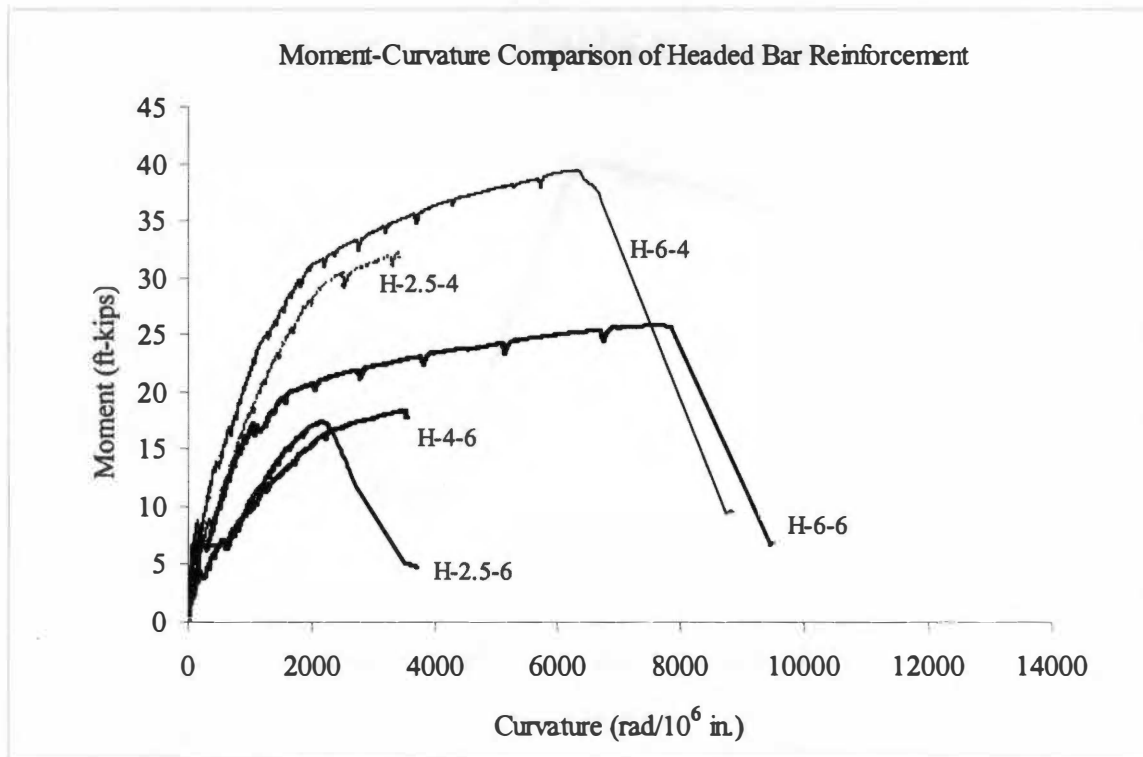


Figure 3-20: Moment vs. Curvature Diagrams for Headed Bar Specimens

difference in the moment capacity with respect to the lap length can also be detected. The 6 in. lap length provides more moment capacity than the 2.5 in. or 4 in. lap length.

Figure 3-21 compares the moment curvature response for the 4 in. spacing of headed reinforcement. The plot includes the predicted moment curvature for a 4 in. spacing using Response 2000 software. Specimen H-6-4, which has a 6 in. lap length and 4 in. spacing, had a larger moment capacity than Specimen H-2.5-4 and the predicted Response 2000. The largest moment of Specimen H-6-4 was 39.4 ft-kips when the curvature was 6,320 rad/(10⁶ in). The maximum curvature of Specimen H-6-4 was 8,850 rad/(10⁶ in). When comparing the behavior of Response 2000 for a continuously reinforced beam with Specimen H-6-4, the moment capacity for Specimen H-6-4 was almost 25% more than the moment capacity predicted by Response 2000, and the ductility of Specimen H-6-4 was over 90% larger than the ductility of Response 2000. Specimen H-2.5-4 failed suddenly due to the 2.5 in. lap length which can be recognized by the abrupt stop in the moment curvature. Specimen H-2.5-4 had a moment

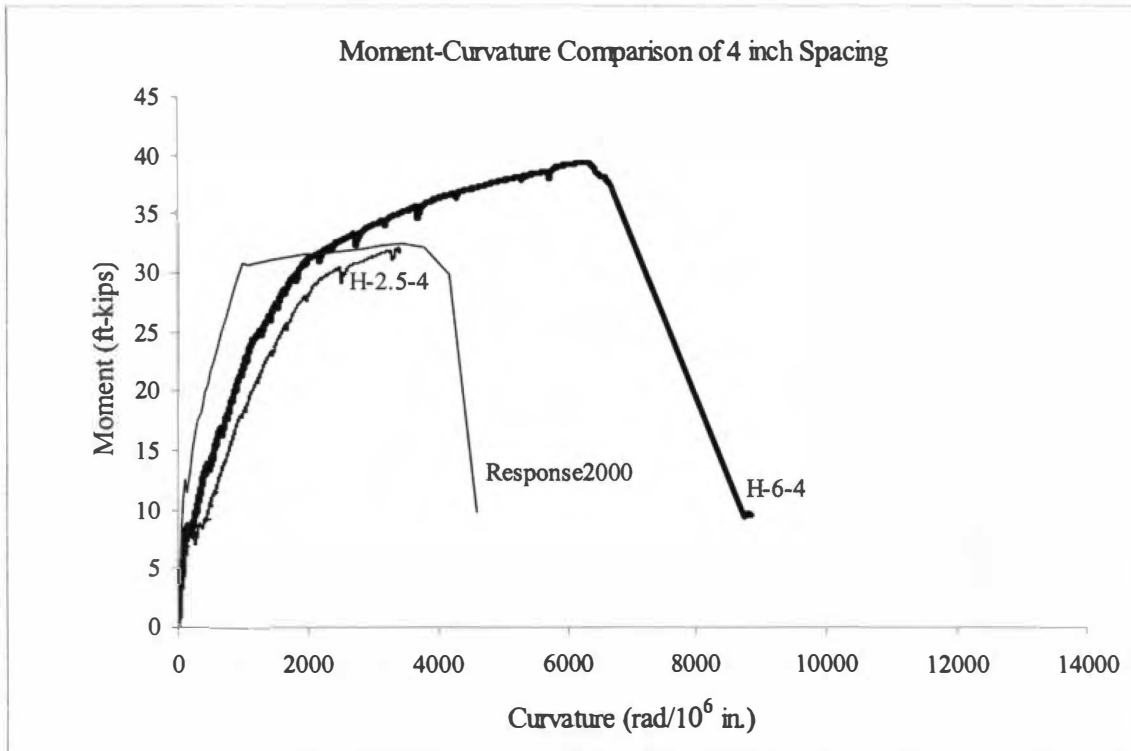


Figure 3-21: Moment vs. Curvature Diagrams for 4 in. Spacing

capacity of 25.83 ft-kips which was very similar to the projected moment capacity of Response 2000.

Figure 3-22 and 3-23 compare the moment curvature response for the 6 in. spaced specimens with 6 in. spacing and the predicted curve from Response 2000. The specimen results were split into two graphs due to the different concrete cylinder strength. Figure 3-22 plots the behavior of the Control Specimen and Specimen H-6-6 which had a concrete strength of approximately 10,000 psi. Both the Control Specimen and Specimen H-6-6 had a higher moment capacity and higher ductility than the projected Response 2000 curve. Specimen H-6-6 experienced a maximum moment of 25.83 ft-kips when the curvature was 7,660 rad/(10⁶ in), and the maximum curvature of Specimen H-6-6 was 9,490 rad/(10⁶in). The Control Specimen was more ductile than Specimen H-6-6 with a maximum curvature of 12,930 rad/(10⁶in). The Control Specimen had a maximum curvature 68% larger than the maximum curvature for Specimen H-6-6. The maximum moment of the Control Specimen was 25.19 ft-kips which was similar to the 25.83 ft-kips moment capacity of Specimen H-6-6.

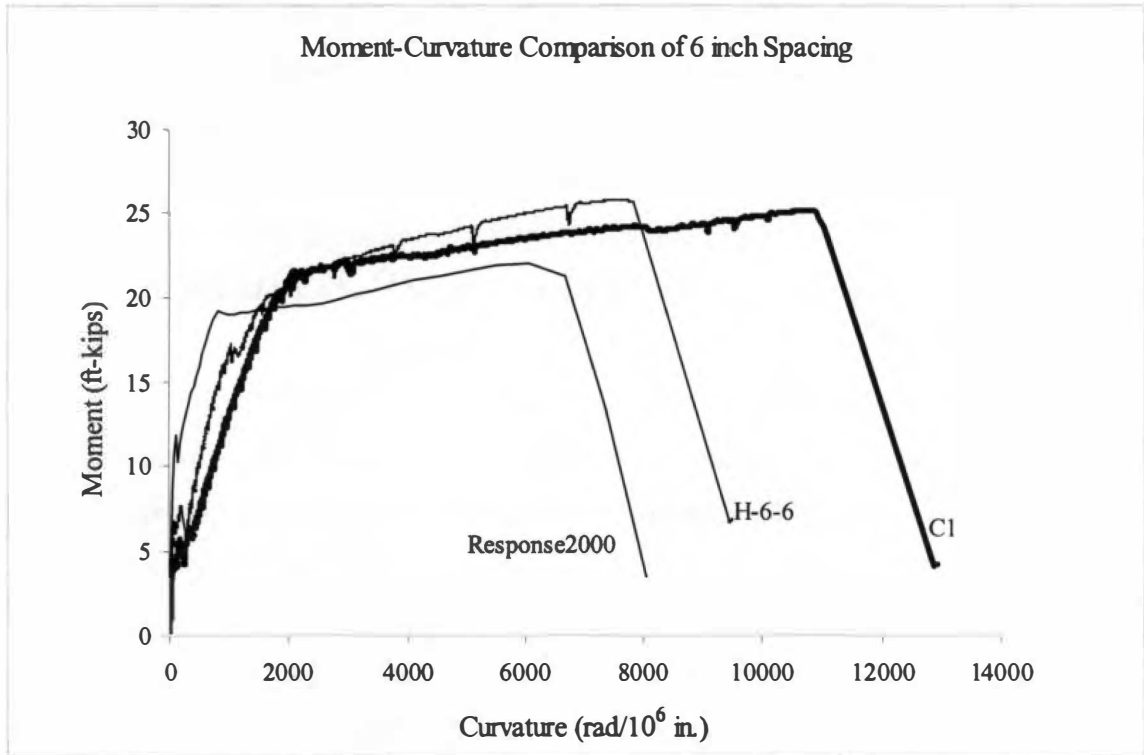


Figure 3-22: Moment vs. Curvature Diagrams for 6 in. Spacing and $f'_c=10,000$ psi

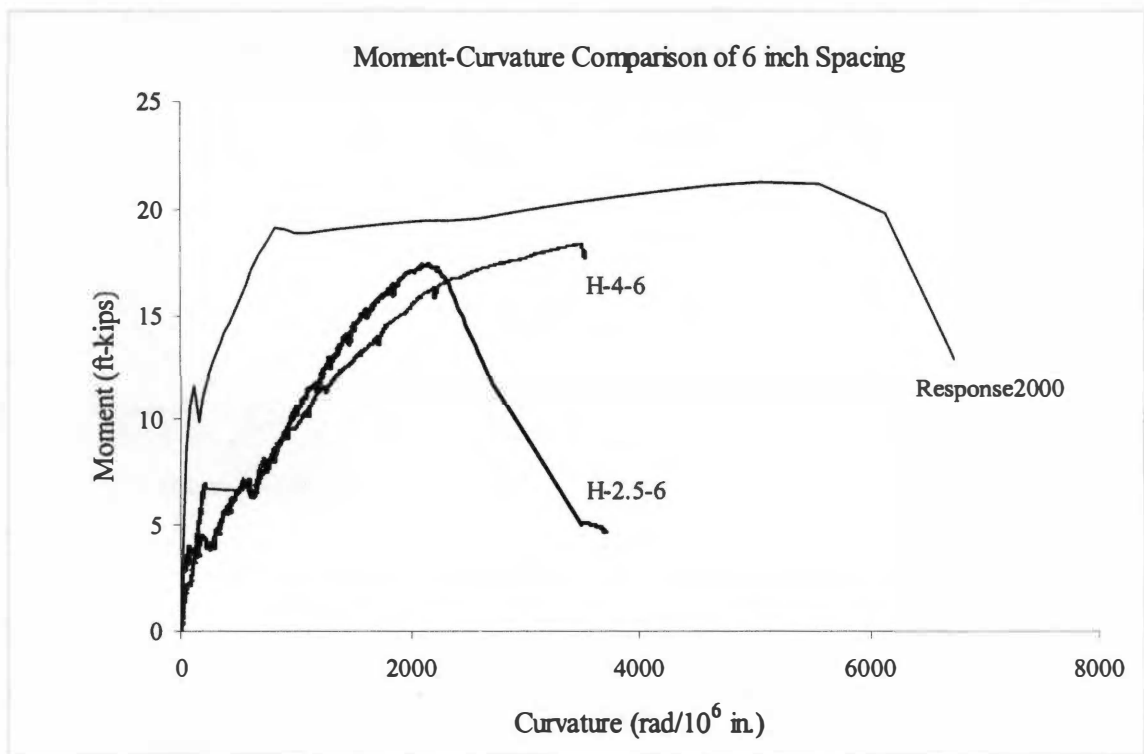


Figure 3-23: Moment vs. Curvature Diagrams for 6 in. Spacing and $f'_c=8,300$ psi

Figure 3-23 charts the moment versus curvature of the specimens with 6 in. and a concrete cylinder strength of approximately 8,300 psi. The 17.4 ft-kips maximum moment capacity of Specimen H-2.5-6 was smaller than the maximum moment of Response 2000. Specimen H-2.5-6 did not have a ductile failure with a maximum curvature of 3,715 rad/(10⁶in). Specimen H-4-6 had a maximum moment of 19.8 ft-kips. As seen by the abrupt stop in the moment curvature curve of Specimen H-4-6, the specimen failed suddenly.

Figure 3-24 shows the moment curvature behavior of the welded wire reinforcement specimens. A Response 2000 curve with a spacing of 4 in. corresponds to the Specimen WWR-4-4, and the Response 2000 curve with 6 in. spacing is comparative to the Specimen WWR-4-6. Neither specimens performed like the expected behavior of Response 2000 and failed prematurely. Specimen WWR-4-4 had a maximum moment of 4.74 ft-kips, and Specimen W-4-6 experienced a maximum moment of 3.68 ft-kips. Specimen W-4-6 had a slightly more ductile behavior than Specimen W-4-4.

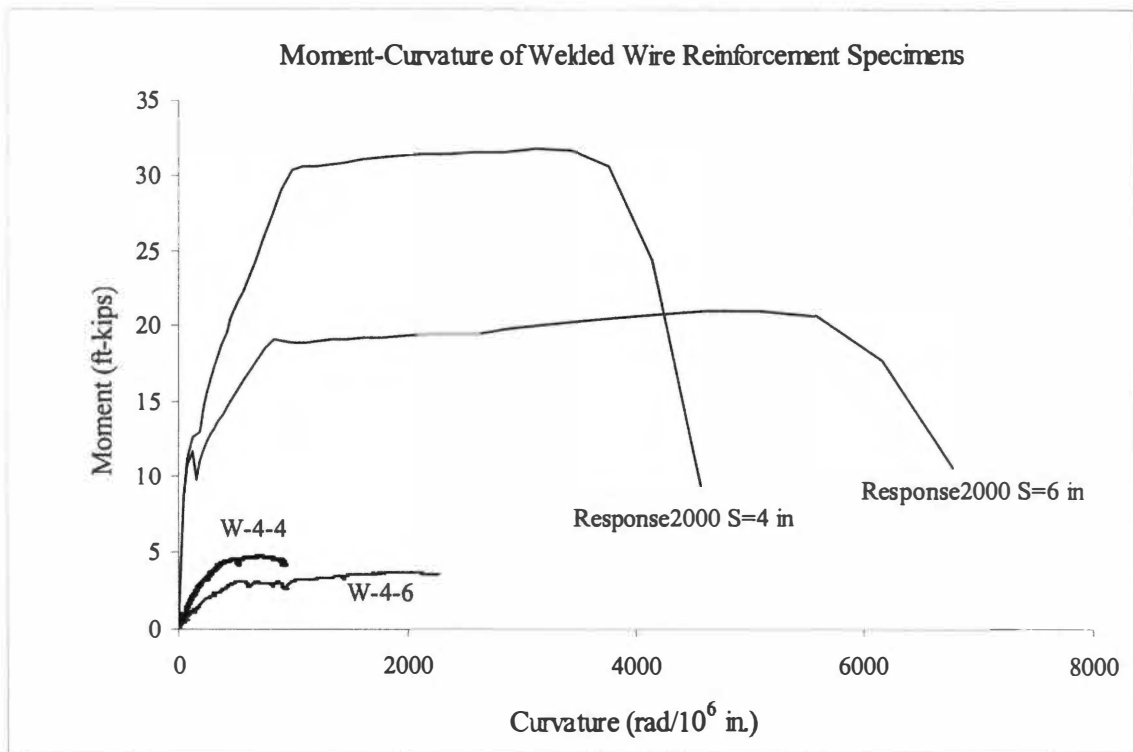


Figure 3-24: Moment vs. Curvature Diagrams for WWR Specimens

CHAPTER 4 Discussion of Results

Moment Capacity

Specimen H-6-6 had a moment capacity of 25.83 ft-kips which was very similar to the maximum moment held by the Control Specimen of 25.19 ft-kips. Specimen H-2.5-6 and Specimen H-4-6 had slightly lower moment capacities of 17.4 ft-kips and 19.8 ft-kips respectively, but the lack of ductility of the specimens is not desirable. The WWR Specimens did not have near the moment capacity of the other six specimens and failed suddenly. Two specimens' moment capacities were significantly more than the Control Specimen. Specimen H-2.5-4 had a maximum moment of 39.26 ft-kips, but the failure was sudden and brittle. Specimen H-6-4 performed the best of all the specimens with a maximum moment of 39.4 ft-kips and a fairly ductile failure. From the inspection of the failure and moment capacity of the specimens, the recommended spacing and lap length under these conditions was the scenario of Specimen H-6-4 with a 6 in. lap length and a 4 in. spacing of headed bar reinforcement.

Strain Comparisons

The results from the strain gauge readings were plotted in a moment versus steel stress plot. The plot then includes the calculated moment versus steel stress for a continuously reinforced beam. For the 6 in. spacing, the cross sectional steel area used for the calculated moment versus steel stress was determined by four #5 bars, and for the 4 in. spacing, six #5 bars were used as the steel area. The solid line for the calculated moment versus steel stress is for the linear relationship between the concrete strength and strain up to $0.5f_c$. A dashed line then connects the moment at which the concrete compression reaches $0.5f_c$ to the nominal moment capacity according to ACI 318-05 code. The dashed line then continues up to a moment and steel stress which considers strain hardening. The following calculations show the method for determining the moment versus steel stress for a beam with continuous reinforcement spaced at 6 in. apart with the property details of Specimen H-6-6. Figure 4-1 shows the cross section of the 6 in. spaced reinforcement beam and stress distribution up to cracking.

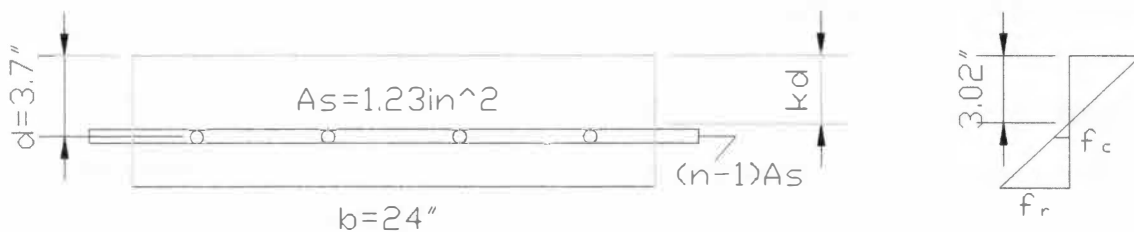


Figure 4-1: Cross Section Before Cracking and Stress Distribution

$$n = \frac{E_s}{E_c} = \frac{29,000 \text{ ksi}}{57\sqrt{10,500 \text{ psi}}} = 4.97 \quad (n-1)A_s = (4.97-1)(1.23 \text{ in}^2) = 4.88 \text{ in}^2$$

$$\sum M_{N.A.} = 0 = (24)(kd)(kd/2) - (24)(6-kd)\left(\frac{6-kd}{2}\right) - (4.88)(3.7-kd)$$

$$\sum M_{N.A.} = 0 = 148.9(kd) - 450.1$$

$$kd = 3.02 \text{ in.}$$

$$I_{\text{uncracked}} = \frac{24 \text{ in.}(3.02 \text{ in.})^3}{3} + \frac{24 \text{ in.}(2.98 \text{ in.})^3}{3} + (4.88 \text{ in}^2)(3.7 \text{ in.} - 3.02 \text{ in.})^2 = 434.3 \text{ in}^4$$

$$M_{\text{crack}} = \frac{f_r(I_{\text{uncracked}})}{h - kd} = \frac{7.5\sqrt{10,500 \text{ psi}} / 1000(434 \text{ in}^4)}{6 \text{ in.} - 3.02 \text{ in.}} = 112 \text{ k-in} = 9.3 \text{ ft-kips}$$

By similar triangles, the stress of the concrete at the steel level can be determined:

$$\frac{0.769 \text{ ksi}}{2.98 \text{ in.}} = \frac{f_c}{0.68 \text{ in.}}$$

$$f_c = 0.175 \text{ ksi}$$

$$f_s = n(f_c) = 4.97(0.175 \text{ ksi}) = 0.872 \text{ ksi}$$

The above calculations summarize the method for determining the cracked moment and steel stress immediately before cracking. The cracking moment is expected to be 9.3 ft-kips with the steel stress equal to 0.872 ksi. The steel stress will greatly increase immediately after the concrete cracks. The following calculations will determine the stress increase at cracking along with the cracked moment versus stress up to a concrete compression stress of $0.5f_c$. Figure 4-2 displays the cross section after cracking and the stress distribution when the concrete compression reached $0.5f_c$.

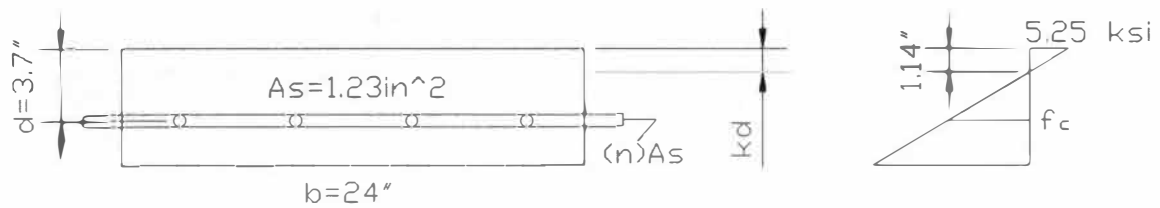


Figure 4-2: Cross Section After Cracking and Stress Distribution

$$(n)A_s = 4.97(1.23 \text{ in}^2) = 6.11 \text{ in}^2$$

$$\sum M_{N.A.} = 0 = (24)(kd)(kd/2) - (6.11)(3.7 - kd)$$

$$\sum M_{N.A.} = 0 = 12(kd)^2 + 6.11(kd) - 22.61$$

$$kd = 1.14 \text{ in.}$$

$$I_{\text{cracked}} = \frac{24 \text{ in.} (1.14 \text{ in.})^3}{3} + (6.11 \text{ in}^2)(3.7 \text{ in.} - 1.14 \text{ in.})^2 = 51.89 \text{ in}^4$$

$$\text{The concrete stress at the level of steel, } f_c = \frac{M(y)}{I_{\text{cracked}}} = \frac{M(2.56 \text{ in.})}{51.89 \text{ in}^4}$$

$$f_s = f_c(n) = \frac{M(2.56 \text{ in.})}{51.89 \text{ in}^4} (4.97)$$

$$\text{The steel stress immediately after cracking, } f_s = \frac{9.3 \text{ ft-kips}(2.56 \text{ in.})}{51.89 \text{ in}^4} (4.97) \frac{12 \text{ in.}}{\text{ft}} = 27.4 \text{ ksi}$$

When the compression concrete reaches $0.5f'_c$, $0.5f'_c = 0.5(10.5 \text{ ksi}) = 5.25 \text{ ksi}$

$$\text{By similar triangles, } \frac{5.25 \text{ ksi}}{1.14 \text{ in.}} = \frac{f_c}{3.7 \text{ in.} - 1.14 \text{ in.}}$$

$$f_c = 11.8 \text{ ksi}$$

$$\text{Linear relationship stops when, } M = \frac{(11.8 \text{ ksi})(51.89 \text{ in}^4)}{2.56 \text{ in.} (12 \text{ in./ft})} = 19.9 \text{ ft-kips}$$

In summary, the steel stress increases to 27.4 ksi immediately after the concrete starts to crack. The linear relationship between the concrete compression stress and concrete strain is estimated to stop when the top compression of the concrete reached 5.25 ksi. The moment at which the concrete compression is 5.25 ksi is determined to be

19.9 ft-kips. Below summarizes the calculations for the nominal moment capacity at which the steel stress reaches yielding and the moment and steel stress considering strain hardening.

$$a = \frac{A_s f_y}{0.85 f'_c b} = \frac{1.23 \text{in}^2 (60 \text{ksi})}{0.85 (10.5 \text{ksi}) (24 \text{in.})} = 0.345 \text{in.}$$

$$c = \frac{a}{\beta_1} = \frac{0.345 \text{in.}}{0.65} = 0.53 \text{in.}$$

$$\frac{\epsilon_s + 0.003}{3.7 \text{in.}} = \frac{0.003}{.53 \text{in.}} \quad \epsilon_s = 0.018 \text{ (Steel yielded)}$$

$$M_n = A_s f_y (d - \frac{a}{2}) = (12 \text{in.} / \text{ft}) (1.23 \text{in}^2) (60 \text{ksi}) (3.7 \text{in.} - \frac{0.345 \text{in.}}{2}) = 21.7 \text{ ft} - \text{kips}$$

Considering strain hardening:

$$\text{Statics:} \quad 0.85 (10.5 \text{ ksi}) (c) (0.65) (24 \text{in.}) = f_s (1.23 \text{in}^2)$$

$$\text{Strains Compatibility:} \quad \frac{c}{0.003} = \frac{3.7}{0.003 + \epsilon_s}$$

$$f_s = \frac{1.26}{0.003 + \epsilon_s}$$

Plotting the formula for steel stress on a stress versus strain curve for Grade 60 steel,

$$f_s = 73 \text{ ksi} \quad \text{and} \quad \epsilon_s = 0.0142$$

$$a = \frac{A_s f_s}{0.85 f'_c b} = \frac{1.23 \text{in}^2 (73 \text{ksi})}{0.85 (10.5 \text{ksi}) (24 \text{in.})} = 0.42 \text{in.}$$

$$M_n = A_s f_y (d - \frac{a}{2}) = (12 \text{in.} / \text{ft}) (1.23 \text{in}^2) (73 \text{ksi}) (3.7 \text{in.} - \frac{0.42 \text{in.}}{2}) = 26.1 \text{ ft} - \text{kips}$$

Figure 4-3 compares the above sample calculations of moment versus steel stress for a continuously reinforced beam with four #5 bars spaced 6 in. apart with the strain gauge results from Specimen H-6-6. Strain gauges 3-2 and 3-3 from Specimen H-6-6 used in this comparison are located 2 in. and 6 in. away from the head respectively, as shown in Figure 3-5. Specimen H-6-6 has 6 in. spacing with three headed bars on the left span and four headed bars on the right span. Gauges 3-2 and 3-3 are located on the right

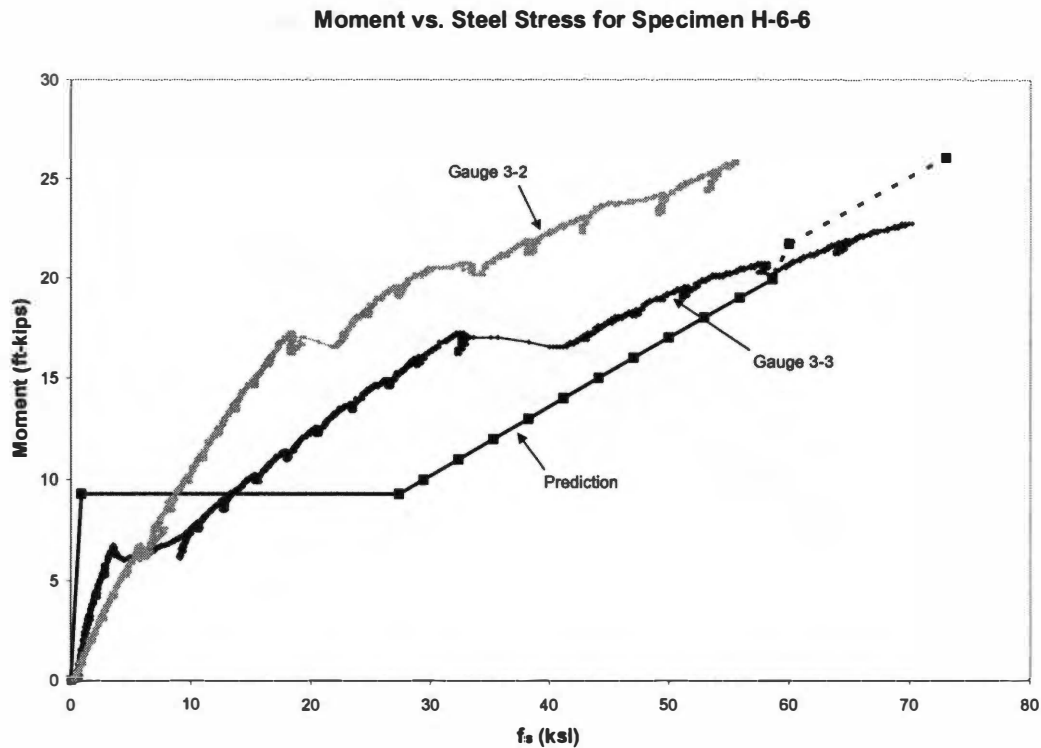


Figure 4-3: Moment versus Steel Stress Comparison for Specimen H-6-6

span with four headed bars which is why the comparison is made with the calculated moment versus steel stress using four bars. Notice in Figure 4-3 that the steel stress 2 in. away from the head did not develop stress as quickly and did not reach full capacity. The moment versus steel stress 6 in. away from the head behaved much more closely to the continuous bar behavior. Figure 4-3 indicates a beam with a 6 in. spacing can be near full development at 6 in. lap length.

Figure 4-4 examines the moment versus steel stress behavior for the side right of the centerline for Specimen H-6-4. This specimen has a 6 in. lap length and 4 in. spacing of bars. Gauges 2-2, 2-3, and 2-4 produced the strain data at locations 2 in., 4 in., and 6 in. away from the head, respectively. Figure 3-9 shows the strain gauge locations which are on the right side of the centerline. The cross sectional area of steel on the right side had five #5 bars while the left side had six #5 bars. The gauge 4 in. away from the head produced a moment versus steel stress behavior similar to the calculated behavior of a continuous bar at 4 in. spacing. By the end of the lap zone length, gauge 2-4 recorded

Moment vs. Steel Stress for Specimen H-6-4 (Right of Centerline)

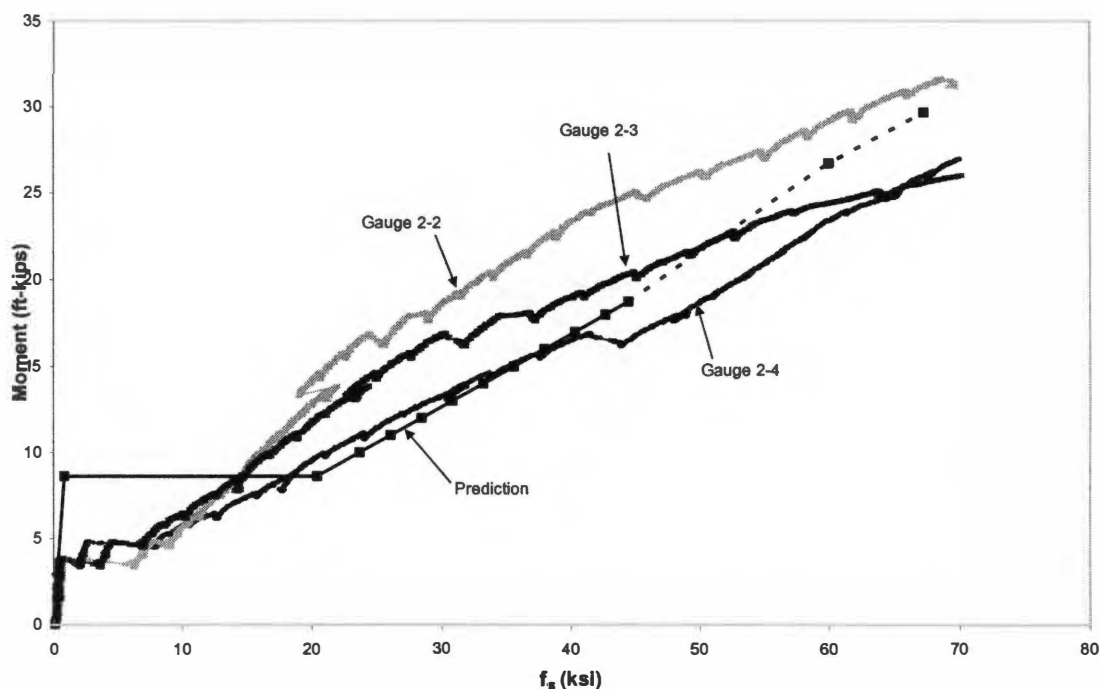


Figure 4-4: Moment versus Steel Stress Comparison for Right Side of Specimen H-6-4

steel stress larger than the steel stress calculated by continuous bars for a given moment. By comparison of both plots in Figure 4-4, the 6 in. lap length specimens developed and behaved as a continuous bar specimen. The 4 in. spaced reinforcement behaved more like a continuously reinforced specimen closer to the head of the bar than the 6 in. spaced bars. For both 6 in. lap length specimens, the beams reached the calculated nominal moment capacity.

Figure 4-5 plots the moment versus steel stress for the left side of the centerline for Specimen H-6-4. As shown in Figure 3-9, the left side had one more headed bar of reinforcement. Gauges 5-2 and 5-4, with locations 2 in. and 6 in. away from the head, can be seen in Figure 3-9. Gauges 5-2 and 5-4 developed steel stress close to the calculations for the left side of the beam. Like the right side of the beam shown in Figure 4-4, the left side of the beam developed more steel stress with respect to increasing moment at 6 inches away from the head. Figure 4-4 and Figure 4-5 validates that the

Moment vs. Steel Stress for Specimen H-6-4 (Left of Centerline)

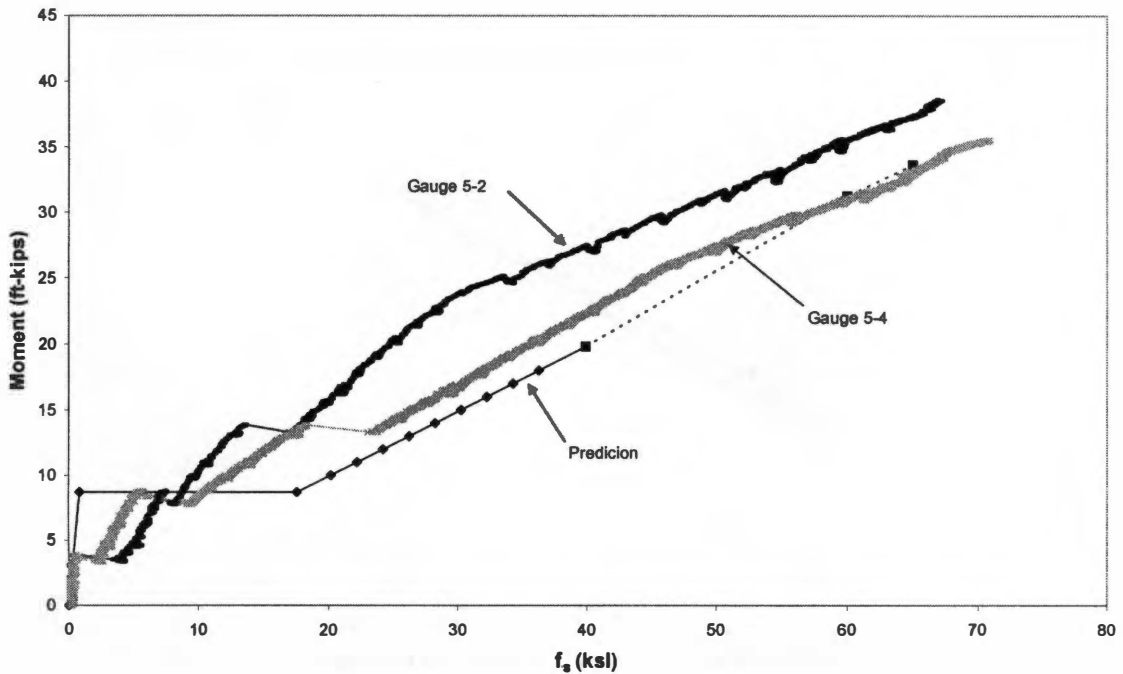


Figure 4-5: Moment versus Steel Stress Comparison for Left Side of Specimen H-6-4

gauges 6 inches away from the head on either the left or the right side of Specimen H-6-4 behaved like the predicted calculations.

Moment versus steel stress plots were made for all other headed specimens to compare the effect of lap length with the steel stress development of the bars. Figures 4-6 through 4-8 include these plots. Figure 4-6 and 4-7 plots the moment versus steel stress for the 2.5 in. lap length beams with either a 4 in. or 6 in. spacing of the bars. The locations of the strain gauges used in the plots can be seen in Figure 3-7 for Specimen H-2.5-6 and Figure 3-11 for Specimen H-2.5-4. Both beams behaved very similarly to the calculated behavior. The difference between the moment versus steel stress plots for the 6 in. lap length and the 2.5 in. lap length was the 6 in. lap length bars reached yielding and nominal moment capacity. Specimen H-2.5-4, which is more heavily reinforced, reached closer to the nominal moment capacity than Specimen H-2.5-6.

Moment vs. Steel Stress for Specimen H-2.5-4

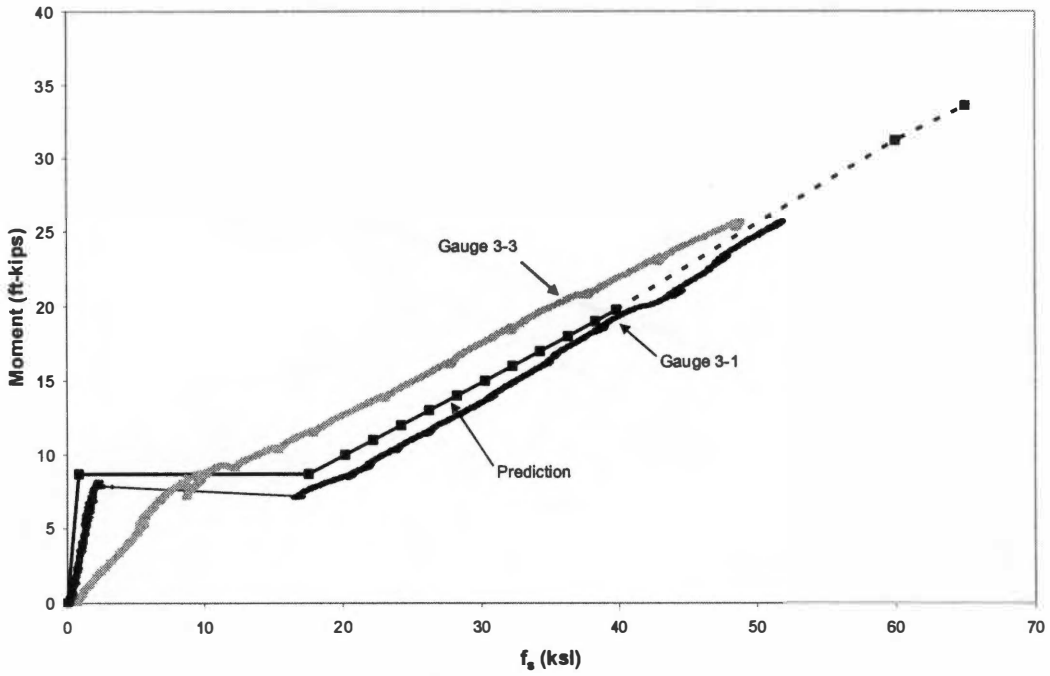


Figure 4-6: Moment versus Steel Stress Comparison for Specimen H-2.5-4

Moment vs. Steel Stress for Specimen H-2.5-6

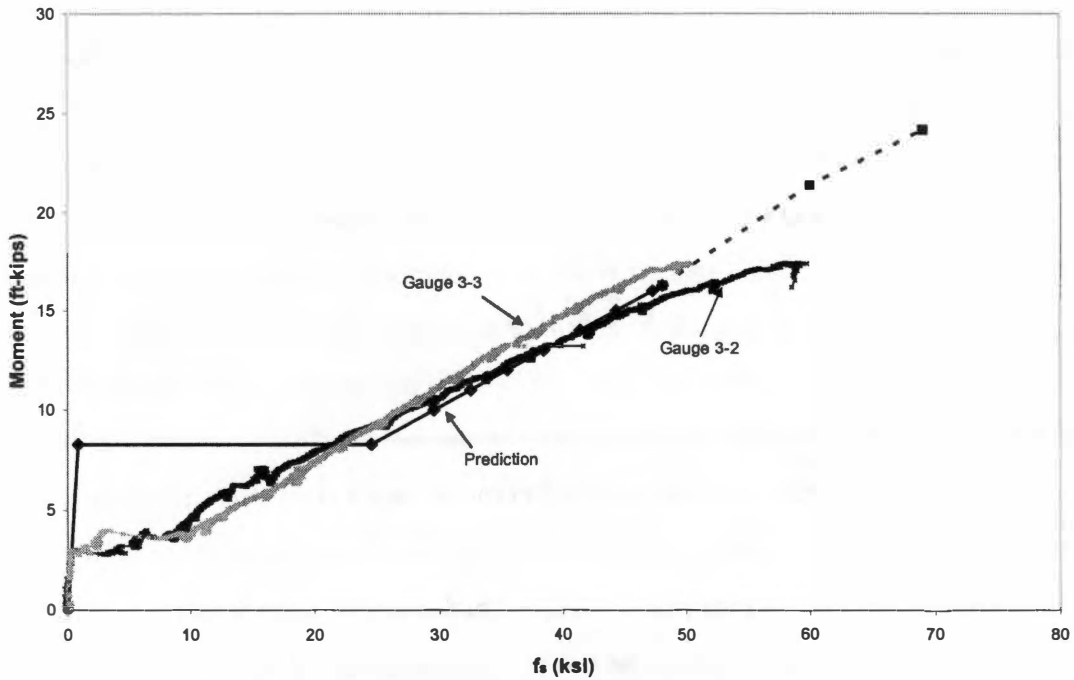


Figure 4-7: Moment versus Steel Stress Comparison for Specimen H-2.5-6

Moment vs. Steel Stress for Specimen H-4-6

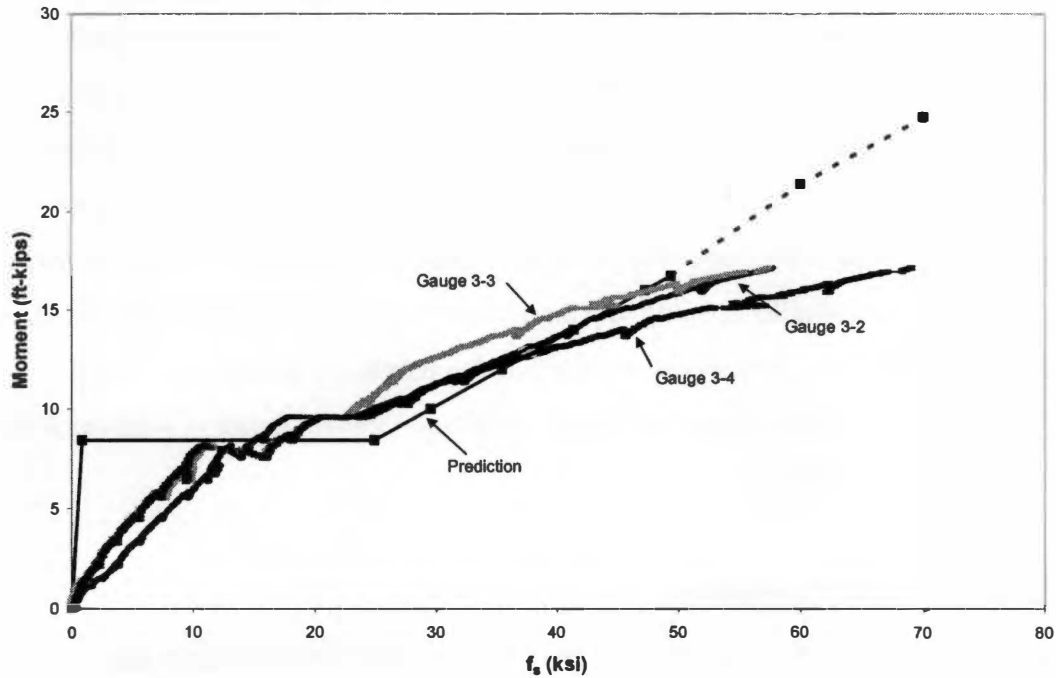


Figure 4-8: Moment versus Steel Stress Comparison for Specimen H-4-6

Figure 4-8 shows the moment versus steel stress for Specimen H-4-6. The gauge locations are shown in Figure 3-13. Gauges 3-2, 3-3, and 3-4 are located 2 in., 4 in. and 6 in. away from the head respectively. The bar's stress developed as expected and bar reached yield 6 in. away from the head. The steel stress developing more quickly further away from the head can be noticed. However, the beam did not meet the nominal moment capacity.

As shown in the moment versus strain behavior of the WWR specimens, at no locations did the bars develop strain. All of the strain gauge readings of W-4-4 and W-4-6 are on the order of magnitude of micro strain. Along with the bars not developing, the specimens failed prematurely and abruptly. A large crack would continue to propagate the center of the span of these specimens until a brittle failure would occur. The reason for the poor performance of the welded wire reinforcement was the inability of the concrete to form between the welded wires. The specimens went against the Article 12.18.1 of the ACI code requirement of a minimum 2 in. distance between the overlap of

the outermost cross wires. Specimens W-4-4 and W-4-6 had bars wires overlap distance of 1 inch in order to reduce the lap zone area.

By comparing the moment versus strain plots for the 2.5 in. lap length, the four inch spacing can be determined as the better spacing condition. The moment versus strain curves for Specimen H-2.5-6 rarely developed passed yield, and the bars did not reach full capacity. Specimen H-2.5-4 performed better than H-2.5-6 with respect to reaching yielding stress of the bars. However, Specimen H-2.5-4 had a sudden, brittle failure, and despite the smaller spacing, the 2.5 in. lap length was not adequate to transfer loads across the specimen. In conclusion, the 6 in. lap length developed steel stress adequately with increasing moment and reached nominal moment capacity with the 4 in. spacing being more desirable.

Moment-Curvature Discussion

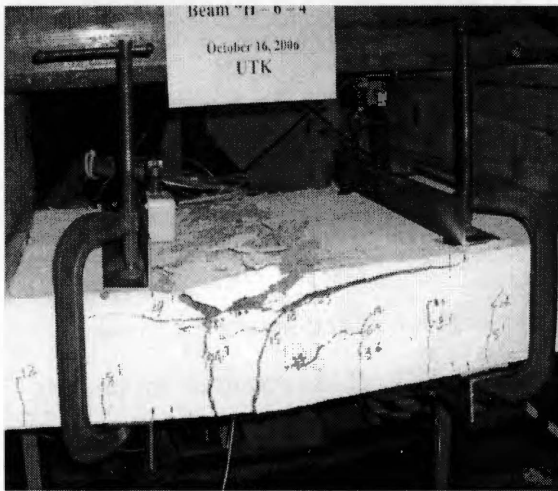
By comparison of the moment-curvature relationships for the headed bar specimens, the 4 in. spacing provided much more moment capacity to the specimens. The smaller spacing provides more steel area in the cross section which will improve the flexural strength and thus the moment capacity. However, if the steel ratio is increased too much, the ductility of the beam can be sacrificed. Specimen H-6-6 proved to be slightly more ductile than Specimen H-6-4 due to reduced area of steel. The slight increase in the ductility of Specimen H-6-6 is not as beneficial as the significant moment capacity improvement of Specimen H-6-4. In summary, the 4 in. spacing provided much more flexural strength than the 6 in. spacing.

The moment-curvature plots reveal the lap length also causes an effect on the behavior of the moment curvature. The 6 in. lap length can clearly be determined as the optimum design for lap length. Specimens H-6-6 and H-6-4, which both have a 6 in. lap length, had substantially more curvature capacity than either the 2.5 in. or 4 in. lap length. The moment capacity of Specimen H-2.5-4 was one of the strongest of the eight specimens, but as seen from the moment curvature plot, the specimen failed abruptly due to the lack of development of the bars in the 2.5 in. provided. In summary, the 6 in. lap

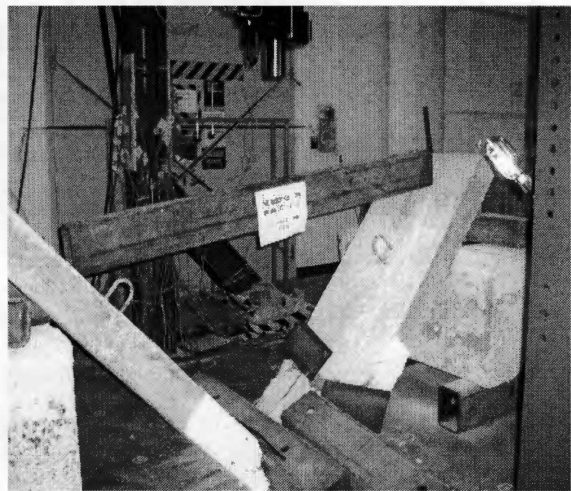
length can be identified as the required lap length to provide development length and curvature capacity.

Failure Types

The specimens exhibited two different failure types during testing. Figure 4-9 displays both a ductile, slow failure and a sudden, brittle failure. The WWR specimens and H-2.5-4 experience a sudden, brittle failure which is undesirable for design implementation. The Control Specimen, H-6-6, H-6-4, H-4-6, and H-2.5-6 had a ductile failure. As shown Figure 4-9, the compression zone began to crumble until moment could not longer be carried.



(a) Ductile Failure



(b) Brittle Failure

Figure 4-9: Failure Types

CHAPTER 5 Conclusions and Recommended Future Research

From the moment-curvature analysis, the optimum lap length was 6 inches. This lap length provided enough development of the bars to largest moment capacities and ductility. The 4 inch spacing specimens had larger moment capacities than the 6 inch spacing. By comparing the 6 inch lap length specimens, the moment capacity of the 4 inch lap length had a moment capacity that was 50% larger than the 6 inch spacing without compromising much ductility.

The moment versus steel stress analysis indicated a required lap splice length of 6 inches. The bars yielded in the 6 inch lap length specimens. For the gauge located 6 inches away from the head, the moment versus steel stress behaved as the calculated prediction for a continuously reinforced specimen. For the 4 inch lap length specimen, the bar yielded 6 inches away from the head while the bar did not yield 2 and 4 inches away from the head. This also suggests that the required lap length was 6 inches. For the 2.5 inch lap length specimens, the bars did not yield, and they did not reach the predicted nominal moment capacity.

Based on the experiments conducted, the required lap splice length for these specimens is estimated to be close to 6 inches. In comparison of the required lap lengths from the ACI code for straight and hooked bars in Chapter 2 of this paper, this conclusion seems reasonable. As expected, the headed bars reduced the required lap length compared to the straight bar which had a required splice length of 25.4 inches. The required development length for hooked bars was 6.8 inches which is closer to the length required for headed reinforcement.

For the 6 inch bar spacing, the design method proposed by the University of Texas at Austin (UTA) produced a slightly larger required lap splice length than the concluded 6" lap length made by the testing results. There are a couple of reasons why the proposed method is slightly conservative. The minimum anchorage length of $6d_b$ controlled for both the 6 inch and 4 inch spacing. Research at UTA indicated that the head bearing capacity was overestimated for an anchorage length of $6d_b$ or less. The formulas used to calculate head bearing capacity were based on existing ACI code for bearing strength and side blowout capacity. For anchorage lengths of $6d_b$ or less, the

head bearing capacity was less than the calculated capacity. This resulted in designing for less bond stress than required, and to prevent overestimating the head bearing capacity, the anchorage length limit of $6d_b$ was added. More research should focus on whether this lower limit for anchorage length is accurate. Another reason for the conservative estimate of the 6 inch spacing beam could be from the 55° strut line path recommended for determining the lap splice length from the anchorage length. For the 6 inch spacing, the strut line addition increased the anchorage length of 3.75 inches up to a required lap splice length of 7.03 inches which was almost a factor of 2. For the ACI code for a straight bar with Class B splices, the factor for converting development length to lap splice length is 1.3. Reducing the ratio of anchorage length to lap splice length will result in a value closer to the 6 inch lap length determined in this research.

For the 4 inch bar spacing, the proposed method by UTA required lap length of 5.6 inches was smaller than the 6 inch lap length from the testing results. From the results for 4 inch spacing specimens, it is possible that the required lap length could reduce to 5.6 inches. The next smallest splice length with a 4 inch spacing was H-2.5-4, which had a 2.5 inch splice length. The lap length could not reduce down to 2.5 inches according to the test results for H-2.5-4 which had a brittle failure. In conclusion, the testing results showed some variation with the design method proposed by the University of Texas at Austin. Further research on the minimum anchorage length, the bearing head capacity, and the strut line path should be pursued.

List of References

List of References

ASTM A 970, "Standard Specification for Headed Steel Bars for Concrete Reinforcement," American Society for Testing and Materials, West Conshohocken, Pennsylvania, 2007.

ACI International Committee 318. 2005. *Building Code Requirements for Structural Concrete (ACI 318-05)*. Farmington Hills, MI: American Concrete Institute International.

Bentz, Evan C., and Michael P. Collins. 2000. *Response-2000 Reinforced Concrete Sectional Analysis*. Bentz, Evan C., and Michael P. Collins.

MacGregor, James G., and James K. Wight. 2005. *Reinforced Concrete: Mechanics and Design*. Fourth Edition. Upper Saddle River, New Jersey: Pearson Education, Inc.

Oesterle, R. G., Ma, Z. J., Eriksson, R., and Prussack, C. 2004. Design and Construction Guidelines for Long-Span Decked Precast, Prestressed Concrete Girder Bridges. *NCHRP 12-69 Interim Report, December*. 125 pp.

Thompson, M. K., Ledesma, A. L., Jirsa, J. O., Breen, J. E., and Klingner, R. E. 2003. *Anchorage Behavior of Headed Reinforcement*. Springfield, VA: National Technical Information Service.

Thompson, M. Keith, James O. Jirsa, and John E. Breen. 2006. Behavior and Capacity of Headed Reinforcement. *American Concrete Institute Structural Journal*. Volume 103 Number 4 522-530 pp.

Thompson, M. Keith, Antonio Ledesma, James O. Jirsa, and John E. Breen. 2006. Lap Splices Anchored by Headed Bars. *American Concrete Institute Structural Journal*. Volume 103 Number 2 271-279 pp.

Vita

Mary Elizabeth Griffey was born in Muncie, IN on December 19, 1983. Mary was raised by her parents, Richard and Susan Griffey, along with her brothers, Bryan and Joseph, in Muncie, IN and Franklin, TN. In 2002, Mary graduated from Centennial High School in Franklin, TN. Following high school, she attended the University of Tennessee, Knoxville to study civil engineering. She received her B.S. in Civil Engineering. Mary is currently pursuing a Master of Science degree in structural engineering at the University of Tennessee, Knoxville.

1422 5103 26
02/20/08 VN 